Automatic extraction of potential impact structures from geospatial data – examples from Finnmark, Northern Norway

Svein Olav Krøgli

Dissertation for the degree of Philosophiae Doctor (Ph.D.)

Department of Geosciences

Faculty of Mathematics and Natural Sciences

University of Oslo

2010

Series of dissertations submitted to the
Faculty of Mathematics and Natural Sciences, University of Oslo
No. 948

ISSN 1501-7710

Cover: Inger Sandved Anfinsen.
Printed in Norway: AiT e-dit AS.

Produced in co-operation with Unipub.
The thesis is produced by Unipub merely in connection with the
thesis defence. Kindly direct all inquiries regarding the thesis to the copyright
holder or the unit which grants the doctorate.

Preface

This work constitute my Ph.D. study that started with the working title "Automatic and semi-automatic detection of meteorite impact structures in the Fennoscandian shield using pattern recognition of spatial data". The study area was constrained to Finnmark, Northern Norway, due to data accessibility. The thesis presents results from my three year employment as a Ph.D. research fellow at the Department of Geosciences, University of Oslo (2006 – 2009), with supervisors Professor Henning Dypvik and Professor Bernd Etzelmüller. It consists of a summary, three papers and two peer reviewed extended abstracts describing different automatic search techniques. Sometimes a description of the novel Beyond Sleep by W. F. Hermans fits the study: "A classic of post-war European literature, this is the tale of a man at the limits of physical and mental endurance beyond the end of the civilised world", where the limits of physical and mental endurance is crater search and the end of the civilised world is Finnmarksvidda.

This project is part of an international program between (groups from) the Universities of Oslo and Helsinki, the European Space Research and Technology Centre (ESA/ESTEC), and the Geological Surveys of Norway and Finland (data supply) (Chicarro et al. 2007; Dayioglu et al. 2006). The program is titled "The search of meteorite impact structures in the Fennoscandian Shield – a novel technique". The program outline is to develop workable automatic or semi-automatic search algorithms to discover new impact structures in Fennoscandia. The idea comes from the Finnish discoveries of several impact structures during the nineties using digital maps (Abels et al. 1997a; Abels et al. 1997b).

List of papers

Paper I: *Krøgli, S.O., Dypvik, H., Etzelmüller, B., 2007. Automatic detection of circular depressions in digital elevation data in the search for potential Norwegian impact structures. Norwegian Journal of Geology 87, 157-166.*

Paper II: *Krøgli, S.O., Dypvik, H., 2010. Automatic detection of circular outlines in regional gravity and aeromagnetic data in the search for impact structure candidates. Computers & Geosciences 36, 477-488.*

Paper III: *Krøgli, S.O., Dypvik, H., Chicarro, A.F., Rossi, A.P., Pesonen, L.J., Etzelmüller, B. The Impact Crater Discovery (ICDY) tool applied to geospatial data from Finnmark, Northern Norway. Submitted to Canadian Journal of Remote Sensing.*

Peer reviewed extended abstract I: *Krøgli, S.O., Dypvik, H., Etzelmüller, B., 2007. Automatic and semi-automatic detection of possible meteorite impact structures in the Fennoscandian shield using pattern recognition of spatial data, In: ScanGIS'2007: The 11th Scandinavian Research Conference on Geographical Information Science, Ås, Norway, 227-235.*

Peer reviewed extended abstract II: *Krøgli, S.O., Dypvik, H., Etzelmüller, B., 2009. Correlation of radial profiles extracted from automatic detected circular features, in the search for impact structure candidates, In: Geomorphometry 2009, Zurich, Switzerland, 50-54.*

Acknowledgements

Thanks to: Supervisor Henning Dypvik for always asking how it is going, clearing up my complicated sentences and for company on field trips; supervisor Bernd Etzelmüller for believing in GIS and me and for being a man of structure; Elin Kalleson for discussions, company on conferences and feedback on my work; Bård Romstad for technical discussions during "GIS-lunsjer"; the English proof readers Christopher Nuth (paper II and thesis) and Kimberly Ann Casey (paper III); Rutger Dujardin for spending time reflecting in the office at ESTEC while tourist trams waved outside and for inspiration from his master thesis; The European Space Research and Technology Centre (ESA-ESTEC) with Agustin Chicarro and Angelo Pio Rossi for making it possible to stay a three months period (Sep-Nov 2007) and a two weeks period (May 2009) at the ESTEC facilities (The Netherlands), learning and using the Impact Crater Discovery (ICDY) tool; The Geological Survey of Norway (NGU) with Odleiv Olesen for providing geophysical data and a meeting in Trondheim and Jan Sverre Sandstad for providing exposure maps of Finnmark that greatly helped the field work; Anne Solberg for making it possible to attend an image analysis course when not scheduled; Odd Nilsen for microscopy help; the Network on Impact Research (NIR) for sponsoring relevant workshops, Ph.D.-courses, conferences and creating an impact structure student environment; the lunch group Karianne and Lars Eivind, fellow geofag students, staff, the Småkasins, Ingeborg, family and friends for making things go around.

Thanks to the Research Council of Norway (Norges forskningsråd) for financially supporting this project (nr# 170617).

Abstract

Impact cratering is a fundamental process in the Solar System, and on solid planetary bodies like Mars and the Moon, impact cratering may be the most prominent landforming process. On the Earth several processes compete in shaping the surface. Consequently, the impact structures on Earth are often poorly preserved, difficult to spot and found in limited numbers (only 176 terrestrial impact structures are confirmed). Potential terrestrial impact structures waiting to be found are therefore expected to be partly masked by erosion and depositional processes. This makes detection more difficult than on solid planetary bodies and requires the use of multiple techniques and multiple datasets. The findings of new impact structures would contribute information to scientific questions such as better understanding of impact processes and their importance in the Earth's geological history.

The impact crater formation process results in a circular shape of fresh craters, except for impacts at low angles. This circularity is found in e.g. morphology, the distribution of impact rocks and in geophysical anomalies. The analytical choice is then to use the circular shape as a feature descriptor in search approaches. This thesis describes a new technique, established techniques and an existing tool, all applied to automatic extract circular features from appropriate geospatial datasets, i.e. to locate potential impact structures. The data cover parts of Finnmark county, Northern Norway, and include digital elevation models, geophysical potential field data and multispectral images. The presented techniques deal with circular depressions, circular borders and circular symmetry, and the results show them suitable to identify various circular features.

Remote sensing or image analysis methodologies can only detect potential impact structures, the most promising structures for further field studies. Evidence must later come from sampled rocks. The methods are semi-automatic since the researcher needs to set thresholds appropriate for the different regions, and thereafter inspect the detected features to prioritize and select the sites to be visited in the field. An impact structure search should not be based on a single technique or a single dataset because of the diverse impact crater catalog, but rather a combination of several techniques applied on various data, utilizing data fusion to improve the detection process. Interesting patterns first found by automatic detections and then evaluated by the researcher can prove rewarding, possibly emphasizing structures that

would not have been considered without the automatic step. Unlike previous terrestrial search approaches of purely visual analysis of data or the use of automatic techniques relevant to only a limited set of data, the presented methodology (collection of techniques) offers a framework to search large regions and several types of data to extract promising structures prior to the visual inspection. The sites at the researcher's disposal are all exhaustive and objectively extracted based on circularity.

Sammendrag

Asteroide- og kometnedslag med påfølgende dannelse av nedslagskratre (ofte kalt meteorittkratre) er fundamentale prosesser i vårt solsystem, inkludert utformingen av jorda, fra dens dannelse til i dag. Resultat av nedslag kan tydelig ses på planetære overflater som månen og Mars, der kratre ofte er den mest dominerende landformen. På jorda er det mange prosesser som former overflaten (erosjon, platetektonikk og sedimentasjon), og dette gjør at nedslagskratre forringes over tid eller forsvinner helt. Det har bare blitt funnet et fåtall bekreftede nedslagsstrukturer på jorda sammenlignet med andre terrestriske planeter (ca. 176). Mulige nye nedslagskratre er forventet å være dårlig bevart og delvis fjernet av erosjon eller skjult av sedimentære prosesser. Dermed blir deteksjon av meteorittkratre vanskeligere på jorda enn på mange andre planeter og måner, og det vil kreve bruk av flere teknikker og datasett. Funn av nye nedslagskratre kan gi svar på vitenskapelige spørsmål som fører til økt forståelse av nedslagsprosesser og kraterdannelse, og deres viktighet gjennom jordas geologiske historie.

Selve nedslagprosessen resulterer i at ferske kratre ender opp som sirkulære fordypninger (elliptiske hvis nedslagsvinkelen er under ti grader fra horisontal). I tillegg til sirkulære topografiske mønstre er den sirkulære formen også typisk blant nedslagsbergartenes oppsprekking og oppknusing, samt de resulterende geofysiske anomaliene. Den sirkulære formen ble derfor valgt som egenskapsbeskrivelse og analysekriterium i utviklingen av søketeknikker for å finne potensielle nedslagsstrukturer. Formen er et minste felles multiplum for alle kratre, men det en stor forenkling. En enkel modell gjør imidlertid at algoritmene kan benyttes på flere datatyper. Denne avhandlingen beskriver en nyutviklet teknikk, etablerte teknikker og et eksisterende verktøy, alle benyttet for automatisk ekstraksjon av sirkulære strukturer eller rester av sirkulære strukturer fra relevante digitale regionale datasett. Dataene dekker et område i Finnmark fylke (Nord-Norge) og inkluderer blant annet digitale høydemodeller, geofysiske anomalikart (tyngde, magnetisme) og multispektrale bilder. De presenterte teknikkene dekker forskjellige sirkulære aspekter; sirkulære groper, sirkulære grenser og sirkulær symmetri. Resultatene viser at teknikkene er egnet til å detektere varierende sirkulære former.

Form alene er imidlertid langt fra nok til å si at man har et nedslagskrater. Metoder innen fjernanalyse og bildeanalyse kan kun detektere potensielle nedslagsstrukturer. For eventuelt å bevise et nedslagsopphav må det foretas detaljerte feltundersøkelser av de mest lovende automatisk detekterte strukturene. Metodene er halvautomatiske siden operatøren må sette terskelverdier som er hensiktsmessige for hvert område, og deretter inspisere resultatene for å prioritere hvilke steder som bør besøkes i felt. Leting etter nye nedslagskratre bør ikke basere seg på en enkelt teknikk eller datatasett, fordi strukturene er så forskjellige på jorda. En fusjon (sammensetting) av resultater basert på flere teknikker anvendt på topografisk, geologisk, geofysisk og satellittbilde informasjon vil forbedre deteksjonsprosessen. Dette gir likeledes et kostnadseffektivt verktøy for en første identifisering av sirkulære objekter i romlige data. Interessante mønstre som først er funnet med automatiske metoder og deretter evaluert av operatøren, gir muligheter for å fremheve strukturer som ellers kanskje ikke ville ha blitt vurdert. Den presenterte metoden (samling av teknikker) gir et rammeverk for å søke i store områder og i flere typer data, i forhold til tidligere søketeknikker på jorda som har omhandlet visuell analyse av data, eller bruk av automatiske teknikker relevante for få bestemte datasett.

Contents

1. Introduction and objectives

Impact cratering is a fundamental process in the Solar System, from planetary evolution to landscape formation. On solid planetary bodies like Mars and the Moon, impact cratering may be the most prominent landforming process, whereas on the Earth several processes compete in shaping the surface. Consequently, the impact structures on Earth are often poorly preserved and difficult to spot. Nonetheless, "impacts of extraterrestrial objects on the Earth, once regarded as an exotic but geologically insignificant process, have now been recognized as a major factor in the geological and biological history of the Earth" (French 1998, p. 1). Impacts from asteroids, comets and meteorites also act as natural hazards, possibly causing mass extinctions and environmental changes (climatic effects on local, regional and global scale) (e.g. Keller and Blodgett 2006). Craters are important in planetary analysis whereby numerous craters within a region is an indication of an older surface. For example, if two different types of Martian volcanoes are found on old crater plains or young crater plains, respectively, they can be relatively dated and provide information about the evolution of the planet from the age of processes creating the specific volcano type (e.g. Plescia and Saunders 1979).

On the Earth today 176 proven impact structures are known (Earth Impact Database 2009), but "the recognition of craters on Earth's surface is highly biased by the accessibility of the area and the research activity within a specific region" (Werner 2006, p. 8). In Fennoscandia, 21 structures are confirmed (Dypvik et al. 2008). There are probably even more impact structures to be found in Fennoscandia, due to the large areal extent and the older bedrocks that have the potential to record impact events over a long period of time. In Norway, research activity focused on identifying new impact structures has in addition been relatively low. The search for impact structures may be triggered by exploration for natural resources (e.g. water, ore, oil), but mainly for mapping and information contribution to scientific questions towards a better understanding of impact processes and their importance in the Earth's geological history.

Images of solid extraterrestrial bodies (e.g. Mars) often display craters with a clean, well preserved morphology due to the lack of an active lithosphere, with little to no tectonic, erosion or depositional processes. On Earth, these processes modify or erase the

morphological imprint of impact craters. Well preserved structures are predicted to be found in an explored area as Norway, and unidentified terrestrial impact structures are expected to be partly masked by erosion, making detection more difficult than on solid planetary bodies. In the search for new terrestrial impact structures we have to look for suspicious patterns in the spatial data (e.g. topography, gravity). Impact structures often display a circular shape in spatial data, and candidate sites may therefore be detected based on similarities to this signature.

To find new possible impact structures, large areas have to be searched preferably using automatic methods. The sciences of geomorphometry, remote sensing and automatic pattern recognition have developed a multitude of digital techniques to extract specific features based on a regularly spaced matrix of discrete values (e.g. elevation, gravity or spectral reflection values). This data structure enable convenient possibilities to investigate spatial relations between cell values (pixels), either in close proximity or at a distance away from each other (DeMers 2002). A broad perspective is needed, using multiple techniques, multiple datasets and data fusion to improve the detection process. This is required because of the complexity of impact structures. They contain a wide range of modification levels and sizes, are found on different terrains, and in limited numbers. The methods of remote sensing or image analysis only allow us to detect possible impact structure candidates whereas additional field investigations and laboratory analyses are required to disclose their origin.

The aim of this study is to develop a search methodology to detect potential impact structure sites. The general research aims of this thesis are to:

1) Identify feature descriptors; impact structure characteristics as manifested by geological, geophysical and morphological signatures and their relation in space.
2) Develop techniques, use established techniques or apply existing tools to extract the chosen feature characteristics from appropriate datasets.

The underlying questions are then: If an impact structure is present, what will the spatial data display, and can we detect similar places automatically?

2. Scientific background and theory

2.1. Impact structures

Our Solar System consists of the Sun, eight planets, three dwarf planets and moons, asteroids and comets. The Earth's Moon is covered by impact craters (Fig. 1a) due to the lack of atmosphere and geologic activity. Many can be seen by a normal telescope. The terrestrial planets, except for Earth and Venus, are all dominated by impact craters (Fig. 1b), as are several of the moons/satellites of planets (Fig. 1c). Even asteroids and comets have been hit by other asteroids, comets or meteorites resulting in crater formation (Fig. 1d).

2.1.1. Crater formation, morphology and geology

Asteroids and comets create craters when colliding with planets, moons or other asteroids and comets. The event is a hypervelocity impact which acts as an explosion, creating a circular depression (e.g. Gifford 1924; Melosh 1989). Gifford (1924) presented in 1924 an impact-explosion analogy, claiming that the crater is not due to the impact itself, but to the explosion resulting from the kinetic energy, the "violent heat produced by the sudden stoppage of the meteor" (Gifford 1930, p. 379). Circular craters are generally produced for impact angles greater than 10 - 12 degrees from horizontal (Bottke et al. 2000). Lower impact angles produce elongated or ellipsoidal craters. Both the projectile properties (i.e. composition, density, size, mass, velocity, angle) and target properties (i.e. gravity, material, density, strength, porosity) effect the size and morphology of the resulting impact crater. A hypervelocity impact (typically a velocity of 10 – 30 km/s at an impact angle of 45 degrees from horizontal) may result in shock pressures generally reaching hundreds of GPa, possibly causing melting and vaporization of both projectile and target (Melosh 1989). The cratering process is conventionally divided into three stages (Melosh 1989; Turtle et al. 2005): *i)* Contact and compression (shock wave initiation and propagation), *ii)* crater excavation (transient crater, the drive of material out of the crater is gravity dependent), and *iii)* crater collapse and modification (final crater structure).

The circularity of impact craters has been the subject of quantitative studies. Ronca and Salisbury (1966) examined the circularity of lunar craters by calculating a circularity index for several craters. The circularity of terrestrial features like calderas, collapse pits, ring

complexes, maars and tuff-rings, cinder and spatter cones, artificial explosion craters and meteorite craters, together with lunar features like well-preserved craters, large craters with flooded floors, elementary rings, small lunar craters, secondary craters and lunar calderas, were compared by Murray and Guest (1970), concluding that meteorite craters are more circular than most volcanic craters (calderas). Using quantitative expressions of circularity to discriminate between impact structures and other features was also shown by Pike (1977a), describing a difference between most impact craters and most large volcanic craters. The reason that calderas are not as circular as impact craters may result from the difference between a single explosion that form impact craters, as opposed to calderas that may derive from a series of explosions (Murray and Guest 1970) or by the collapse of magma chambers along irregular lines of weakness in the rock (Oberbeck et al. 1972). Martian craters show similar circularity values as terrestrial impact structures and different from indices of terrestrial calderas, explained by a significant difference between the mean circularity of meteorite craters and volcanic craters (Oberbeck et al. 1972).

Fresh craters are circular in shape but display different morphology depending on size, recognized on the lunar surface: “To my eye the interiors of most craters under four miles and all under two miles appear as simple cups” (Gilbert 1893, p. 245). The craters may be simple bowl shaped, complex or multi-ringed impact basins. Crater morphology displays the same characteristics throughout the Solar System. On Earth, the two dominant types of impact structure are the 1) simple structures, with a raised rim surrounding a bowl-shaped depression, and the 2) complex structures, larger in diameter, with a central peak, surrounded by an annular trough and a slumped rim (e.g. Grieve 1990; Melosh 1989) (Fig. 2). The transition between simple and complex craters occur on Earth at diameters of about 2 km or 4 km, in sedimentary or crystalline rocks respectively (Dence 1965; Grieve 1990). Concentric peak rings are found for larger craters, occasionally surrounding the central peak. Even multi-ring craters exist, with several ring structures creating annular basins (e.g. Turtle et al. 2005). Resurfacing processes such as tectonics, erosion and deposition will after formation eventually modify or erase the surface expression. These processes are very active on Earth.

Breccias are an important recognizable geological feature within impact craters. Breccias can be formed by the crushing of target rock during impact or after impact by (angular) fragments falling back into the crater after being thrown up in the air. Other impact related rocks are melt rocks, e.g. suevite and tektites. The central uplift in complex craters typically exposes rocks from deeper levels in the crust that are uplifted from considerably depth to reach the surface. The lithologies exposed in the central peak thus contrasts with the

surrounding stratigraphic sequence around the impact structure (Koeberl 2007). Several additional shock metamorphic mineral features may be found at a microscopic level. These differences in lithological properties may appear as anomalies relative to the surrounding area unaffected by impact and commonly exhibit roughly circular/symmetric patterns.

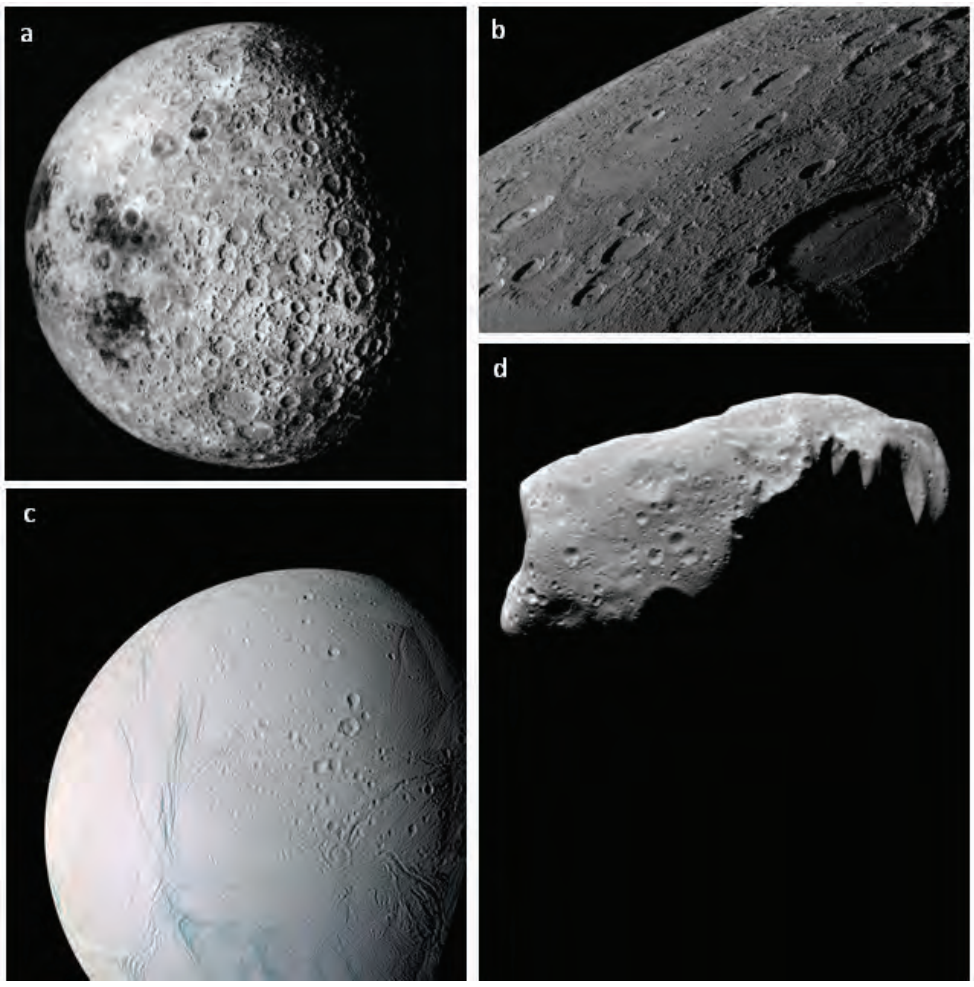

Fig. 1. A compilation of impact craters as seen on different solid bodies in the Solar System. (a) The Earth's Moon. (b) Mercury's horizon as seen from the MESSENGER satellite. (c) Saturn's icy moon Enceladus. (d) Asteroid Ida. All images credit NASA.

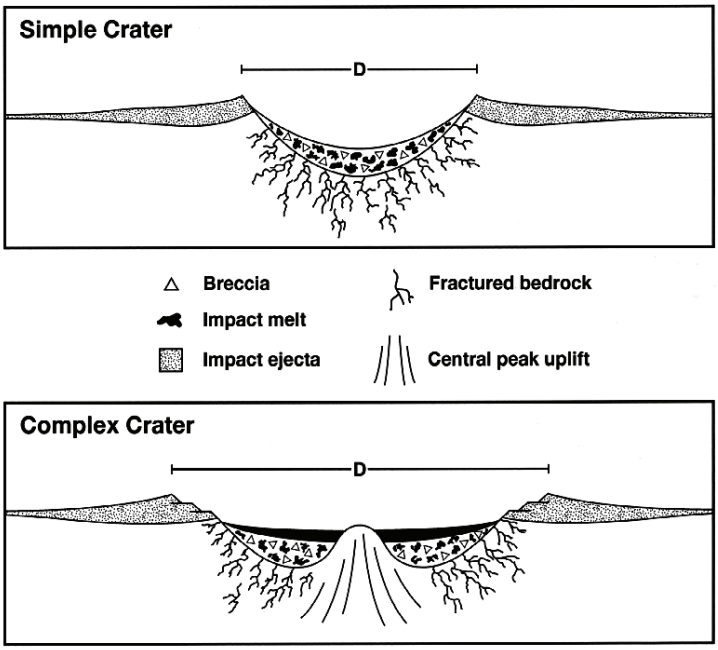

Fig. 2. Morphology of simple and complex craters. Image credit NASA.

2.1.2. Crater chronology

The interpretation of the geologic evolution of the planetary bodies is somewhat dependent upon the ability to identify impact craters and establish the best possible crater record. The result of planetary crater counting, either performed manually or automatically (crater detection algorithms), is the number of impact craters and their size. The frequency distribution of the diameters can be used to derive an estimate of age related to the local erosional history of the analyzed surface area. Generally, the more impact craters a surface has, the older it is. Going from relative age to absolute dating requires information about the bombardment flux (frequency at which bolides of a given diameters collide with planetary bodies), impact conditions and scaling laws for planetary crater size comparison given a fixed projectile size (Ivanov 2008a).

Data sampled during the Apollo missions to the Moon have been used to establish a lunar crater production rate, "the number of impact craters accumulated on a unit area per unit of time" (Ivanov 2008a). The crater chronology is based on the number of craters as a function of age. The age is derived from radiometric measurements of the rocks from the

landing sites. The relationship can be used to calculate the age of a surface (in million of years) on the Moon and has also been transferred to other solid planetary bodies, e.g. Mars (e.g. Neukum et al. 2001; Neukum et al. 2006). Criticism of the methodology is that it only considers crater density as a function of time. "More generally, the terrestrial planets should also possess a variation in impact density with latitude" (Le Feuvre and Wieczorek 2006), with more hits on equator (on Earth, however, plate tectonics have changed location of continental plates during geologic times) (Thackrey et al. 2006).

Gasselt et al. (2006) divides the process of age determination of a surface in three steps based on crater-size frequency distribution: (1) Find diameters of impact craters within a surface area, (2) calculate a size-frequency distribution, and (3) determine age using one of the techniques: Isochrones or production function fit, combined with the application of a chronology model (impact flux estimates). The production function is the impact crater size-frequency distribution line that marks the approximate saturation or equilibrium of craters on a surface. That is when each newly formed crater destroys one or several previously formed craters, and on average the line would remain about the same. The production function is a replica of the point not yet changed by planetary resurfacings and impact crater overlapping. The real frequency records may be different from the ideal production function due to surface processes working on the individual planetary bodies (Ivanov 2008a). The impact flux have changed through time, but the shape of the production function has not changed dramatically over the last 4 Ga (Neukum et al. 2001). This procedure transfers a crater-size frequency found through crater counting of a particular surface unit to a surface model age.

2.1.3. The terrestrial distribution

The Earth has been subjected approximately to the same bombardment flux by asteroids and comets as the Moon (Ivanov and Hartmann 2007). But there are only 176 proven impact structures on Earth (Earth Impact Database 2009) (Fig. 3). The term "impact structure", as opposed to "crater", is used to entitle the structures after the original impact crater shape has been modified and is thus the proper label for all terrestrial entities. New impact structures on Earth are constantly suggested and proposed. Several databases exist for impact structure recognition (e.g. Earth Impact Database 2009; Impact Database 2009) and they have different ways of registering (operating with different numbers). Regardless which database is applied, the number of terrestrial impact structures is very low compared to the Moon and Mars. The low number is mostly due to the active lithosphere, plate tectonics and geologic activity, i.e.

degradation over time (erosion, covering by later sediments). For example, the ocean floor is relative young (65 Ma on average, with a complete rejuvenation in ca. 200 Ma) and not many impact structures have accumulated there. The shielding effect of the atmosphere and sea water prevents numerous smaller craters. Additionally the late acceptance and research (including search) of impact craters on Earth (Koeberl 2004) has led to a too small number of recognized craters. The diameters of the proven impact structures vary from just a few meters up to 300 km (Vredefort, South Africa). Ages range from the oldest having an age of ~2.4 Ga (Suavjärvi, Russia) up to present day (Earth Impact Database 2009). Different levels of preservation, from "fresh" to buried or eroded, are found in the terrestrial record.

Despite the differences between Earth and other planetary bodies, there should still remain many undetected impact structures (e.g. Trefil and Raup 1990). The distribution of detected impact structures on Earth's surface is biased by the activity of impact research in a region and the accessibility of areas. For example, several Finnish impact structures were found during an active search in the nineties (e.g. Deutsch 1998).

Fig 3. Distribution of recognized impact structures on Earth. Edited from McCall (2009). New structures included according to Earth Impact Database (2009).

2.1.4. The Fennoscandian/Norwegian distribution

Scandinavia and the Baltic states holds about thirty confirmed impact structures (Abels et al. 2002; Dypvik et al. 2008) (Fig. 4), of these about twenty lay on the Fennoscandian shield. More structures have been proposed as impact structures in the last decades (e.g. Abels et al. 2002; Pesonen 1996). Fennoscandia is one of the most densely crater-populated terrains on Earth which might be due to its long existence as a continental shield, but also due to the level of research activity, coupled with a deterministic view of what to look for (Dypvik et al. 2008). The ages and diameters of the structures vary, but many are relatively small (<10 km) and mostly of Paleozoic age (Abels et al. 2002).

In Norway there are three proven impact structures. The Gardnos impact structure is 5 km in diameter, containing a roughly circular area of fractured and brecciated rocks. Zones of the original crater-floor and sequences of crater-fill breccias are present (French et al. 1997). The Mjølnir impact structure in the Barents Sea is 40 km in diameter, located in water depths of 350 - 400 m beneath a younger sedimentary strata of thickness 400 m (Dypvik et al. 1996). The Ritland impact structure in West Norway is a 2.5 km wide and 350 m deep circular depression, displaying crushed/fractured basement rocks and sedimentary, post impact breccias. Cambrian shales, sandstones and thrust nappes cover about one third of the interior (Riis et al. 2008). Both Gardnos (Kalleson et al. 2009) and Ritland (Riis et al. in press) are old (600 – 500 Ma) and eroded structures.

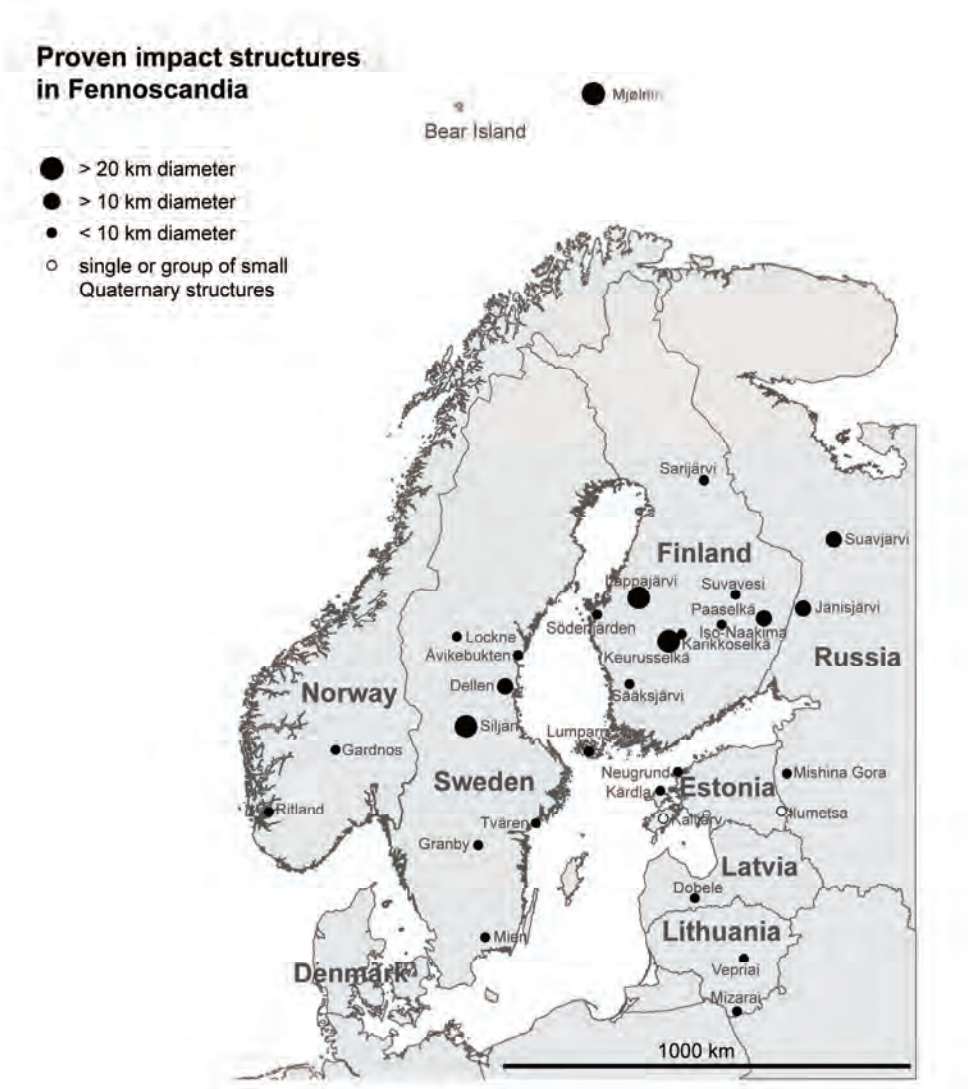

Fig. 4. A compilation of recognized impact structures in Fennoscandia (based on Abels et al. 2002; Dypvik et al. 2008; Henkel and Pesonen 1992). Notice the lack of structures discovered in the north. Courtesy Elin Kalleson.

2.1.5. Proofs of impact origin

The starting point in the search for new impact structures through automatic or semi-automatic candidate detection is the discovery suspicious patterns. The next step is field work and sampling of rocks from the suspected sites. To prove an impact origin of larger impact

structures (only diameters larger than 0.5 - 1 km was considered in the analyses) requires the detection of either shock metamorphic effects in minerals and rocks, and/or the presence of a meteoritic component in these rocks (e.g. French 1998, p. 99). Shock metamorphic effects are, for example, shatter cones on the macroscopic scale and planar deformation features (PDFs) in quartz at the microscopic scale. PDFs are created at extreme pressures in which the resulting characteristic microscopic pattern display many thin straight parallel lines close together, occurring as several sets with distinct orientations relative to the quartz crystal axis. The presence of extraterrestrial (meteoritic) components in impact target rocks, melt rocks, breccias or ejecta must be confirmed by geochemical analysis which search for traces of meteoritic material mixed in the rocks, typically deriving from the platinum group elements (e.g. iridium, osmium, platinium). These elements are more abundant in extraterrestrial rocks than on the surface of the Earth (Koeberl 2007).

2.2. Geomorphometry

Digital terrain analysis or geomorphometry is the science of the quantitative representation of topography and the quantitative description and measurements of landforms (Dehn et al. 2001; Pike 2002). It deals with the study of features connected to geometrical shapes, material, the morphological history and topography of landforms (Schmidt and Dikau 1999). Landforms may be considered as containing a structured form rather than chaotic due to the geologic history and the geomorphologic processes that have produced the present landform (Dehn et al. 2001). This implies a connection between the quantitative description and the landforming process. The terrain may be quantified based upon different perspectives (Pike 1995), in which distinctions are made between specific and general geomorphometry (Evans 1972). Specific geomorphometry consider discrete specific landform types or objects while general geomorphometry describes and analyze continuous surfaces. A geomorphometrical object is a clearly defined landform unit (Schmidt and Dikau 1999), e.g. a river channel, a catchment area, V-shaped valleys, glacial cirques (Evans 2009), sand dunes (Guth 2009), talus slopes, rock glaciers or, on most planetary surfaces, impact craters.

On planetary surfaces, craters are often a dominant landform (Lowman 1997). A geomorphometrical study of these features belongs in the category of specific geomorphometry which includes more common terrestrial landforms like valleys, slopes and peaks. However, impact structures are not that distinct on Earth and thus whether specific

geometry applies is up for discussion. Only a few of the terrestrial impact structures are preserved well enough to be distinguishable as a separate discrete landform; as is the case for Barringer crater (Meteor crater). Many of the terrestrial impact structures blend in with other geomorphological shapes.

The z value of a surface (x,y,z) is not restricted to altitude, but may consist of continuously varying attributes or regionalized variables (Burrough and McDonnell 1998) like temperature, annual precipitation, radiation, population density, pollutants in soil and geophysical fields values. In this thesis, various surfaces will be used in the search for impact structures. "Combining ideas from image analysis and geomorphometry can be a fruitful way of developing new parameters and gaining a better understanding of the information in the DEM" (Olaya 2009, p. 146). This is probably true for other surfaces as well, motivating the testing and developing of techniques on various spatial data types.

2.3. Remote sensing and geomorphometry in crater search

2.3.1. Planetary crater detection

When the aim is to detect craters on solid planetary bodies (except the Earth) the desired result is often impact crater counting (e.g. Plesko et al. 2006). The resulting diameter frequency reflects the local erosional history of the surface area, and can be used for age estimation. In such methods "a robust methodology should produce no false detections while detecting all the craters present in the image" (Bandeira et al. 2006). The template matching technique has been used as part of the detection process (e.g. Bandeira et al. 2007; Barata et al. 2004), but often the circular Hough transform is introduced as one of the detection steps. Kim et al. (2005) presents a stepwise algorithm (including a thinning step) and exemplifies it on data from the Mars Orbiter Camera (MOC), Mars Orbiter Laser Altimeter (MOLA) and High Resolution Stereo Camera (HRSC), resulting in relatively good detection quality. Using MOLA digital elevation models, Bue and Stepinski (2007) describes an algorithm applied to topographic data of 500 m resolution. Their comparison between image and DEM crater detection ultimately favored DEMs due to their increasing accessibility and resolution. Their algorithm detected edges using the profile curvature, then divide the DEM into smaller fragments using a "flood" technique in order to perform a morphological closing and thinning

of each fragment where then a circular Hough transform can be applied to detect candidates. After, a confirmation algorithm is applied based on a set of criteria to detect or reject the candidates. Sawabe et al. (2006) presented a multiple approach that consist of four detection algorithms (including a fuzzy Hough transform) combined into one lunar crater detection algorithm, and reported to detect craters of all sizes and shapes. Both the Hough transform and template matching were used by Kim et al. (2004), in which the algorithm first detects crater edges in optical images and DEMs, then locates optimal ellipses using a Hough transform, before finally applying the template matching technique to verify detections. Mathematical morphology techniques have been used in planetary crater detection approaches by e.g. Urbach (2007). In that case a pre-processing step detected bright and dark (shadow) parts of craters in an image and decided if two parts belonged to the same crater based on different criteria. For a comprehensive list of crater detection algorithms (CDAs) see Salamuniccar and Loncaric (2008).

2.3.2. Terrestrial crater detection

The major difference between planetary and terrestrial impact crater detection is the low number of known impact structures on Earth (176), i.e. the absence of a large test data set. The proven impact structures are distributed over a large time span, found in different rocks, and they exhibit a large degree of variation, making the automatic detection of potential impact structures challenging. The structures are too few and varied to make a proper classification scheme, but can be used to investigate what kind of signs we are looking for in automatic detection routines. An advantage on Earth is the opportunity to conduct field work on impact structures in order to determine the details of their shape, geology and formation. Search strategies may be based on the following: Morphology (e.g. circular outline, rim structure, central structure), geophysical anomalies (e.g. gravity, magnetic, seismic) and geology, mineralogy and geochemistry (e.g. brecciation, shock metamorphism, traces of meteoritic material).

Remote sensing of impact structures on Earth has mostly been to study single, already proven or suspicious impact structures. For example, Zumsprekel and Bischoff (2005) analysed Landsat Enhanced Thematic Mapper (Landsat ETM), DEM, European Remote Sensing satellite (ERS) radar, radiometric (gamma ray) and airborne magnetic data to investigate the Strangway impact structure in Australia. Reimold et al. (2006) enhanced features in Landsat Thematic Mapper (Lansdat TM) and Shuttle Radar Topography Mission

(SRTM) data, while Almeida-Filho et al. (2005) enhanced features using Advanced Spaceborne Thermal Emission and Reflection Radiometer (ASTER) and a DEM to investigate the Serra da Cangalha impact structure in Brazil. Garvin et al. (1992) describe remote sensing characteristics of the impact structures Barringer, Bosumtwi and Zhamanshin. Radar images work well in aeolian terrains where the long wavelengths can penetrate deeper revealing structures in sandy places (McHone et al. 2002). A lithological supervised classification from field collected spectral measurements was conducted for the Gosses Bluff impact structure and environments by Prinz (1996), implying that information can be gained by such methods. Volcanic structures (calderas) display similarities in morphology to impact structures and approaches applied there may be transferred to impact studies, e.g. Kouli and Seymour (2006) investigated Landsat, DEM and SPOT images for radial faults, and Szèkely and Karàtson (2004) describe techniques applied to DEMs to enhance radial ridge patterns of degraded volcanic landforms.

Detection of new impact structures through remote sensing or image analysis techniques have mostly been by visual analysis of data (e.g. Di Achille 2005), sometimes integrating several datasets within a Geographic Information System (GIS) software (e.g. Abels et al. 1997a). Before visual inspection, various image enhancement techniques are commonly applied to highlight contrast, linear or circular features. Araujo et al. (2001) presented an automatic processing chain to identify circular forms, impact and volcano craters in satellite remote sensing images (Landsat 5). The methodology consisted of several steps including pre-processing techniques to capture edge pixels and the Hough transform. A circular feature was detected, but the study only showed results for a small region. Though the circular Hough transform is the most frequently used, another algorithm called “the radial consistency algorithm” (calculates symmetry) has been applied in a few detection approaches. Earl et al. (2005) presented this technique together with a prototype tool, the Impact Crater Discovery (ICDY) tool (Chicarro et al. 2009), that incorporates the algorithm. Results were shown from applying and combining SAR, Landsat and Shuttle Radar Topographic Mission (SRTM) data for the Brent crater in Canada. The tool is applied in this thesis. Bruzzone et al. (2004) presented the same algorithm with results from several impact structures, though not over larger regions.

A regional approach searching new impact structures was performed in Canada in the 1950s and 1960s. The approach evolved from the fact that even though there was high human activity in and around the Brent crater, it remained undiscovered until detected on aerial photographs. This led to a systematic study of aerial photographs, hoping that other craters

might be found in that way. The study, starting out with the Canadian Shield as the area of search, revealed several craters or crater-like objects, and some of these structures were later proved to have an impact origin (Beals et al. 1956a; Beals et al. 1956b).

The best performance regarding impact structure search by remote sensing or image analysis is to detect candidates, the most promising structures for further field studies (Koeberl 2004). Remote sensing methods can tell us where to look, but proof must later come from sampled rocks.

2.4. Relevant datasets

Combining several types of relevant data increase the amount of information and may improve the analysis. The succeeding sections describe different datasets that apply to impact search studies.

2.4.1. Digital elevation models (DEM)

Digital elevation models (DEM) represent the surface and hence the topography/morphology of an area. The elevation models may consist of contour lines (lines of equal elevation) or TINs (set of adjacent, non-overlapping triangles with x, y coordinates and z vertical elevations for their vertices), but the most common representation for analysis is the raster data model. The raster model is a set of regularly spaced points/cells (altitude matrix), made from elevation points interpolated to a continuous pixilated surface. The elevation points may come from field measurements, digitized contours from aerial or satellite photogrammetry, interferometry of radar data, or laser altimetry.

Elevation models have been used to investigate morphology and geometry of craters; for example the size and relations of rim height, central peak height, crater depth and crater diameter (e.g. Pike 1977b). Digital elevation data "provide a good means to investigate crater morphology" and various structural elements (Reimold et al. 2006). It is possible to extract profiles across a structure, usually exaggerating the elevation axis to visually enhance features and possibly to separate the different parts of the structure. Shaded relief models, also based upon DEMs, can be used for visual interpretation. Erosion and depositions covering the craters make elevation models less appropriate for Earth impact structure search studies. However, one reason to still apply DEMs is due to possible differential erosion of rocks, e.g.

the Gardnos and Ritland impact structures have both been covered by kilometres of sediments and thrust nappes through geological time, and then eroded so the structures became re-exposed. Their partly circular appearance could reflect the shape of the underlying bedrock or the preferential erosion of weaker crater infill rocks. An old impact event may consequently still influence present landforms.

2.4.2. Geophysical data

Geophysical surveys measure "the variation of some physical quantity, with respect either to position or to time" (Kearey et al. 2002, p. 8). Our goal is to search local anomalies that may be caused by visually concealed geologic features, e.g. resulting from an impact. Target areas that has been subject to impact and related processes (explosion, excavation, etc.), will differ from their surrounding. The resulting changes in the geophysical properties can be described as impact related geophysical signatures. Gravity and aeromagnetic data often display such signatures. These signatures can be used to search undiscovered impact structures. The shape and size of the Chicxulub impact structure was revealed by circular features in gravity and magnetic fields in which drill cores provided the proof (Hildebrand et al. 1991). The erosional effects on geophysical anomalies could lead to a spatial offset compared to the morphological feature (e.g. Hawke 2003). Still circularity often closely coincides with the structural boundaries (French 1998).

Electric resistivity data (e.g. Henkel 1992) and seismic data (e.g. French 1998) may also display impact characteristic patterns. Some main reviews of impact structures and geophysical signatures are found in Grieve and Pilkington (1996), Pilkington and Grieve (1992), Henkel (1992) and Pesonen (1996).

Gravity signatures

A gravity low is commonly associated with impact structures (Fig. 5). Such negative density anomalies are typically circular (Henkel 1992; Pilkington and Grieve 1992), e.g. the Wanapitei impact structure has a circular Bouguer gravity low (L'Heureux et al. 2005). Fracturing and brecciation of the target rocks creates space/porosity and consequently less dense material. In addition, low-density sedimentary infill will contribute to a gravity low (Grieve and Pilkington 1996). Even if fractured to large depths, a gravity signature may still be present in an eroded structure. However, the effect is smaller at deeper erosion levels and the impact effects on gravity distribution may be minor as compared to gravity differences

caused by the original lithological distribution in target area (Henkel 1992). In complex impact structures, an exposure of rocks uplifted from considerable depth contrasts with the surrounding (Koeberl 2007) and may lead to a positive anomaly at the central uplift (e.g. Pilkington and Grieve 1992). This uplift is often more resistant to erosion than the rest of the impact structure, and it may be the only remnant that can be identified in old eroded structures (Chicarro et al. 2009). Positive anomalies are thus also important in impact structure detection.

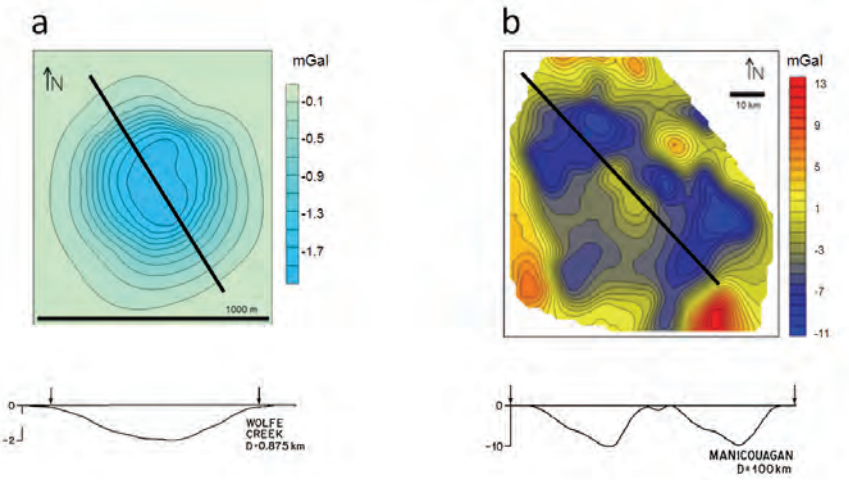

Fig. 5. Bouguer residual gravity anomaly maps and profiles. (a) The simple Wolfe Creek impact structure. (b) The complex Manicouagan impact structure. Residual gravity anomaly profiles are scaled to crater diameter and maximum gravity anomaly value. Arrows indicate crater rim (Pilkington and Grieve 1992). Black lines in maps correspond to possible position of profiles. (Map credits: www.impact-structures.com).

Magnetic signatures

There is a lack of consistency between magnetic signatures and impact structures. The magnetic character may contain large variations with both positive and negative anomalies occurring, where circularity also may be present (French 1998; Pilkington and Grieve 1992). The Manicouagan impact structure (Canada) has a relatively subdued positive circular magnetic anomaly over the central uplift (Cowan and Cooper 2005) while the Acraman impact structure in South Australia exhibits a circular magnetic low (Williams et al. 1996); the most common impact generated magnetic signature. This may be caused by reduction in susceptibility from contributions of fractured target rocks, brecciation and alteration (Grieve

and Pilkington 1996; Pilkington and Grieve 1992), and post-impact nonmagnetic sedimentary infill (Grieve and Pilkington 1996; Scott et al. 1997). A central magnetic anomaly could in some cases be the result of mafic basement rocks uplifted to the surface and shock re-magnetised by the impact (Pilkington and Grieve 1992). Large impact structures may have magnetic contributions from a combination of regional magnetic trends disrupted by shock and/or thermal demagnetization and high amplitude, short wavelength magnetic anomalies primarily produced by natural remanent magnetization of impact melt rocks, breccias and rocks below the crater floor. The latter is related to thermal alteration (Ugalde et al. 2005). Short-wavelength, intense magnetic anomalies have been described by both Hawke (2003) and Hildebrand et al. (1991). Hawke (2003) show that a short wavelength circular anomaly coincide with the position of the Wolfe Creek crater and correlates with the crater rim and present day inner walls. The magnetic response was slightly offset to the north due to the dipolar nature of the magnetic field. The discovery of high magnitude, but small in size, magnetic anomalies should lead to further attention, especially if other data display impact related features close to the same locality.

The inverse problem in geophysics

In geophysics, a circular anomaly may be the result of several processes. Impact structures may be represented by circular anomalies, but circular anomalies do not necessarily represent impact structures as "any given anomaly could be caused by an infinite number of possible sources" (Kearey et al. 2002, p. 139). This "non-uniqueness in the conclusions that can be drawn" (Kearey et al. 2002, p. 6) is the geophysical inverse problem. In Finnmark, circular anomalies may come from hinges, faults, fractures, domes, basin folds, dykes, large intrusive bodies, etc. One approach to reduce this problem is to analyse various data types to determine if the circular feature is located at or near impact supporting features in several datasets, thereby reducing the ambiguity.

2.4.3. Multispectral images and images

Multispectral and panchromatic images derive from passive sensor systems (e.g. satellites) that capture the reflected solar radiation of the surface. When the reflectance is measured in different wavelengths (spectral bands), the result is a multispectral image. Unlike digital elevation models and geophysical field models, image conditions like cloud coverage and illumination are crucial components that must be considered. When detecting craters on

planetary surfaces it is common to use panchromatic images; i.e. images that capture the reflectance over the entire visible spectrum (ordinary images). There is a huge library of digital image processing and analysis techniques available for such images. Crater detection and measurements in images are limited by the signal to noise ratio, the optical point-spread function, illumination geometry, target background roughness and (crater) shape deviation from a simple circle or ellipse (Ivanov et al. 2008).

There is no specific multispectral signature that can distinguish all impact structures from their surroundings, like the Landsat Thematic Mapper (TM) band ratio TM3/TM5 for glacier enhancement or the Normalized Difference Vegetation Index (NDVI) for vegetation enhancement. This is because impacts structures are both created and found in different environments, such as crystalline rocks, sedimentary successions, in the ocean, on land, in deserts and in highly vegetated regions, etc.

2.4.4. Radar images

Radar images are not explored in the present papers. A radar image is the result of an active imaging radar system, capturing backscatter of surface material in the microwave spectrum. Synthetic Aperture Radar (SAR) images may, in particular, prove useful for crater detection because of the higher resolution than ordinary radar images due to the system configuration acting as an aperture antenna; e.g. Envisat Advanced Synthetic Aperture Radar (ASAR) of 150 m or 30 m spatial resolution. Chicarro et al. (2003) presents several terrestrial impact structures and their SAR images, while McHone et al. (2002) display radar results of ten impact structures. Radar images would probably be difficult to use in techniques requiring edge detection due to the speckle effect, but filters may minimize this effect (e.g. Lee, Frost, Gamma, Kuan, Local Sigma and enhanced versions of the mentioned). The filters preserve image sharpness and suppress the noise. SAR images of different polarization and captured at various times (temporal) may detect differences in dielectric properties through the year. Some of these differences may be triggered by impact related structures.

2.4.5. Drainage patterns

Drainage patterns often reflect the underlying rocks and structures. Mihàlyi et al. (2008) provide an overview of drainage patterns of four complex impact structures, concluding that they have characteristic patterns despite being later modified. The recognition of these

features can be an important first step of discovering new sites. Reimold et al. (2006) studied the drainage pattern at the Serra da Cangalha impact crater in Brazil. They found the structure to be characterized by a strong concentric drainage pattern extending outwards from the crater rim. L´Heureux et al. (2005) mention that the circular shape of Lake Wanapitei was a first clue towards indication of an impact origin. Dence and Popelar (1972) used the drainage pattern of the lake to support the presence of an impact structure, describing a concentric pattern of streams and smaller lakes within 5 km of the Wanapitei impact crater. The use of lake data can be to detect circular lakes or circular combinations of lakes, while network data can be used to determine if a local drainage pattern is distincly different from the larger regional pattern.

2.4.6. Fracture patterns

Radial or concentric patterns of fractures, faults, folds and transpression ridges are often connected with impact structures (Kenkmann 2002; Kenkmann and Dalwigk 2000). Such features may indicate a potential impact structure if the local pattern varies from the regional pattern. L´Heureux et al. (2005) mention that concentric joint and fracture patterns peripheral to the lake were observed early in the study of the Wanapitei impact structure. Kenkmann et al. (2005) report that radial folds and concentric stacking of imbricated thrust slices are among the prominent deformation features in Upheaval Dome impact crater, Utah. Data of fractures and faults may be accessible as geodata files (e.g. lineaments), or found using satellite images, e.g. Gabrielsen and Ramberg (1979) found circular features in Landsat images during a lineament study of Norway.

2.4.7. Other datasets

Data of lithology distributions is already classified, but a detection of circular features may explain detections in other data, or shed light on a feature. Geochemical distribution data, if available as raster data models, can be used in the same way as the lithologic data. Bathymetry data can, and have been used to detect circular depressions (Webb et al. 2009). The Smith and Sandwell (1997) global digital bathymetric map of the oceans (horizontal resolution of 1 to 12 km) represents a possibility for global ocean floor analyses. The geographic information software, Google Earth, and the web mapping service, Google Maps,

can also be used to detect suspicious circular structures. The ICDY tool has the potential to operate on such data whenever a reasonable method to include it in the software is developed.

2.4.8. Pre-processing of data

Several possibilities exist to enhance data prior to use in automatic procedures. Conventional data processing techniques are image transformations (e.g. principal component analysis, RGB to HIS, NDVI, contrast stretching), band rationing and noise removal (e.g. by median or mean filters). A classification of remotely-sensed multispectral images may be performed to detect common textures through a supervised or unsupervised classification. This can either be for geological mapping or the enhancement of lithologic boundaries. Data can also be resampled to fit other data in an analysis or to fit the analytical scale of the analysis, e.g. detection of large features do not need a high resolution.

Among the pre-processing techniques, separation of the different wavelengths (deconvolution) in the models may prove useful (Cowan and Cooper 2005). The geophysical potential fields can be considered the sum of features operating at different frequencies. The separation of such frequencies is possible, performing filter operations in the frequency domain. Short or long frequency anomaly enhancements are commonly performed by deconvolving a model into regional-residual and local-residual models. A discrete Fourier transform, computed using the Fast Fourier transform (FFT) algorithm, converts the models into the frequency domain. Convolving with Butterworth designed high- and low-pass filters, focusing only on the magnitude of the frequency response of the gravity and aeromagnetic intensity data, will emphasize small or large scale features, respectively sharpening or smoothing the model. The latter may be rewarding regarding large scale impact structures because a low-pass filter reduces small “spikes”, noise and “spurious” effects. The opposite may also be rewarding, removing regional wavelengths, trends larger than the features of interest. Uncertainties comes in selecting filter parameters and “there are many considerations to be made in the way you select, and the manner in which frequency components are retained or excluded” (Nixon and Aguado 2002, p. 64).

3. Setting

Norway comprises the western part of the Scandinavian Peninsula. The bedrock geology of Norway is dominated by Precambrian basement rocks and Caledonian successions (e.g. metamorphic Cambro-Silurian sediments stacked in nappe units). Limited areas of Devonian to Permian sediments and volcanics are also present. The larger part of the bedrock is, however, covered by various Quaternary formations of mainly marine, glacial and fluvial origin. Geomorphologically, the present topography of Norway is governed by peneplanation and stripping of marine strata during the Mesozoic (Lidmar-Bergstrøm et al. 2000; Peulvast 1985), the Tertiary uplift (Gjessing 1967; Strøm 1948) and related fluvial-dominated landscape formation in a warmer and partly drier climate than today (Gjessing 1967; Lidmar-Bergstrøm et al. 2000; Strøm 1948), followed by numerous Quaternary glaciations (Kleman and Borgström 1994). The latter accentuated the Tertiary fluvial valley pattern, while areas in central and northern mountainous areas underwent little or no erosion due to the thermal conditions of the ice sheets (Lidmar-Bergstrøm et al. 2000; Sollid and Sørbel 1994).

The search area of this thesis is located in Finnmark county (specifically Finnmarksvidda), Northern Norway (Fig. 6). The search area is situated on a plateau (Finnmarksvidda) 300 – 500 m a.s.l. and has a relative low relief, except for the large river valleys. The Finnmark geology is dominated by large areas of eroded Precambrian bedrock. It is composed of Archaean gneiss complexes acting as basement for early Proterozoic greenstone belts (supracrustal sequences), partially covered by Caledonian formations (Olesen and Sandstad 1993). The landscape is covered by thick and widespread Quaternary glacial deposits, making it difficult to locate outcrops over large areas. Interpretation of regional geophysical data has therefore been crucial for the geological understanding of the area (e.g. Midtun 1988; Olesen et al. 1992; Olesen and Sandstad 1993; Sindre et al. 1983). It is thus an area of fairly good gravity and aeromagnetic coverage.

The search area is part of the Fennoscandian Precambrian Shield, displaying a very long geological history (Henkel and Pesonen 1992). The Precambrian gneisses and meta-sediments are normally hard and have good preservation potential, with descent chances of displaying impact structures. However, in a non-sedimentary setting such as the crystalline rocks of the Canadian Shield, the identification of impact structures is difficult because of the

lack of prominent marker horizons in geophysical datasets, often reducing diagnostic approaches to analysis of potential field data (L'Heureux et al. 2005). Crystalline target rocks may in addition be too poorly stratified for a significant contrast between uplifted rocks (central peak) and the surrounding, often not sufficient to provide remote sensing signatures based upon differences in spectral properties or erosional resistance (Abels et al. 2000).

The Caledonian orogeny may have altered possible earlier structures and the last glaciations in Scandinavia likely both eroded and covered possible pre-Quaternary impact structures. Earlier geological researches on Finnmarksvidda have, in addition to general mapping, mostly been focused on studying locations for ore occurrences. These are commonly found along the border of the greenstone belts, which possibly resulted from rift developments (Olesen and Sandstad 1993). As of today, Finnmark area has no proven impact structures. It does, however, belong to a part of the Fennoscandian shield which holds several proven impact structures. Finland has, in particular, had a very high success rate in detecting possible impact structures through the use of detailed geophysical surveys.

Finnmark is a promising place to search for undiscovered impact structures because it is an area of old bedrocks (long exposed) with high competence, large areal extent and good data availability (including DEMs, gravity and aeromagnetic potential field data). The possibility of success in Northern Norway may therefore be promising.

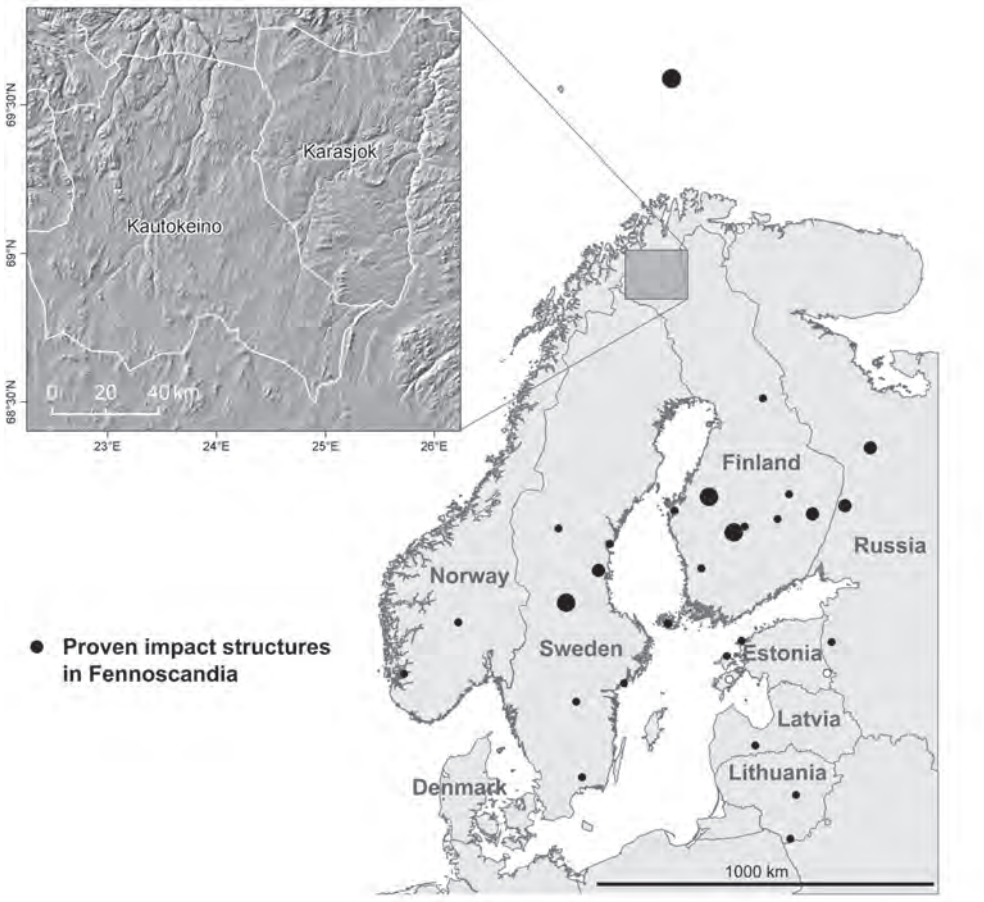

Fig. 6. Recognized impact structures in Fennoscandia (see Fig. 4 for names). Grey square marks location of search area. The search area is part of Finnmark county, covering the municipalities of Kautokeino and Karasjok (white borders on inset map). To get an impression of the topography, the search area is displayed as a shaded relief map.

On Earth, the number of impact structures found is a combination between the production rate and the erosion rate. Is it statistically reasonable to find any impact structures in our search area, and what would the expected number of impact structures be? Such questions need to address the age and areal extent of the area, together with impact flux, distribution (if a random process), degradation (erosion, obliteration) and the size of impact structures. A rough estimate of the exposed age of the search area is 2.1 Ga. The Precambrian bedrock with an approximately mean age of 2.4 Ga, has a complex history and has been covered by a total

cover duration of about 300 Ma (e.g. by Caledonian nappe units). The search area covers ca. 25.000 km^2.

Two approaches have been conducted to determine the number of expected structures in the search area. The first is based on Ivanov (2008b, p. 109), who present a table of the cumulative number of impacts for the Earth's continents (Fig. 7). If the line of 1 Ga is used, to be conservative, the number of craters with diameter larger than 2 km on the surface of the Earth should be 100.000. The Earth's total surface is ca. 510.072.000 km^2. This results in an estimate of ca. 5 impact structures for the search area in Finnmarksvidda.

A "production function may be used to interpolate crater counts obtained on surfaces of various ages" (Ivanov 2008a). The techniques of crater chronologies and production functions are not directly applicable to Earth because the terrestrial record is not extensive enough. Despite this, the second method use the software "Craterstats" (Michael and Neukum 2007) to estimate the number of expected structures based on the already known distribution of Fennoscandian impact structures. Craterstats apply the methodology of the production function fit combined with the application of a chronology model. From the size of the Fennoscandian surface unit (ca. 1.411.911 km^2) and the record of proven impact structures (17), the crater-size frequency distribution and the surface unit modeled age are calculated within the software. A crater production function for the Moon and a chronology function for Earth, both Neukum (1983), were used to estimate an age. The resulting age was 707 +- 250 Ma (Fig. 8), an underestimate indicating the lack of impact structures in the area compared to other planetary surfaces. Insetting a 2.1 Ga chronology function display that a bit more than 10^{-4} craters larger than 2 km per km^2 should be present, that is ca. 3 craters for the study area.

The approaches are highly approximate and erosion has not been accounted for. The overall picture is that not many impact structures can be expected in our search area, though a couple might be reasonable based on the above.

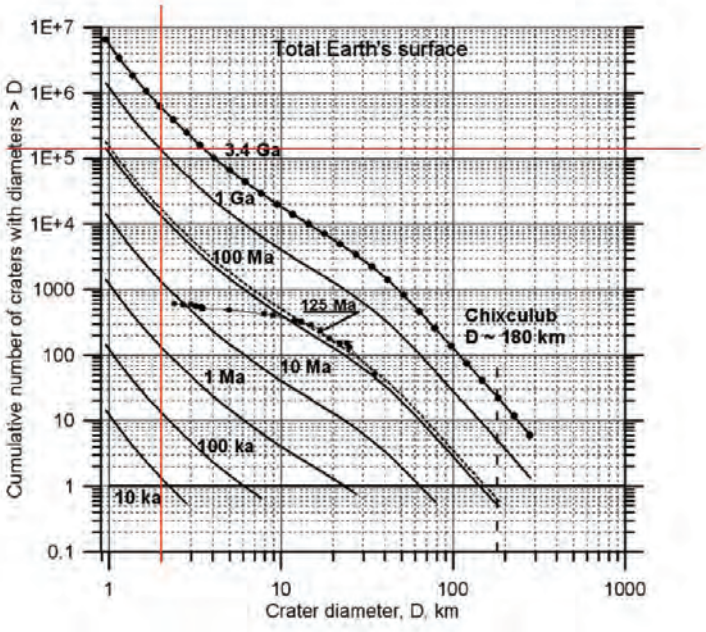

Fig. 7. Cumulative number of craters for the whole Earth surface (Ivanov 2008b, p 109). Red vertical line denote the intersect between impact diameter larger than 2 km for a surface of 1 Ga. Red horizontal line intersect with the cumulative number of craters (larger than 2 km in diameter), given 1 Ga.

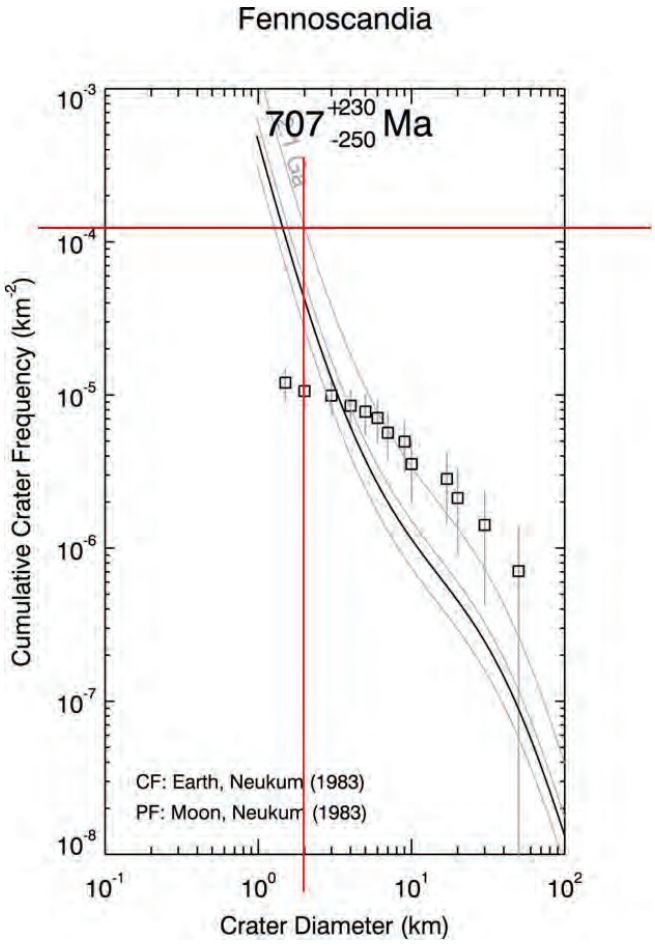

Fig. 8. The software "Craterstats" (Michael and Neukum 2007) was applied on the 17 proven impact structures in Fennoscandia in order to estimate an age of the region based on the impact crater distribution. The crater production function parameters of "Moon, Neukum 1983" and the chronology function parameters of "Earth, Neukum 1983" were used in the analysis. The chronology function is an equation of the form $N(1) = A(e^{Bt} - 1) + Ct$, where A, B, C are constants; 4.15E-14, 6.93E0 and 6.39E-4 for "Earth, Neukum 1983", respectively. "Moon, Neukum 1983" includes the coefficients of a twelfth-order polynomial that describes the production function (Neukum 1983). (Craterstats: http://hrscview.fu-berlin.de/craterstats.html).

4. Data

Two DEMs from the Norwegian Mapping Authority are used in the analysis, one with 25 m spatial resolution and another with 100 m spatial resolution. The Geological Survey of Norway (NGU) provided access to regional gravity and aeromagnetic data (e.g. Olesen and Sandstad 1993). The gravity data has a spatial resolution of 1500 m, while the two aeromagnetic datasets have spatial resolutions of 1000 m and 100 m. They are available as raster data models interpolated from ground stations (gravity) or flight measurements (aeromagnetic). In the detection algorithms, the data are treated as surfaces with intensity (z) values as mGal or nT. The gravity Bouguer values range from -51.23 mGal to -3.02 mGal, and the magnetic field values range from -1267.11 nT to 7093.42 nT. Bouguer corrected gravity anomalies have been reduced for variations in the Earth's gravitational field that do not result from the density differences of the underlying rocks (e.g. latitude, elevation and terrain) (Kearey et al. 2002). The International Geomagnetic Reference Field (IGRF) is used to remove a theoretical undisturbed Earth surface magnetic field from the aeromagnetic data (Kearey et al. 2002). This has been applied, but the aeromagnetic data have not been reduced to the pole (RTP) due to the high latitude of search area. Both gravity and aeromagnetic data are thus of a residual format since large regional fields are removed.

This study used multispectral images from the Landsat Enhanced Thematic Mapper Plus (ETM+) sensor, orthorectified by the Global Land Cover Facility (GLCF 2009). Data of lake distributions are available as vector data from the Norwegian Mapping Authority (N250 and N50 series), and vector data of lithology distributions (N250 series) are available from the Geological Survey of Norway (NGU). All vector data were converted to a raster data structure before analysis.

The data must be georeferenced and co-registered into consistent datum and reference coordinate systems in order to be combined (Fig. 9). In these analyses the datum for all the data are within the World Geodetic System from 1984 (WGS84) in a Universal Transverse Mercator (UTM) projection and coordinate system (Zones 32N, 33N, 34N and 35N).

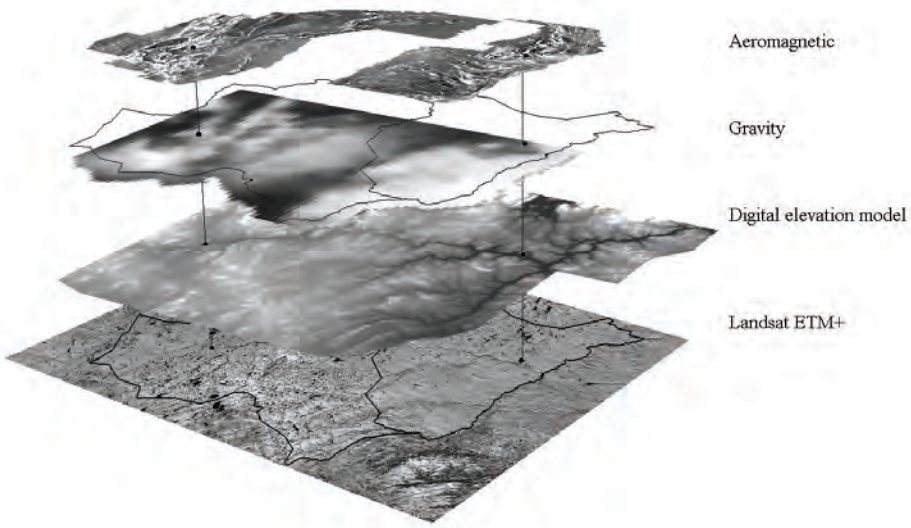

Fig. 9. Various datasets are used in the analyses to improve detection (see Fig. 6 for location and scale). From below; Landsat satellite image (ETM+), digital elevation model, gravity and aeromagnetic data. The municipalities of Kautokeino and Karasjok are displayed with black borders, and the vertical lines pass through the villages Kautokeino (left) and Karasjok (right).

5. Methods

In a first attempt to detect potential impact structures (Dypvik et al. 2006) we explored the simple idea; are there places that look like an impact crater in Norway? This was evaluated through a template matching technique performed on DEMs (*Paper I*). The circular Hough transform technique was tested on aeromagnetic data (section 5.2.2) and a shaded relief model (*Peer reviewed extended abstract I*), but the technique was ineffective for terrestrial data due to the edge detection step that makes it difficult to extract both subtle and strong anomalies. *Paper II* describes the circular outline algorithm applied to DEMs and geophysical data, an algorithm that searches for circular rims independent of the strength of the anomalies. *Paper III* evolved from the possibility to include multispectral images and to apply an already developed tool, the Impact Crater Discovery (ICDY) tool. An example of a filter technique that can be used to reduce the number of detected features from analysis on DEMs and potential field data is presented in *Peer reviewed extended abstract II*. The methodology sketch then consist of different techniques applied to a variety of datasets (Table 1), combination of results (data fusion) and possible post-processing steps, before conduction of field analysis (Fig. 10).

Table 1. Overview of technique and data combinations presented. The template matching technique may apply geophysical data, but it is not straight forward to make proper templates. Converted vector to raster data may be bedrock, lake, drainage patterns and lineament data.

Techniques \ Data	Digital elevation models (DEM)	Geophysical potential field data	Remotely-sensed images	Converted vector data
Template matching	Paper I			
Circular Hough transform	Ext.abs. I	Ext.abs. I		
Circular outline algorithm	Paper II	Paper II		
ICDY	Paper III	Paper III	Paper III	Paper III

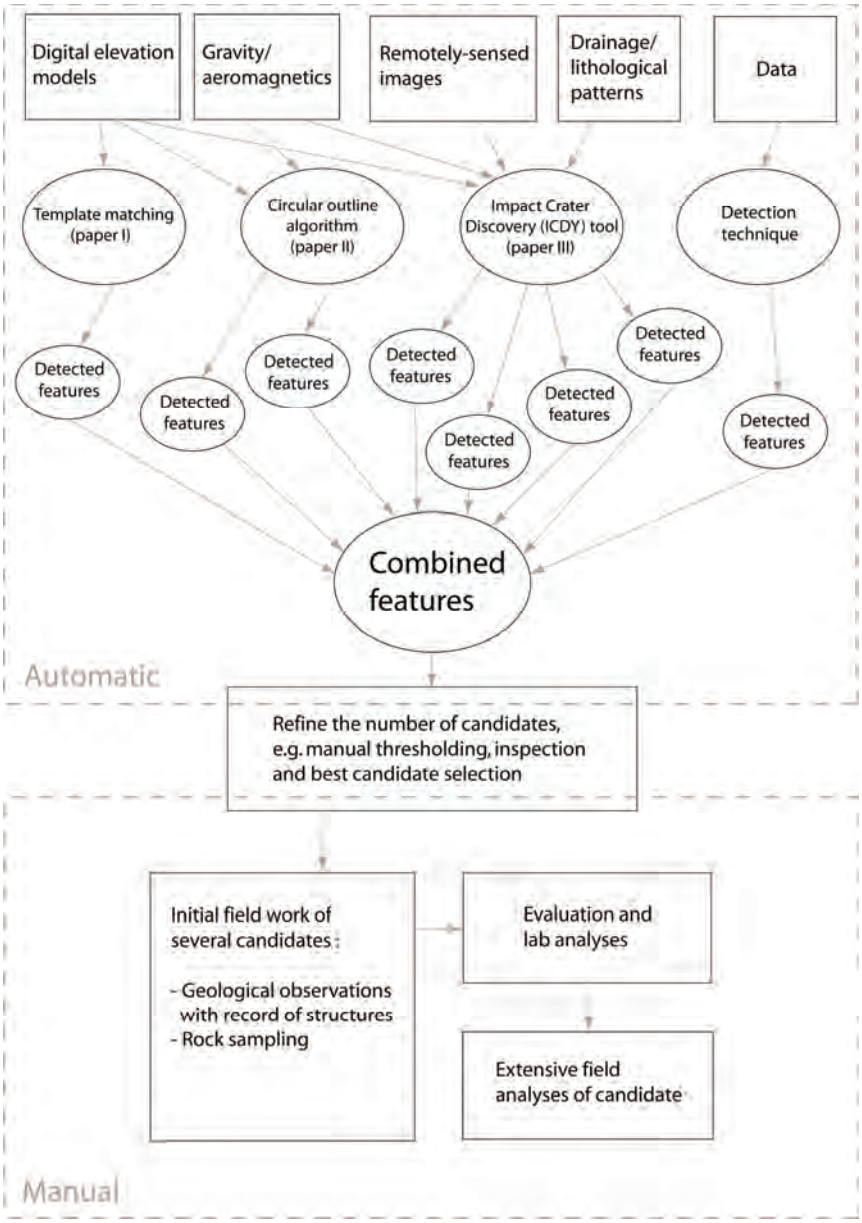

Fig. 10. Methodological sketch of the search for new impact structures. The automatic and manual parts are connected. A terrestrial impact structure can not be proven without field work, and in the presented search model the sites to visit in field are based on automatic detections. The flow chart emphasize that several data types and techniques should be used to get the most out of the automatic procedures.

5.1. Detection characteristics

Detection of spatial objects requires defining feature characteristics or feature descriptors that describes the object. This is often the essential object features without details, however, the number of false detections usually increase with simplicity of the description. Impact crater formation typically results in circular shaped craters, except when impacts occur from low angles (< 10˚). The circularity is found both in morphology (Fig. 11) and in the distribution of impact rocks (e.g. breccias) for all crater sizes. Other features related to impact structures could also be connected to circularity, e.g. "the circular shape of lake Wanatapei was one of the first and most obvious clues indicating its origin" (L'Heureux et al. 2005). Numerical simulations display circular impact features, and shows that oblique impacts in water (e.g. 45 degrees) starts as asymmetrical (elliptical) though ends up as a symmetric (circular) feature after a short time (e.g. Gisler et al. 2003). Geophysical signatures also display circularity which may be found even if the structure is less apparent morphologically, or even eroded.

The choice of detection descriptor or classifier is a tradeoff between being either too specific or too generalized. The analytical choice for terrestrial impact structure search is to use a simple characteristic, the circular shape. Too specific characteristics will lead to no feature detections at all. The original circular appearance of impact structures on Earth has been through many processes and, in addition to possible deviation from a circle, maybe just a part of the circularity is still present. The applied search methods should find the structures even if the circularity is only covering half the structure or found in broken forms.

The analyses is here operating on a regional level, aiming at relative large-scale structures. Of the 176 proven terrestrial impact structures, 160 have a diameter of 40 km or less (Earth Impact Database 2009). In order to keep the resulting amount of data on a practicable level and to detect reasonable sized structures to visit in the field, the search interval diameters are set from 500 m to 40 km or from 1 km to 40 km in the present analyses depending on algorithms and geospatial data resolutions.

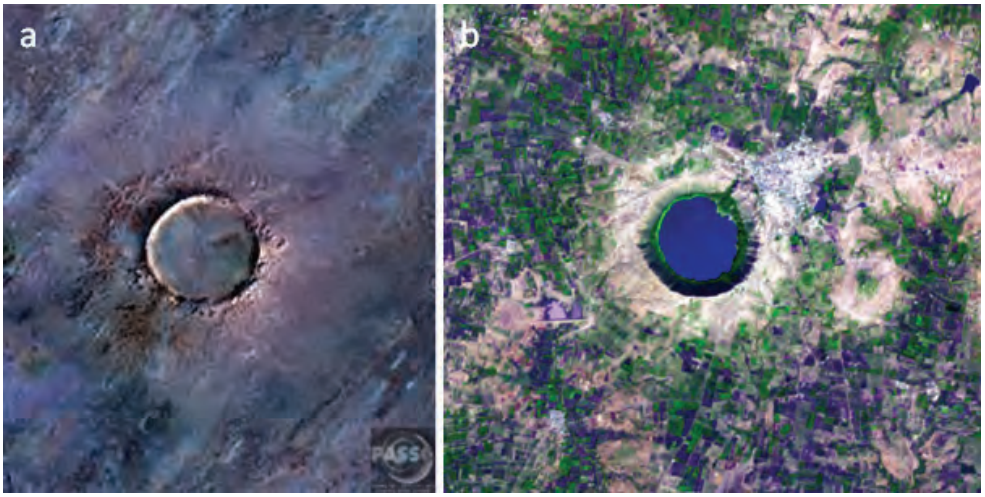

Fig. 11. Two almost perfect circular terrestrial impact structures. (a) Tenoumer impact structure (Mauritania), 1.9 km in diameter, ca. 0.0214 Ma. Landsat Thematic Mapper image. Credit: Earth Impact Database (2009). (b) Lonar impact structure (India), 1.83 km in diameter, ca. 0.052 Ma. Advanced Spaceborne Thermal Emission and Reflection Radiometer (ASTER) image. Credit: NASA.

5.2. Techniques/algorithms

A visual inspection of data is here classified as a separate technique, where several of the data pre-processing techniques may be applied. It may prove useful to visually enhance or highlight structural information in data to possibly discover features not seen before. Such enhancements can involve making colour images, shaded relief images, high/low pass filtering (sharpening or smoothing), first and second order surface derivatives (e.g. slope, curvature), horizontal profiles, image transformations (e.g. RGB to IHS, principal component analysis), colour composites and gradient images. Cooper (2005) demonstrated a method analysing aeromagnetic and gravity datasets from South Africa based on a visibility algorithm, where a calculation of viewshed enhanced details. Usually, multiple techniques or combinations of techniques are required to enhance the desired features.

There is a difference between enhancing features (e.g. edge enhancement) and extracting features (e.g. circular structures). We seek techniques that automatically extract impact structure candidates. These techniques should strive to be scale independent, operational for both 1 m and 1000 m spatial resolution models. With spatial data, x and y

coordinates represent the location of an intensity value z (e.g. height or gravity) or a binary value (e.g. a lake or not a lake). The presented techniques evaluate if these values are arranged (x,y,z) in a circular way, interesting for impact structure search.

5.2.1. Template matching

The template matching technique and results are presented in *Paper I* (Krøgli et al. 2007b). Template matching involves correlating a template and an image over a moving window, resulting in an image of correlation values or similarity (matches). *Paper I* used template matching to locate crater shape similarities in the topography (DEMs), followed by an approach to reduce the number of localities. Template matching has also been used in locating kimberlite pipes. Keating (1995) compute first-order regressions over a moving window between a typical magnetic kimberlite anomaly and regional aeromagnetic data. In the same manner, Keating and Sailhac (2004) calculate correlations between the analytical signal of a magnetic field and typical kimberlite target anomalies. A similar approach for gravity signatures and impact structures is possible, but it is difficult to make proper templates. In archaeology, detection of circular features (possible cultural remains) are attempted using DEMs, template matching, and Hough techniques (Risbøl et al. 2007; Risbøl et al. 2008).

Matching techniques have been incorporated in several planetary detection algorithms (Bandeira et al. 2007; Kim and Muller 2003; Michael 2003). Bandeira et al. (2007) describes a method using template matching of binary images, where rims are extracted first within a candidate selection phase. Their binary templates (not greyscale as in *Paper I*) consist of a circular white crown (rim) on a black square background in which several radii are defined by different templates. This leads to a probability volume where regional maximums are found using morphological operators. The approach reported to have good quality results. On solid planetary bodies, the craters are often uniform, while on Earth, the topography is more varied thus low correlation coefficient thresholds must be set to produce any matches (there are few places that actually looks like the templates). This will often result in the findings of too many structures. The Gardnos impact structure shape of a hanging valley was found by the template matching technique (Fig. 12), however, there are hundreds of additional structures with comparable correlations in Norway.

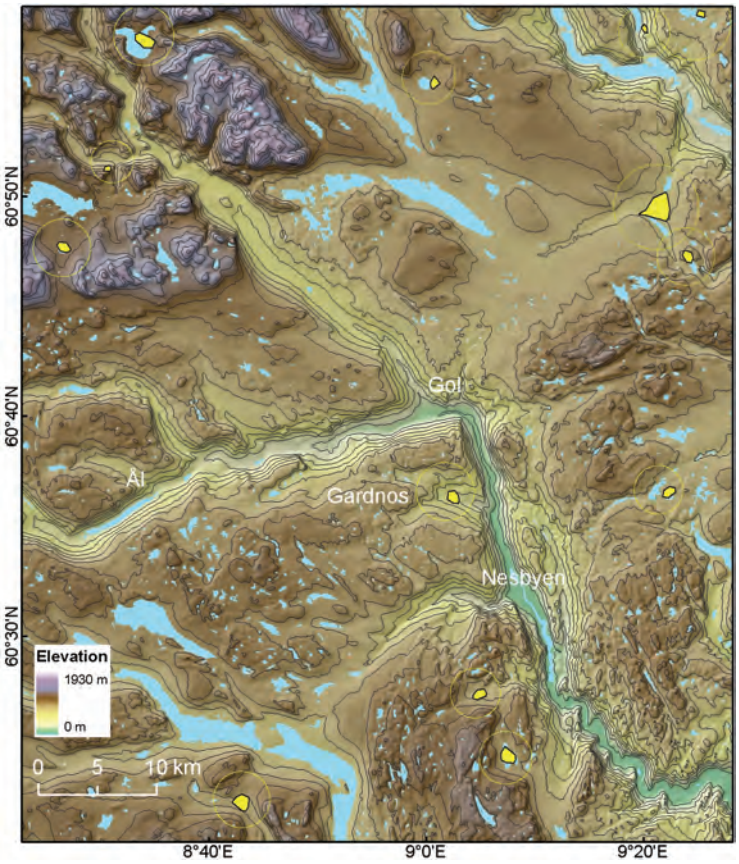

Fig. 12. The template matching technique detects the Gardnos impact structure using a crater model of 5 km diameter. At the same time hundreds of other ca. 5 km in diameter features are detected in Norway. This is a high number, but the detected depressions can be used in later analysis for comparison. Yellow circles mark the approximate borders of the high correlated areas (yellow polygons). Contour interval is 100 m.

5.2.2. The circular Hough transform

The original Hough transformation technique, introduced by Hough (1962), has been adapted for image shape analysis, detecting first linear features in images (Duda and Hart 1972), and thereafter extended to detect other shapes like circles and ellipses. The circular Hough transform has a variety of applications; some examples include automatic fruit recognition robots (Jiménes et al. 1999), finding circular gas seepage locations on images (van der Werff et al. 2006) and in medicine to localize cell nuclei of cytological smears (Smereka and Duleba 2008). Cooper (2006) demonstrates the use of the Hough transform on aeromagnetic and

gravity datasets from South Africa. He extends it to work on spherical global geoscientific datasets. Cooper and Cowan (2004) use the Hough transform to detect circular anomalies in irregular spaced data as opposed to gridded data using an aeromagnetic dataset. They apply this approach because large flight line separation during sampling as compared to flight direction sampling may distort features, resulting in information loss by the gridding process.

The circular Hough transform is a voting technique, accumulating a parameter space that must be followed by peak detection (e.g. global or local thresholds, cluster methods) to locate objects. The transform is usually applied to binary images consisting of edge pixels (result of edge detection). It calculates the possibility that such edge pixels are lying on a circle. For each edge pixel, it locates possible circle centres; all pixels a distance *r* (radius) away from the considered edge pixel. These potential circle centres are stored in a three-dimensional accumulator matrix, the size of radii interval and input image (r_{min}-r_{max}; x_{min}-x_{max}; y_{min}-y_{max}). This procedure is performed for all edge pixels and all interesting radii, accumulating possible circle centers in the matrix. The frequency of the accumulated values correspond to the probability of several edge pixels belonging to the same circle (Gonzalez and Woods 1993; Sonka et al. 1999), as displayed in Fig. 1 of *Peer reviewed extended abstract I* (Krøgli et al. 2007a). High values in the accumulation matrix indicate the presence of a circle in the original image. If some of the edge pixels along a circle in the original image are missing (as is often the case) the algorithm will result in a lower value in the accumulation matrix, though it may still be high enough for detecting the circle.

The circular Hough transform was applied on a shaded relief model in *Peer reviewed extended abstract I* and on aeromagnetic data (Fig. 13), using a simple code from Nixon and Aguado (2002). The results showed high dependency on the number and location of the edge pixels. *Paper II* (Krøgli and Dypvik 2010) presented some of the difficulties of localizing edge pixels (edge detection).

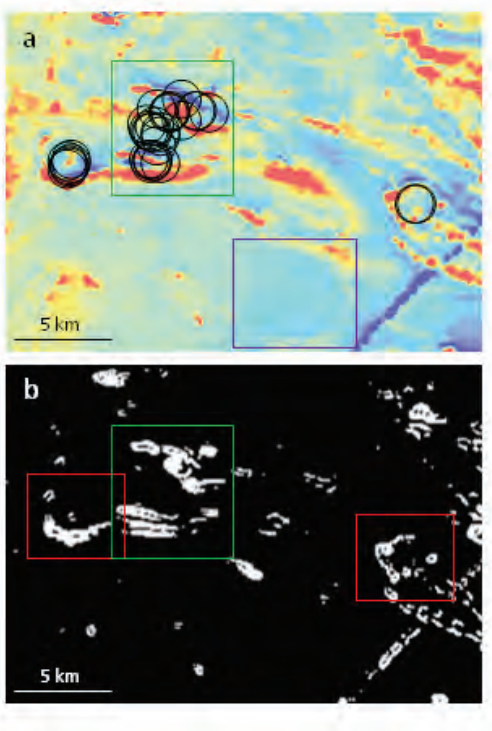

Fig. 13. (a) Circular features (black circles) detected by a circular Hough transform in regional aeromagnetic field data from the search area (100 m spatial resolution). (b) Edge pixels found by Sobel edge operator and a global threshold. The two distinct circular features in (a) are detected where a circular pattern of the edge pixels are seen (red squares). A more "chaotic" pattern of edge pixels lead to the detection of several circles (green rectangles). It requires a lower threshold to detect the subtle half circular feature in lower central of image (a) (purple square), but this will lead to more edge pixels in the image and probably more examples of "chaotic" patterns.

Edge detection

"An edge is the boundary between two regions with relatively distinct grey-level properties" (though also used with other contrast/intensity properties like in colour images and DEMs), most often assuming "that the regions in question are sufficiently homogeneous so that the transition between two regions can be determined on the basis of grey-level discontinuities alone" (Gonzalez and Woods 1993, p. 416). The Hough transform is dependent on finding edge pixels (edge points) in an image. This usually involves gradient calculation (ordinary thresholding and thinning also work) followed by extraction of edge pixels from this gradient image. The result is dependent upon the quality of these steps. The human brain can evaluate

if an edge in an image is meaningful. Edge detection operators like the Sobel or Roberts techniques (Nixon and Aguado 2002; Roberts 1965; Sobel 1970) enhance edges in images, but the edges are not necessarily meaningful. Edge pixels are localised from the resulting gradient magnitude image (edge enhanced image). The final result of the operation is a binary image displaying edge pixels and non edges pixels. The result are dependent on the choice of edge operator and binarization method (Albregtsen 1993; Trier 1995). Binarization methods are typically global and local (adaptive) threshold techniques (Fig. 1 in *Paper II*). There are problems of using only threshold techniques at this step because of possible diffuse boundaries, noise that can produce high gradients, and the possibility of a thick band of pixels in an edge map (Efford 2000). The process of binarization or extracting edge pixels may result in information loss when inappropriate thresholds are used. Edge-based segmentation works well in images with high contrast between object and background, but have disadvantages on images with smooth transitions and low contrast.

The circular Hough transform is a common step in several crater detection algorithms. On solid planetary bodies, craters are commonly clearly visible with reasonable contrast to the surroundings. This is not the case for terrestrial data. Bruzzone et al. (2004) showed that the circular Hough transform did not give satisfactory results if the structures where not clearly visible in the images. Boschetti (2005) described an edge detection technique using gradients, specifically made for high and low amplitude geophysical fields. Nonetheless, to cope with the difficulties of making reliable edge detections, an approach without requiring the localisation of edge pixels are sought in the next section.

5.2.3. The circular outline algorithm

This technique is developed in order to bypass the difficulties of edge detection and is presented in *Paper II* (Krøgli and Dypvik 2010). It is primarily made for use on regional geophysical potential field data but can also operate on DEMs. In geophysical potential field data "it is almost impossible in practice to achieve satisfactory results when anomalies of widely varying sizes are present" (Cooper 2005). The algorithm differs from the more common circular Hough transform in that edge detection is not a prior requirement. If there is not a large enough difference (gradient) between adjacent pixels, edge enhancement might be difficult. In such cases subtle circular anomalies (small gradients) might be difficult to extract. These subtle circular anomalies are considered to be as important in an impact structure search as strong circular anomalies (Fig. 14). Therefore, the algorithm is constructed to

operate on even the smallest numerical differences between an anomaly and its surrounding. The algorithm searches for a circular "contour" around a point and determines how complete it is by calculating the number of pixels that have a gradient direction (aspect) in the direction of the centre pixel. A tolerance of the direction angle may be set. Different radii are analysed and only pixels along the outline of the circle are considered. The inside of the circular outline may then consist of any values. An accumulation matrix (similar in size to a corresponding Hough transform accumulation matrix) records the values where a high value indicates the detection of a circular outline. The pixels on the circular outline can be of various intensities because the aspect value is relative (the same aspect value can be at e.g. different elevations), and there can also be various edge magnitudes around the circle, e.g. weak on one side and strong on the other side. Both downslope and upslope attitudes towards a centre pixel can be evaluated (negative and positive anomalies).

Fig. 14. The left and right feature features are considered equally valuable in the analysis. The right feature has a steeper gradient, but it is the shape, not the gradient magnitude that is important.

Aspect

A digital terrain model (DTM) is a "general model of the landscape that includes other parameters such as slope and aspect" (Burrough and McDonnell 1998) which are related to a topographic surface (Florinsky 1998). The method of Horn (1981) use eight neighbouring cells to calculate the aspect of a kernel pixel. This method is considered high in quality by Jones (1998) and was used for calculating aspect. Hodgson (1995) demonstrated that calculating slope or aspect for an elevation model of a certain grid-cell size, yields a result that better depicts a surface of 1.6 to 2 times the grid-cells. This has a minor effect as elevation and parameter data are not directly compared in these analyses (as would be the case in cartographic modelling).

A gradient vector has 2 components, magnitude and direction. In geographical information analysis, a pixel in a DEM (or other surface) has slope and aspect, where aspect

(0 to 360 degrees) is the direction of slope (directional component of the gradient vector). Figure 15 display some well exposed craters on Mars. At first glance, the corresponding aspect image may seem chaotic, even for these craters, but a closer look reveals the presence of a pattern that can separate craters from their surroundings.

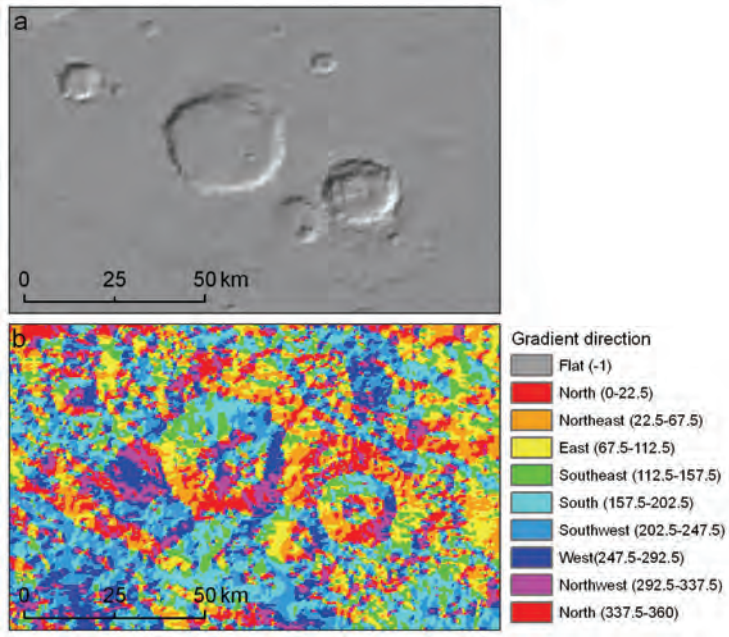

Fig. 15. (a) Martian impact craters displayed using a shaded relief model (based on MOLA data, 463 m spatial resolution). (b) Aspect values (0 – 360 degree gradient directions) calculated from the DEM that was the source of the shaded relief model in (a). Notice how the aspect values display a pattern that coincidence with the craters.

5.2.4. Impact Crater Discovery (ICDY) tool

The Impact Crater Discovery (ICDY) tool and results are presented in *Paper III* (Krøgli et al. in prep). The tool is based on the radial consistency algorithm (Bruzzone et al. 2004; Earl et al. 2005) that calculates the amount of circular symmetry about a point. This technique is applicable to a broad range of data, including remotely-sensed satellite images. In addition to Landsat ETM+ images it was applied to DEMs, geophysical data, data of geological boundaries and lake distributions. The advantage of the tool is the multi-source possibilities and, as the circular outline algorithm, that it operates without prior edge detection.

The radial consistency algorithm is a moving window operation evaluating differences in pixel values along and between profiles (16 default profiles) radiating from a centre pixel (Bruzzone et al. 2004). An area of circular symmetry has altogether larger pixel contrast differences along radial profiles than between adjacent profiles. A value (*A-B)-(A-C)* is calculated, where the considered pixel is *A*, the next outward pixel is *B* and the pixel on profile to the right, but on the same level as *A* is *C* (Fig. 2 in *Paper III*). The resulting values are summarized for all pixels on profiles in the window, before moving the window to the next step. At each step, the value is modified to make the calculation more dependent upon geometry rather than contrast differences, e.g. black or grey circles on a white background would receive similar values. Results from multiple data sources should be comparable due to this modifying step. The result is a crater likelihood image (CLI). A high value indicates that the pixel is the centre of a region of circular symmetry. Such pixels are isolated by peak detection (global threshold). Then, the most probable radius of each site is found, the radius that contributed most to the CLI value. This means that the CLI value "depends on contributions from all specified radius values about a point, while the preferred radius depends on finding the radius providing the maximum contribution to the overall measure" (Bruzzone et al. 2004).

The algorithm only looks at the intensity differences between adjacent pixels, it does not evaluate the pixel values background. It is the contrast that is important and highlighting the spectral contrast of surface features in an image may prove useful. An example of this is to enhance vegetation to detect spectral anomalies that may reflect the lithology, either directly by nutrients or indirectly by topography. It is less desirable to use pre-processing steps that reduces dimensionality to fewer bands (e.g. principal component analysis) since it is preferred to utilize as much information as possible, and ICDY can be applied on several bands simultaneously.

6. Martian crater detection/comparative results

In order to compare the performance of the Impact Crater Discovery (ICDY) tool on different planetary surfaces, it was applied to Martian and terrestrial DEMs (Fig. 16) (Krøgli et al. 2009a). The Martian DEM (463 m spatial resolution) is based on altimetry data acquired by the Mars Orbiter Laser Altimeter (MOLA) and cover a region known as Southern Thaumasia, a region of diverse topography including a rift system (Grott et al. 2007). The terrestrial DEM (100 m spatial resolution) covers the search area in Finnmark, Northern Norway. The ICDY tool has shown promising results with planetary data (Earl et al. 2005). We compared automatic and manually detected craters on Mars to find the best global crater likelihood (CLI) threshold for use in crater counting. Results showed that a threshold of 2.2 seems reasonable for a broad range of Martian topographies, being a compromise between detecting too many false positives and leaving too many craters undetected. Although resolution of models and sizes of detected circular features are different, some tendencies are apparent in Figure 16. Most of the craters present on the Mars test-site were detected and there were in addition two false positives (black arrows in Fig. 16). A similar CLI threshold on the terrestrial data extracts more varied structures than on Mars. None of the terrestrial structures resembles the shape of the Martian craters, and the findings suggest that the aim of such methods on Earth would be to detect circular depressions or partly circular structures for comparison with related analysis. A stricter CLI threshold and a morphology filter (e.g. removal of features that include non-circular peaks) may refine the detected structures.

The application of both the ICDY and the circular outline algorithm result in several overlapping features (several detections of the same crater) when applied on Martian data (Fig. 16, Fig. 3 in *Paper II* and Fig. 17). This results in lower quality when counting craters because false positives reduce the performance. In terrestrial impact structure search studies, an overlap is of minor significance because the focus is on location rather than the number of circles. The algorithms can be used to count craters on planetary surfaces if overlapping features (redundancy) are merged. ICDY uses a minimum separation value to exclude some of the overlapping craters; if two peaks are within this separation value the highest value is kept.

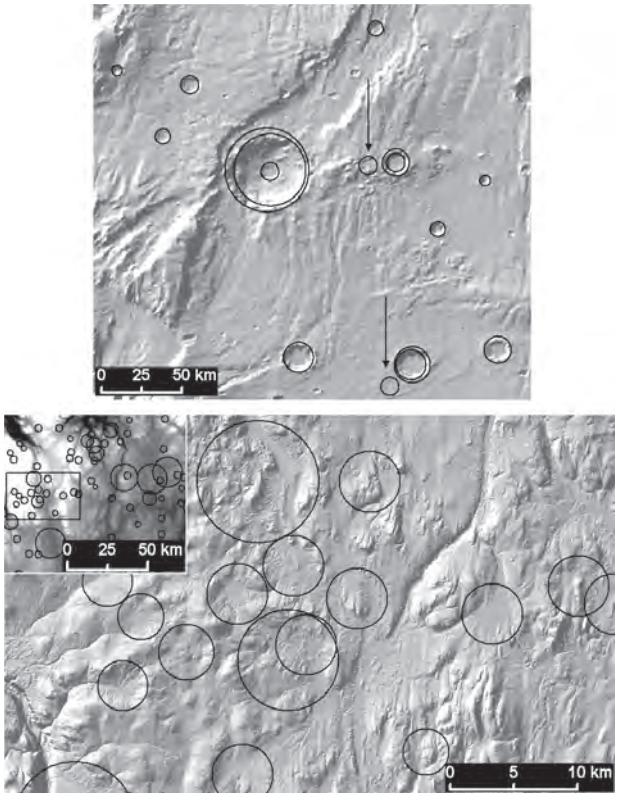

Fig. 16. Automatic detected regions of circular symmetry, CLI > 2.2. Upper image displays a region on Mars, while the lower image displays part of the search area in Finnmark, Northern Norway. Inset Finnmark map in same scale as Mars map above.

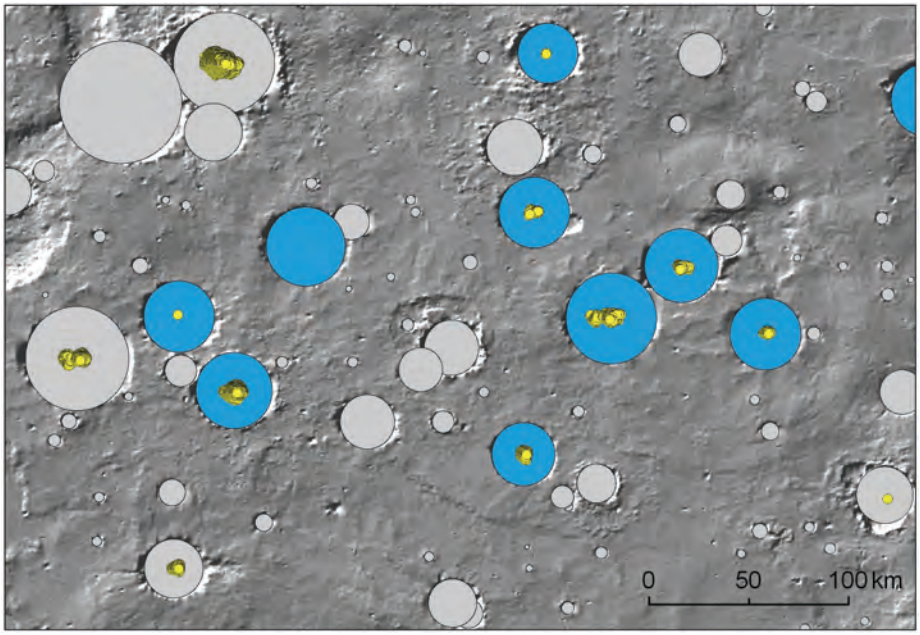

Fig. 17. Circular outline algorithm detections (yellow dots) on Martian MOLA data using a search diameter interval of 30 – 50 km and a threshold of 80 are displayed on a shaded relief model. Manually detected craters are displayed with grey or blue circles, where the blue circles have diameters between 30 km and 50 km. All but one of the craters in the search interval (blue) is detected, but there are also detections of larger and smaller craters (grey). There are also several detections of each crater (yellow dot overlap). These two factors deem the algorithm unsuitable to establish frequency distributions by crater counting because of incorrect diameters and numbers.

7. Terrestrial potential impact structures (or circular features)

Papers *I*, *II* and *III* presented results of the different techniques. This chapter provides important comments about circularity, how to proceed when refining the number of automatic detected features and how the field work might be accomplished.

7.1. Non-impact circular features

On Earth, there are several kinds of natural circular features such that circularity is not diagnostic proof of an impact origin. Several other processes can explain a circular shape besides potential impact structures. Such resulting features may be: Curved valleys, cirques, kettle holes, pockmarks, collapsed pingos (loss of water), volcanic features (e.g. calderas, maars), kimberlite pipes and circular moraine features. Pockmarks are crater like structures on the seabed, usually explained by fluid or gas expulsions that leave circular depressions (Webb et al. 2009). Kimberlites have distinctive geophysical signatures and in the Canadian Shield their aeromagnetic signature is often circular in shape (Keating 1995). Circularity is also connected to concentrically intrusions, ring dikes, basement domes and fault bounded crustal blocks (Pesonen 1996). In addition ring structures may be caused by differential erosion above an intrusion or by diapirism (Reimold et al. 2006).

7.2. Non-circular impact structures/craters

Not all craters or impact structures have a circular shape. An elliptical and asymmetric appearance results if the impact incident angle is lower than 10 - 12 degrees from horizontal, which is the case for about 5% of craters on Mars, Venus and the Moon (Bottke et al. 2000). The polygonal shaped impact craters (rims composed of several straight segments) are common features on the surface of various planetary bodies (Öhman et al. 2008). Garvin et al. (1992) discusses this shape in connection with the Bosumtwi impact structure (Ghana). As

impact structures are affected by geological processes they may over time deviate from the original circular shape.

7.3. Refining the number of features

The number of circular or partly circular structures detected is usually high and thus are too many for detailed follow up field analysis (the variety of terrestrial impact structure expressions demand low thresholds). Three methods to refine the number of candidates are discussed:

(1) The first method is to combine detected features. *Paper III* discussed data fusion and concluded that fusion at the decision level is most relevant for impact structure search studies. The rationale is that the different methods and data complement each other, such that a circular feature in a remotely sensed Landsat image is more interesting if also found as a depression in a DEM, or if an almost circular lake is accompanied by a geophysical anomaly, or if a topographic depression or peak coincidence with a geophysical anomaly without the appearance of an explaining circular lithological feature in the geologic map data. Common located features are detected if all the different results are displayed in a geographical information system. A visual interpretation of the overlaid features is preferred because the data can be slightly shifted from each other (e.g. geophysical anomalies that have different centres than original impact structure because of erosion), small magnetic anomalies may be found close to gravity anomalies, and the extent of an impact structure may be larger than the detected feature. Before overlaying the data, it is possible to weight the importance of the different data types; e.g. gravity more than magnetism. Several coincident features may be of great significance, but some data may be correlated to each other e.g. gravity may be correlated to topography (DEM).

(2) The application of filter techniques may remove less probable candidate sites. The filtering could be based on a morphology test if a DEM is available and, at least on planetary bodies, verify if the circular feature exhibit crater morphology. On Earth, the active erosional and depositional surface makes a specific crater morphology test alone difficult. *Peer reviewed extended abstract II* (Krøgli et al. 2009b) presents a filter technique based on the correlation between eight radial profiles in a detected circular feature. Symmetry exists if they are correlated in several directions, and features of non-symmetrical characteristics are removed. On Martian data, Bue and Stepinski (2007) found several detections of small craters

to represent terrain between two ridges. A separation between two ridges (e.g. a valley) and a possible impact structure could be obtained if symmetry is present around the complete circular feature or larger parts of the circle.

A second example of a filter is to keep only detected circular features that are situated in a geologic homogeneous area, i.e. areas where a “clear-cut” geological explanation of the anomaly is lacking in the geologic digital data. This could be implemented to remove features appearing close to a lithologic boundary. However, this also requires caution since lithological maps sometimes are compiled with geophysical support in areas with poor exposures.

(3) The third method is to manually compare the candidates with available maps (e.g. of geology or topography). An experienced analyst may remove less likely impact structures (Fig. 18) or highlight a selection of candidates.

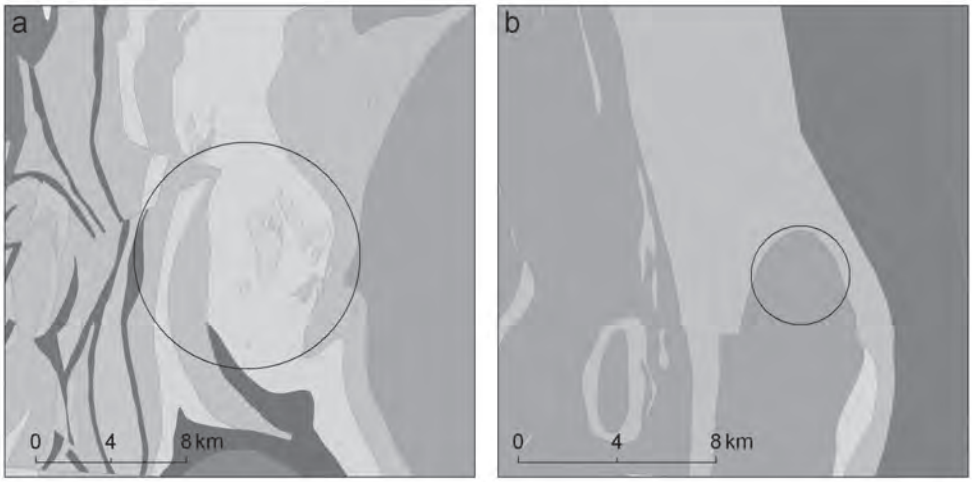

Fig. 18. Geophysical anomalies (black circles) from search area that can be removed, because they to some extent reflect the geological data (circular boundaries situated at boundaries between different lithologies).

7.4. Field work

Field work is crucial in order to prove if a suspected structure found by automatic techniques is an impact crater. A detailed "ground based" geological analysis may dismiss a candidate, lead to more attention or even find proof of impact origin. The morphology might be the first target, e.g. if a circular outline, any rim, a bowl shape or a central peak is present. It may be hard to retrieve an infield overview of a large structure. This is also why remote sensing techniques can help. Further field observations should include looking for impact supporting features such as various degrees of brecciation, melt rocks, fractures and shatter cones, features which might have been missed during regional geological mapping.

Two field excursions to Finnmark occurred during the work of this thesis in which a total of nine structures were visited (Fig. 19 and Table 2). The sites where chosen from the automatic detected structures, a closer map inspection and site accessibility (roads, etc.). The search area is ca. 25.000 km^2 and it is far between the outcrops. Maps displaying exposures were kindly made available by the Geological Survey of Norway, aiding the field work. Several locations were visited at each site covering both external and internal outcrops related to the circular feature. Lithological observations were taken at each locality (possible crushed bedrock, fractures and brecciation), main localities sampled (for thin sections, mineralogy) and structural measurements recorded (foliation, bedding, bands and fractures). The main objectives for these observations are to study the circular feature both macroscopically and microscopically, and to determine if the structure varies outside and inside the circular boundary (Figs. 20 and 21). Microscopic analysis of rocks from the Finnmark localities was performed in order to characterize the rocks and search for planar features and planar deformation features (PFs and PDFs) in the minerals. The thin section studies did not reveal any PFs or PDFs. No clear-cut signs of impact supporting material have this far been found in any of the candidates that could legitimate more detailed field inspections of those picked. The structures Kautokeino, Ravdojavri and Stuorra Cadjejavri did though display some interesting attributes; conglomerate, a breccia zone and inhomogeneous lithology from border to centre of feature, respectively. The structures visited did all reveal circular structures, either as circular lakes or depressions, or circular combinations of lakes, ridges, hills and valleys, thereby confirming the algorithms ability to detect such features (Fig. 21e).

Extensive field analyses are required if the initial field work detects impact supporting material. The Ritland structure was proposed as an impact structure based on geological mapping of the circular structure and the deformed basement (Riis 2002). The first systematic, detailed field work with focus on the crater structure were carried out in 2006. As

a proposed, but not confirmed impact structure at that time, it is well suited as an example of the detailed field techniques and methods required to prove an impact structure. The field work and succeeding laboratory analysis are presented in Riis et al. (in press). The work entailed general geological mapping with detailed analysis of several sections of the sedimentary successions (crater infill), textural measurements of bedding planes (fracture basement characteristics) and thin section analyses (shocked quartz grains with PFs and PDFs are presented in the paper).

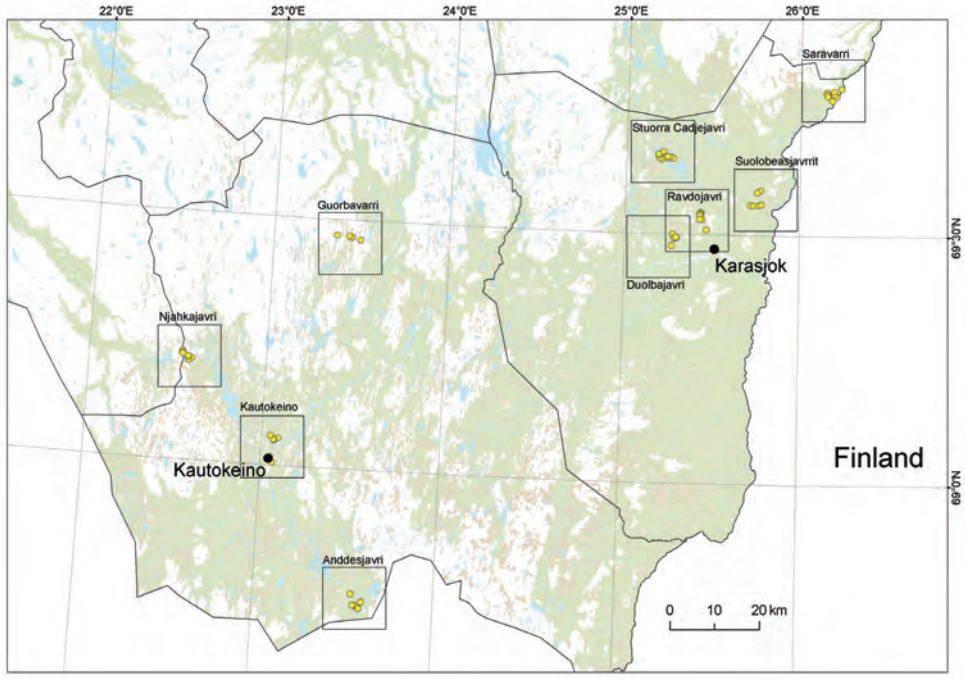

Fig. 19. The nine field targets visited during the field seasons of 2008 and 2009. Yellow dots represent visited field locations.

Table 2. The nine field targets with name, main lithology and diameter of detected circular boundary (see Fig. 19 for location).

Name	Main lithology	Diameter (km)
Ravdojavri	Banded amphibolitic gneiss / gabbroitic gneiss with quartz and feltspar veins	5.4
Suolobeasjavrrit	Banded amphibolitic gneiss / granitic gneiss	3.7
Kautokeino	Conglomerate / finely bedded amphibolitic gneiss	16.9
Anddesjavri	Granitic gneiss / banded gneiss	2.9
Duolbajavri	Fine grained layered amphibolitic gneiss	1.2
Stuorra Cadjejavri	Fine laminated banded micaceous amphibolitic gneiss	4.8
Saravarri	Banded quartzitic gneiss with garnet	4.7
Njahkajavri	Fine laminated coarse amphibolitic gneiss / granitic gneiss	1.4
Gurbavarri	Banded micaceous gneiss with amphibolitic and quartzitic bands / amphibolitic gneiss / phyllite	17.7

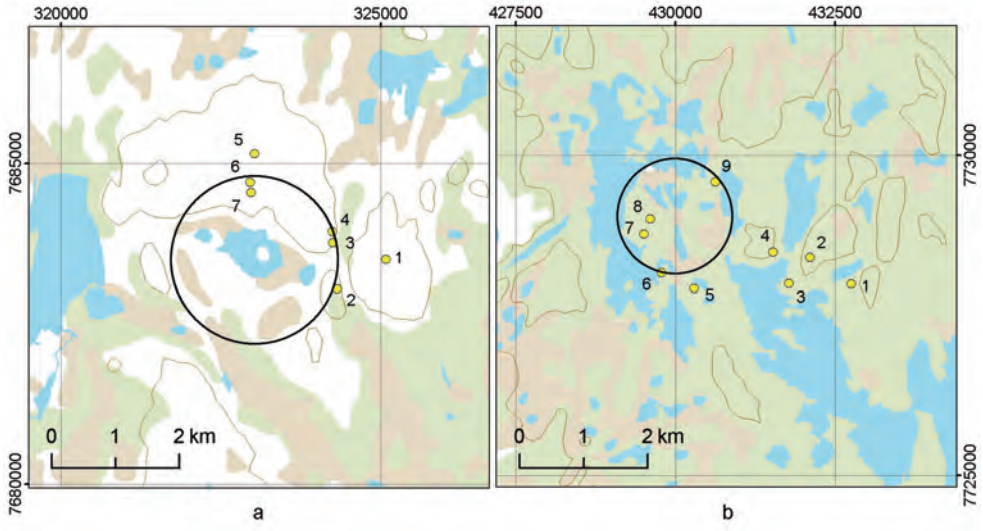

Fig. 20. The maps display the localities of the two field targets Njahkajavri and Stuorra Cadjejavri (see Fig. 19 for location). In the Njahkajavri structure (a) no significant lithological variations were observed from the outside to the inside of the circular outline. In the Stuorra Cadjejavri structure (b), localities 7 and 8 have different lithological appearance compared to the other localities of the area (Fig. 21). Contour interval is 50 m.

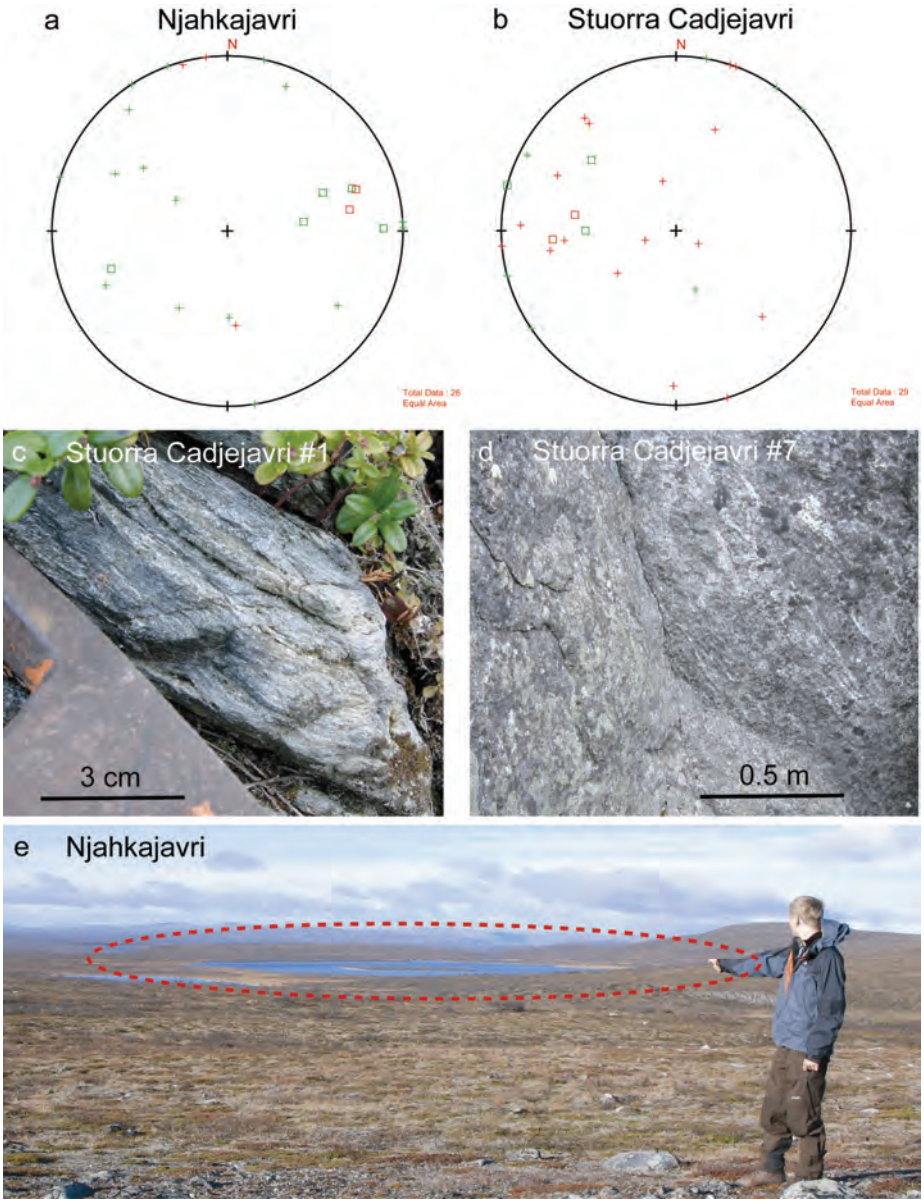

Fig. 21. The fractures (cross) and foliation/bedding (square) of the Njahkajavri (a) and Stuorra Cadjejavri (b) structures displayed in stereographic projection, both for localities inside the detected circle (red) and outside the detected circle (green). The plots display no patterns that indicate differences between the external and internal appearance of the detected circular features. However, while the lithology of Njahkajavri were homogeneous, the lithology of Stuorra Cadjejavri showed variation from fine laminated amphibolitic gneiss of bottle green colour, with occasionally light

coloured schlieren of quartz or feldspar (c) (in localities 1 – 6 and 9, see Fig. 20), to banded gneiss, deformed and fragmented (d) (in localities 7 and 8, see Fig. 20). (e) In field the Njahkajavri structure turned up as a partly circular lake with a three quarter circumference of ridges in a circular pattern.

8. Paper summary

8.1. Paper I

Krøgli, S.O., Dypvik, H., Etzelmüller, B. 2007. Automatic detection of circular depressions in digital elevation data in the search for potential Norwegian impact structures. Norwegian Journal of Geology 87, 157-166.

Technique: Template matching
Data: Digital elevation models

Template matching is a simple technique, but it is an obvious technique to test and a natural place to start when searching for possible impact structures. It addresses the shape of a feature and search similarities. The technique was applied for the whole of Norway and this paper presents selected results from Finnmark. In order to find potential impact crater structures, crater templates and topography were compared by correlation. The templates (models) represent the shape of impact craters with spatial relations based on scale and size characteristics from the Moon and Earth. The topography was represented by digital elevation models (DEM). A good match (correlation) between a template and DEMs is resembled by a high value at the specific location. The methodology is non-scalable and static, so templates for several crater sizes needed to be analysed. The study resulted in detection of a number of circular and partly-circular depressions. There are, however, many features which have the shape of partly circular depressions, e.g. curving valleys and valley intersections, and the many detected circular features must consequently be further evaluated. The technique with DEM as input were together not distinct enough to detect really promising impact structure candidate sites, but the detected circular depressions may be important for comparison with results from other techniques and data.

8.2. Paper II

Krøgli, S.O., Dypvik, H. 2010. Automatic detection of circular outlines in regional gravity and aeromagnetic data in the search for impact structure candidates. Computers & Geosciences 36, 477-488.

Technique: Circular outline algorithm
Data: Gravity, aeromagnetics, digital elevation models

This paper utilize geophysical data; magnetic and gravimetric data in particular. These data may display signatures in relations with impact structures. Circular gravity and magnetic anomalies are common. The geophysical signatures are preserved longer than surface expressions, which is a great advantage when searching in old terrestrial terrain. An algorithm were developed to detect circular anomalies in gravimetric and magnetic potential field data, and the analysis were carried out on a part of Finnmarksvidda were regional gravity and aeromagnetic data are available. The algorithm counts the number of pixels on the boundary of a circle (given a radius) that have a gradient vector which points (within a tolerance) to the circle centre. This approach is possible when the geophysical potential fields are treated as surfaces. Both negative and positive circular anomaly outlines may be found. A few sites were chosen based on detections of the algorithm and the comparing of those sites to geologic and topographic maps. The sites were examined in the field without finding major impact supporting material.

8.3. Paper III

Krøgli, S.O., Dypvik, H., Chicarro, A.F., Rossi, A.P., Pesonen, L.J., Etzelmüller, B. The Impact Crater Discovery (ICDY) tool applied to geospatial data from Finnmark, Northern Norway. Submitted to Canadian Journal of Remote Sensing.

Technique: Impact Crater Discovery (ICDY) tool
Data: Landsat ETM+ images, digital elevation models, gravity, aeromagnetics, geology, lakes

The ICDY tool was developed by the European Space Agency (ESA) and LogicaCMG UK. It can be used on a broad range of data, including remotely-sensed multispectral images which had not yet been explored by our group at that time. The ICDY tool detects rotational symmetry (radial consistency) using the pixel values and their context to each other. Symmetry is calculated from the whole circle, not only evaluating the border as the circular outline algorithm did (*Paper II*). It may be several reasons for the possible symmetry, and one explanation might be that the circular symmetric feature is the result of an impact. Compared to the often used circular Hough transform, the radial consistency approach needs no prior edge detection, making it more applicable to terrestrial data. The tool was applied to several datasets and the paper also includes some ideas regarding pre- and post-processing of data. The high contrasts between lakes and their surroundings in Landsat Enhanced Thematic Mapper Plus (ETM+) data made circular lakes among the most prominent detected features during these experiments. Five sites were chosen as promising for field analysis based on the comparison of detected symmetric features from the different input data. The sites were examined in the field without finding impact supporting material.

8.4. Peer reviewed extended abstract I

Krøgli, S.O., Dypvik, H., Etzelmüller, B., 2007. Automatic and semi-automatic detection of possible meteorite impact structures in the Fennoscandian shield using pattern recognition of spatial data, In: ScanGIS'2007: The 11th Scandinavian Research Conference on Geographical Information Science, Ås, Norway, 227-235.

Techniques: Template matching, circular Hough transform
Data: Digital elevation model, shaded relief model

A template matching algorithm and a circular Hough transform algorithm were applied on data covering the same area. The matching technique used a digital elevation model (DEM), while the Hough analysis was performed on a gray level (8 bit) shaded relief model, calculated from the digital elevation model. A shaded relief model imitates how the topography is affected by an artificial light source, creating light and shadow effects. The resulting model will have similarities to images of e.g. craters from solid planetary bodies (optical images also capture light effects). Gradient pixels to be used in the Hough transform were found using the Sobel edge detection operator. A radius interval between 20 and 60 pixels (ca. 5 - 10 km) was set prior to the analyses. The Hough transform is position, scale and rotation invariant, while template matching only is invariant of position and rotation (rotation due to circularity). Several template sizes must consequently be evaluated. Circular shaped templates (depressions) of fixed diameters (5 – 10 km) were correlated with the DEM, resulting in several structures partly matching the templates. A variety of structures were found, including circular depressions, but also valley intersections. The results showed the Hough transform to be dependent on extracting enough edge pixels to capture a structure. Using the applied edge detector and thresholds, structures of poor contrast were not found by the Hough transform.

8.5. Peer reviewed extended abstract II

Krøgli, S.O., Dypvik, H., Etzelmüller, B., 2009. Correlation of radial profiles extracted from automatic detected circular features, in the search for impact structure candidates, In: Geomorphometry 2009, Zurich, Switzerland, 50-54.

Technique: A possible filter to refine the number of detected features
Data: Detected features and their source data

The techniques presented in *Paper I-III* and *Peer reviewed extended abstract I* detect features with different degrees of circularity. The number of detected features depends on the choice of threshold, but is usually large and requires further manual or automatic analysis to refine the number before field investigations. This extended abstract presented an approach to reduce the number of candidate sites, using a filter technique that removes candidates based on non-symmetrical characteristics.

The symmetry measurement is based on correlation coefficients between radial profiles in the already automatic detected circular features. For each circular feature the algorithm extracts eight profiles from the source data (e.g. DEM or geophysical surface), radiating from centre to the length of the radius. It is the profile shapes that are correlated, indicating that the profiles might be located at different intensities/heights. First only a part, the first three pixels, of each profile is included in the correlation coefficient calculations. That is, the first three pixels when counting from the circular outline towards centre. A profile is marked if it does not correlate with any of the other profiles. Then the next pixel towards centre is added to each profile. Again a correlation coefficient calculation between profiles is performed, this time without the marked profiles. This continues until all profiles have been marked (i.e. no more correlation between profiles) or the end of profiles is reached (i.e. all pixels added). Two profiles may then correlate the whole distance to the centre, even if situated at opposite sides. The number of pixels included in profiles that correlate, compared to the total number of pixels in profiles, is saved as a percentage value. This can be thought of as recording the total length of correlating profiles. The reasoning behind equalizing two features having similar total correlating profile distances is to keep features that have few but long correlation profiles, e.g. in just a corner or half of the circle. They may represent impact structures where only part of the earlier circularity is present.

9. General discussion

9.1. Techniques

The techniques applied are based on the detection of circular features and have been operated on a variety of data. The template matching technique detected many circular depressions in digital elevation models. The circular Hough transform is faster, works with occluded objects and on several types of data but is highly dependent on the quality of the edge detection. The circular outline algorithm is independent of edge detection. Avoiding edge detection is advantageous since edges pixels capturing both subtle and strong anomalies in, for example, gravity and magnetic data are difficult to locate and incorporate in an automated algorithm. Using aspect as part of the methodology makes the algorithm robust enough to apply to various circular shapes and intensities which may be important since the signatures are not always text book examples. This algorithm does not consider the interior pixels inside a circular boundary but rather only the border pixels. The Impact Crater Discovery (ICDY) tool applies a technique that evaluates the symmetry of a feature, applicable to diverse datasets.

The circular Hough transform was not found satisfactory for terrestrial impact structure search studies, due to the edge detection step. Of the remaining three techniques presented in this thesis (papers *I*, *II* and *III*), one looks for circular depressions (*I*), one looks for circular borders (*II*), and the third looks for circular symmetry inside the entire feature (*III*). The techniques do have some common detected features, but several features were detected exclusively by each technique (Fig. 22). This implies that multiple techniques should be used to capture the variety of circular features and that the three approaches complement each other. This further means that combining results is beneficial.

In all of the techniques, thresholds are defined to distinguish promising from less promising sites. A cluster analysis could replace local and global thresholds to detect medium peaks in an accumulation matrix if they are situated in a cluster. They may represent irregularity in the circularity of a feature. Nevertheless, the results show that threshold values should vary between large and small features within the same dataset; large features must be given lower thresholds to be detected.

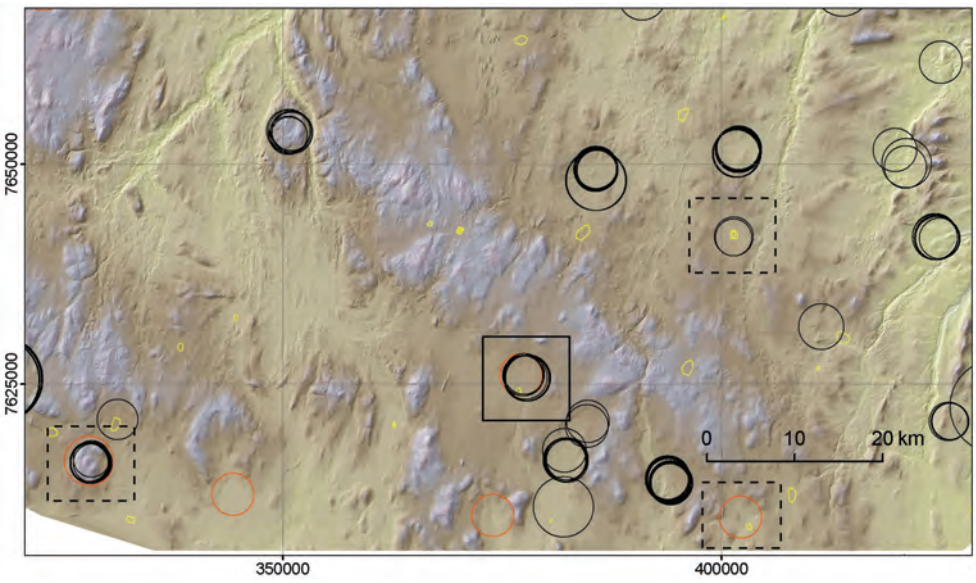

Fig. 22. Results of the three techniques performed on the same DEM (100 m spatial resolution). Black circles denote the circular outline algorithm detections, red circles denote ICDY detections and areas of high correlation from the template matching are displayed with yellow borders. All techniques searched for circular features of about 5 km in diameter. The map display all possible combinations of detection, i.e. a location where all three overlap (black square), locations where two and two overlap (black dashed squares) and locations detected by only one of the techniques. A colourmap from light brown to dark brown to grey has been included to emphasize elevation differences.

9.2. Data

The focus of this thesis is on the application of different techniques but also on the use of different data to search impact structure candidates. Each of the three techniques have their main data input, the data that contain the most significant results; for example; DEMs for template matching, geophysical field data for the circular outline algorithm and multispectral images for the ICDY tool. These datasets also complement each other in an impact structure search, addressing topography, geophysical anomalies and surface spectral properties, respectively. Data fusion is used to detect locations of circularity present in several datasets. *Paper III* discusses data fusion at various levels and concludes that fusion at the decision level (combining results of the different techniques applied on various data), is most relevant. In

section 7.3 it is argued that this fusion should be evaluated manually. In this study, the most promising data types for a remote-sensed impact structure search study have been used. However, radar images, drainage networks and fracture patterns should be considered in future detection studies.

Data derived from ground measurements or remote sensing measurements can be prepared in different ways though must be in a raster (grid) data structure for use in the presented analyses. This interpolation creates continuous surfaces from data points but the surface models are still a simplified version of the real world. Different interpolation techniques yield different models and thereby may result in detection of different circular features. In addition may the flight line spacing as compared to the higher sampling interval in flight direction of for example aeromagnetic surveys have altered the shapes in the interpolated data. The oval shape of the expected circular magnetic anomaly of the Serra da Cangalha impact structure was explained by the large flight line spacing during acquisition (Adepelumi et al. 2005).

To compare and evaluate automatic planetary crater detection algorithms, catalogues of craters and their sizes have been established. However, ground studies searching for proof of impact origin of structures on e.g. Mars are impossible, and thus it is the surveyor and his knowledge that is the basis for the manual detection. Based on this, the accuracy of algorithms may be calculated. On Earth, the lack of a large training and test data catalogue (only ca. 176 proven impacts structures) makes it difficult to verify or evaluate the quality of the algorithms. The search area (Finnmarksvidda) does not include any proven impact structures, but Fennoscandia, and in particular Finland, may provide such data for future studies. However, the data would only contain a minor number of proven impact structures and their expressions or signatures may be to variable to gain valuable information from accuracy evaluations.

9.3. Scale

Various data resolutions (scale) are appropriate to investigate different processes, thus must be considered in an analysis. The spatial resolutions reflect the size of features possible to detect. In addition, resolution may alter the shape or context of the structure. For example, L´Heureux et al. (2005) found an increased sampling rate to show the shape of the studied

anomaly being concordant to a regional geologic framework rather than a simple circular feature.

The information to be extracted (i.e. the size of objects to be detected) determine the proper scale of an analysis. A detailed geophysical investigation of a single structure (e.g. Pesonen et al. 2003) is for example not possible by the low resolution of the gravity and aeromagnetic data. Such analysis would usually require highly sampled profiles or traverses. In the 100 m resolution data only variations in the regional pattern may be detected. The spatial resolution of the applied gravity data (1500 m) is in particular coarse and too low to detect impact structures in the lower range of the 1 – 40 km diameter interval, but the presented methodology may be applied on higher resolution gravity data in future studies. It is important to select an appropriate scale for a particular application and perform analysis within that scale in order to account for scale effects (Woodcock and Strahler 1987). The spatial resolutions of the data in this study vary between 25 m and 1500 m. A circle must contain enough pixels to receive a proper shape. Using spatial resolutions of 30 m (Landsat) and 25 m (DEM) seeking structures from 500 m in diameter (17 - 20 pixel diameter), and using 100 m (aeromagnetic and DEM) data seeking structures from 1 km in diameter (10 pixel diameter) seems reasonable, although in the gravity data (1500 m spatial resolution) structures down to 7.5 km were found (5 pixel diameter).

The resolution is important, but it is the data value precision that determines how small differences the algorithms can detect. Impact generated geophysical anomalies may be too small to be detected on regional data, using for example the circular outline algorithm.

9.4. (Semi-) automatic methods

O´Sullivan and Unwin (2003, p. 362) raise the question: “Can we use (cheap) computer power in place of (expensive) brain power to help us discover patterns in geospatial data?” In other words: Is a visual inspection of data the best way to detect candidates? Do we need automatic methods? Linear and circular structures may be seen by simple data inspection. Several impact structures can be discovered by simply visualizing the data. Ideally the machine vision would detect the same structures as a visual analysis, and in addition structures that the human eye would not see that easily? The techniques proposed in this thesis will probably miss some features that the eye can see, but more important is it if they find something that the human eye cannot see. Circular moraine features have been found on

the Varanger Peninsula, Northern Norway (Ebert and Kleman 2004) and can be seen in images. They are used here as a thought experiment. If the aim is to calculate statistics of the distribution of circular moraines in an area, almost all should be found and incorporated within the statistics. Then, a visual inspection of the data by a professional is required. If the aim is to check the performance of a "circular moraine detection algorithm", one needs to find all features by a visual inspection in order to compare "ground truth" and algorithm results. But if the aim is to find new moraines, which can be features that only partly resembles a circular moraine or fragments of a circular moraine, automatic methods might see geometric patterns not clearly visible, either because the value difference are too small to be captured by the human eye or that it can be hard to see that parts could represent sections of a common circle. In the last case, interesting sites can be detected by automatic methods.

There are few impact structures on Earth and we do not expect to find many new ones in a restricted area like Finnmark. Interesting patterns first found by automatic detections and then evaluated by the researcher can prove rewarding, possibly emphasizing structures that would not have been considerer without the automatic step. The methods are semi-automatic since the researcher needs to set thresholds appropriate for the different regions, and thereafter inspect the detected features to prioritize the sites to be visited in the field. Compared to a purely visual analysis of data, the sites at the researcher's disposal are all exhaustive and objectively extracted based on circularity. Unlike previous terrestrial search approaches of pure visual data inspection with possible data enhancement or data integration steps, or of automatic techniques relevant to only a limited type of datasets, the presented methodology (collection of techniques) offers a framework to search large regions and several types of data to extract promising structures prior to the visual inspection.

9.5. Outlook

The methodology and techniques presented in this thesis are created with interests toward impact structures, specialized to detect impact structure characteristics in consideration of the datasets available. The datasets are all chosen because of their relevance for impact structure search studies. The use of similar techniques and ideas can be used to capture other features, especially those close in shape to impact structures. Structure detection in geosciences that can benefit from the specific techniques derived in this thesis are; kimberlite pipes in geophysical data, circular moraines in images, calderas and cirques in DEMs or pockmarks in

bathymetric data; all circular in shape. Polygonal patterns seen in images from permafrost areas could probably be extracted by some modifications of the presented techniques. The analyses indicated that integrating and combining multisource spatial data can improve extraction of landforms. Example scenarios are: *i)* Extraction of V-shaped valleys using DEMs and drainage network data (e.g. to locate start positions for valley extraction). *ii)* Extraction of large moraine ridges from DEMs could be aided by vegetation data (e.g. remotely-sensed images) due to possible local vegetation differences on and around the moraines. *iii)* Combining DEM and bathymetric data to extract island (volcanic) arcs, an elliptic distribution of islands close to a deep sea trough in global scale DEM and bathymetric data, respectively. Once landforms have been extracted, measures like shape, size, position, orientation and volume can be calculated to include within spatial distribution analysis. The overall methodology to extract a landform is first to identify feature descriptions (could vary for different data), then use or design techniques to find these characteristics.

10. Conclusions

The impact structure search-strategy presented is made for a terrestrial environment and has been demonstrated to require other approaches than planetary crater detection. One can discuss if a methodology that detects impact structure candidates in every terrestrial scene is as useless as a methodology that do not find any craters at all in planetary scenes. However, due to the low number of new impact structures expected in a certain area and the high degree of modification of the ones found on Earth, many candidates extracted from terrestrial data must probably be considered before a new impact structure will be found.

From this study the following main conclusions can be drawn:

- The presented detection techniques seem suitable to identify various circular features, essential since impact structures are associated with circular features that appear in different datasets.
- The techniques provide a powerful and inexpensive tool for a first assessment of circular-shaped features.
- Two existing techniques, the pattern matching algorithm and the circular Hough transform, were found to be inadequate for locating terrestrial impact structures.
- Two new and original techniques, the Circular outline algorithm and the Radial profile correlation algorithm, were developed to improve the search for terrestrial impact structures.
- The analyst should inspect the automatic detected features to pick the most promising sites for field inspection, since an impact structure origin can not be verified by the algorithms applied.
- The field work verified in all cases circular detections of the algorithms.
- None of the nine candidate sites visited in the Finnmark study area proved to be a valid impact structure. However, this negative result almost certainly lies within the error bounds of the expected likelihood of impact structures in the area.
- An impact structure search should not be based on a single technique or a single dataset, but rather a combination of several techniques applied on various data, performing data

fusion at the decision level (combining results). The techniques can be used to extract promising sites in areas with a reasonable coverage of relevant spatial data and resolutions, and may emphasize candidates that would not have been found without these efforts.

References

Abels, A., Pesonen, L.J., Bischoff, L., Lehtinen, M., 1997a. Geographic information system data integration for research on known and search for unknown impact structures in Finland: An outlook, In: Meteoritics & Planetary Science, A5-A147 (abstract).

Abels, A., Pesonen, L.J., Bischoff, L., Lehtinen, M., 1997b. GIS-based data integration for research on known and search for unknown impact structures in Finland: An oulook, In: 60th Annual Meteoritical Society Meeting, Maui, Hawaii,

Abels, A., Plado, J., Pesonen, L.J., Lehtinen, M., 2002. The impact cratering record of Fennoscandia - a close look at the database, In: Plado, J., Pesonen, L.J. (Eds.), Impacts in Precambrian Shields, Springer, Berlin Heidelberg, 1-58.

Abels, A., Zumsprekel, H., Bischoff, L., 2000. Basic remote sensing signatures of large deeply eroded impact structures, In: Impacts and the Early Earth, 91, Springer Berlin, Heidelberg, 309-326.

Adepelumi, A.A., Fontes, S.L., Schnegg, P.A., Flexor, J.M., 2005. An integrated magnetotelluric and aeromagnetic investigation of the Serra da Cangalha impact crater, Brazil. *Physics of the Earth and Planetary Interiors* 150, 159-181.

Albregtsen, F., 1993. Non-parametric histogram thresholding methods - error versus relative object area, In: Proceeding 8th Scandinavian Conference on Image Analysis, 273-280.

Almeida-Filho, R., Moreira, F.R.S., Beisl, C.H., 2005. The Serra da Cangalha astrobleme as revealed by ASTER and SRTM orbital data. *International Journal of Remote Sensing* 26, 833-838.

Araujo, A.A., Hadad, R., Martins Jr, P., 2001. Identification of pattern in satellite imagery - circular forms, In: Nonlinear Image Processing and Pattern analysis, XII, Proceedings of SPIE, 25-34.

Bandeira, L., Saraiva, J., Pina, P., 2006. Automated crater recognition: One goal, many paths, In: First International Conference on Impact Cratering in the Solar System, ESTEC, Noordwijk, the Netherlands, abstract no. 295644.

Bandeira, L., Saraiva, J., Pina, P., 2007. Impact crater recognition on Mars based on a probability volume created by template matching. *IEEE Transactions on Geoscience and Remote Sensing* 45, 4008-4015.

Barata, T., Alves, E.I., Saraiva, J., Pina, P., 2004. Automatic recognition of impact craters on the surface of Mars, In: Campilho, A., Kamel, M. (Eds.), Image Analysis and Recognition, Springer-Verlag, Berlin, 489-496.

Beals, C.S., Ferguson, G.M., Landau, A., 1956a. A search for analogies between lunar and terrestrial topography on photographs of the Canadian Shield, Part I. *Royal Astronomical Society of Canada Journal* 50, 203-211.

Beals, C.S., Ferguson, G.M., Landau, A., 1956b. A search for analogies between lunar and terrestrial topography on photographs of the Canadian Shield, Part II. *Royal Astronomical Society of Canada Journal* 50, 250-261.

Boschetti, F., 2005. Improved edge detection and noise removal in gravity maps via the use of gravity gradients. *Journal of Applied Geophysics* 57, 213-225.

Bottke, W.F.J., Love, S.G., Tytell, D., Glotch, T., 2000. Interpreting the elliptical crater populations on Mars, Venus, and the Moon. *Icarus* 145, 108-121.

Bruzzone, L., Lizzi, L., Marchetti, P.G., Earl, J., Milnes, M., 2004. Recognition and detection of impact craters from EO products, In: Proceedings of European Space Agency (ESA) - European Union Satellite Centre (EUSC) - Theory and Applications of Knowledge-Driven Image Information Mining with Focus on Earth Observation, Madrid, Spain, abstract no. 13.1.

Bue, B.D., Stepinski, T.F., 2007. Machine detection of Martian impact craters from digital topography data. *IEEE Transactions on Geoscience and Remote Sensing* 45, 265-274.

Burrough, P.A., McDonnell, R.A., 1998. *Principles of Geographical Information Systems*, 1st edn. Oxford University Press, Oxford, 333 pp.

Chicarro, A., Earl, J., Milnes, M., Koeberl, C., Marchetti, P.G., Michael, G., Rossi, A.P., 2009. Martian chronicles: Automatic recognition of potential impact craters. *ESA Bulletin* 139, 2-11.

Chicarro, A., Zender, J., Lictenegger, J., Abels, A., Barbieri, M., Paoloni, S., 2003. *ERS Synthetic Aperture Radar imaging of impact craters*. ESA Publications Division, Noordwijk, 69 pp.

Chicarro, A.F., Dypvik, H., Pesonen, L.J., Rossi, A.P., Krøgli, S.O., Zumsprekel, H., 2007. Automatic search for new impact structures in Fennoscandia, In: Bridging the Gap II: Effect of Target Properties on the Impact Cratering Process, Saint-Hubert, Canada, abstract no. 1360, 31-32.

Cooper, G.R.J., 2005. Analysing potential field data using visibility. *Computers & Geosciences* 31, 877-881.

Cooper, G.R.J., 2006. Geophysical applications of the Hough transform. *South African Journal of Geology* 109, 555-560.

Cooper, G.R.J., Cowan, D.R., 2004. The detection of circular features in irregularly spaced data. *Computers & Geosciences* 30, 101-105.

Cowan, D.R., Cooper, G.R.J., 2005. Enhancement of magnetic signatures of impact structures, In: Kenkmann, T., Hörz, F., Deutsch, A. (Eds.), Large Meteorite Impacts III, Special paper 384, The Geological Society of America, 51-65.

Dayioglu, S., Pesonen, L.J., Salminen, J., Dypvik, H., 2006. A new search strategy for detecting impact structures - examples from Fennoscandia, In: First International Conference on Impact Cratering in the Solar System, European Space Research and Technology Centre (ESTEC), Noordwijk, The Netherlands, abstract no. 292192.

Dehn, M., Gartner, H., Dikau, R., 2001. Principles of semantic modelling of landform structures. *Computers & Geosciences* 27, 1005-1010.

DeMers, M.N., 2002. *GIS modeling in raster*. John Wiley & Sons, New York, 203 pp.

Dence, M.R., 1965. The extraterrestrial origin of Canadian craters. *New York Academy of Science, Annals* 123, 941-969.

Dence, M.R., Popelar, J., 1972. Evidence for an impact origin for Lake Wanapitei, Ontario, In: Guy-Bray, J.V. (Ed.), New developments in Sudbury geology: The Geological Association of Canada Special Paper, 10, 117-124.

Deutsch, A., 1998. New pathfinders to impact structures: The Finnish way. *Meteoritics & Planetary Science* 33, 3.

Di Achille, G., 2005. A new impact site in northeastern Sudan detected from remote sensing, In: Lunar and Planetary Science Conference (LPSC) XXXVI, Houston, Texas, USA, abstract no. 1606.

Duda, R.O., Hart, P.E., 1972. Use of the Hough transform to detect lines and curves in pictures. *Communications of the ACM (Association for Computing Machinery)* 15, 11-15.

Dypvik, H., Gudlaugsson, S.T., Tsikalas, F., Attrep Jr, M., Ferrel Jr, R.E., Krinsley, D.H., Mørk, A., Faleide, J.I., Nagy, J., 1996. Mjølnir structure: An impact crater in the Barents Sea. *Geology* 24, 779-782.

Dypvik, H., Krøgli, S.O., Etzelmüller, B., Sørbel, L., Thorsen, T.A.A., 2006. The hunt for impact structures in Norway, In: Lunar and Planetary Science Conference (LPSC) XXXVII, Houston, Texas, USA, abstract no. 1013.

Dypvik, H., Plado, J., Heinberg, C., Håkansson, E., Pesonen, L.J., Schmitz, B., Raiskila, S., 2008. Impact structures and events - a Nordic perspective. *Episodes Journal of International Geoscience* 31, 107-114.

Earl, J., Chicarro, A., Koeberl, C., Marchetti, P.G., Milnes, M., 2005. Automatic recognition of crater-like structures in terrestrial and planetary images, In: Lunar and Planetary Science Conference (LPSC) XXXVI, Houston, Texas, USA, abstract no. 1319.

Earth Impact Database. 2009: <http://www.unb.ca/passc/ImpactDatabase/> (Accessed: Dec. 2009)

Ebert, K., Kleman, J., 2004. Circular moraine features on the Varanger Peninsula, northern Norway, and their possible relation to polythermal ice sheet coverage. *Geomorphology* 62, 159-168.

Efford, N., 2000. *Digital Image Processing, a practical introduction using Java.* Addison-Wesley, Harlow, 340 pp.

Evans, I.S., 1972. General geomorphometry, derivatives of altitude, and descriptive statistics, In: Chorely, R.J. (Ed.), Spatial Analysis in Geomorphology, Methuen & Co Ltd., London, 17-90.

Evans, I.S., 2009. Allometric development of glacial cirques: An application of specific geomorphometry, In: Geomoprhometry 2009, Zurich, Switzerland,

Florinsky, I.V., 1998. Accuracy of local topographic variables derived from digital elevation models. *International Journal of Geographical Information Science* 12, 47-61.

French, B.M., 1998. *Traces of Catastrophe: A Handbook of Shock-Metamorphic Effects in Terrestrial Meteorite Impact Structures*. Lunar and Planetary Institute, Houston, 120 pp.

French, B.M., Koeberl, C., Gilmour, I., Shirey, S.B., Dons, J.A., Naterstad, J., 1997. The Gardnos impact structure, Norway: Petrology and geochemistry of target rocks and impactites. *Geochimica et Cosmochimica Acta* 61, 873-904.

Gabrielsen, R.H., Ramberg, I.B., 1979. Fracture patterns in Norway from Landsat imagery: Results and potential use, In: Proceedings, Norwegian Sea Symposium, Tromsø, Norwegian Petroleum Society, NSS/23 1-28.

Garvin, J.B., Schnetzler, C.C., Grieve, R.A.F., 1992. Characteristics of large terrestrial impact structures as revealed by remote sensing studies. *Tectonophysics* 216, 45-62.

Gasselt van, S., Werner, S.C., Michael, G.G., Neukum, G., 2006. XCage: An analysis toolkit for the evaluation of crater size frequency distributions and age determinations, In: First international conference on impact cratering in the solar system, Noordwijk, the Netherlands, abstract no. 312956.

Gifford, A.C., 1924. The mountains of the Moon. *The New Zealand Journal of Science and Technology* 7, 129-142.

Gifford, A.C., 1930. Meteoritic theory of the lunar craters (Astronomical Column). *Nature* 126, 379.

Gilbert, G.K., 1893. The Moon's face: A study of the origin of its features. *Philosophical Society of Washington Bulletin* 12, 241-292.

Gisler, G., Weaver, R., Gittings, M., Mader, C., 2003. Two- and three-dimensional asteroid ocean impact simulations. *International Journal of Impact Engineering* 29, 283-191.

Gjessing, J., 1967. Norway's paleic surface. *Norsk Geografisk Tidsskrift* 21, 69-132.

GLCF. 2009: Global Land Cover Facility (GLCF), University of Maryland, College Park, Maryland, USA (http://glcf.umiacs.umd.edu/)

Gonzalez, R.C., Woods, R.E., 1993. *Digital image processing*, 1th Edition. Addison-Wesley, Reading, Massachusetts, 703 pp.

Grieve, R.A.F., 1990. Impact cratering on the Earth. *Scientific American* 262, 44-51.

Grieve, R.A.F., Pilkington, M., 1996. The signature of terrestrial impacts. *AGSO Journal of Australian Geology & Geophysics* 16, 399-420.

Grott, M., Kronberg, P., Hauber, E., Cailleau, B., 2007. Formation of the double rift system in the Thaumasia Highlands, Mars. *Journal of Geophysical Research* 112.

Guth, P., 2009. Global survey of organized landforms: Recognizing linear sand dunes, In: Geomorphometry 2009, Zurich, Switzerland,

Hawke, P.J., 2003. Geophysical investigation of the Wolfe Creek meteorite crater. *Western Australia Geological survey* Record 2003/10, 9p.

Henkel, H., 1992. Geophysical aspects of meteorite impact craters in eroded shield environment, with special emphasis on electric resistivity. *Tectonophysics* 216, 63-89.

Henkel, H., Pesonen, L.J., 1992. Impact craters and craterform structures in Fennoscandia. *Tectonophysics* 216, 31-40.

Hildebrand, A.R., Penfield, G.T., Kring, D.A., Pilkington, M., Camargo Z, A., Jacobsen, S.B., Boynton, W.V., 1991. Chicxulub crater: A possible Cretaceous/Tertiary boundary impact crater on the Yucatán Peninsula, Mexico. *Geology* 19, 867-871.

Hodgson, M.E., 1995. What cell size does the computed slope/aspect angle represent? *Photogrammetric Engineering & Remote Sensing* 61, 513-517.

Horn, B.K.P., 1981. Hill shading and the reflectance map. *Proceedings of the IEEE* 69, 14-47.

Hough, P.V.C., 1962. Methods and means for recognizing complex patterns. *U.S. Patent No. 3069654*.

Impact Database. 2009: <http://impacts.rajmon.cz/index.html> (Accessed: Dec. 2009)

Ivanov, B., 2008a. Geologic effects of large terrestrial impact crater formation, In: Adushkin, V.V., Nemchinov, I.V. (Eds.), Catastrophic Events Caused by Cosmic Objects, Springer, 163-205.

Ivanov, B., 2008b. Size-frequency distribution of asteroids and impact craters: Estimates of impact rate, In: Adushkin, V.V., Nemchinov, I.V. (Eds.), Catastrophic Events Caused by Cosmic Objects, Springer, 91-116.

Ivanov, B.A., Hartmann, W.K., 2007. Exogenic dynamics, cratering and surface ages, In: Spohn, T. (Ed.), Treatise on Geophysics, 10, Elsevier, 207-242.

Ivanov, B.A., Melosh, H.J., McEwen, A.S., HiRISE team, 2008. Small impact crater clusters in high resolution HIRISE images, In: Lunar and Planetary Science Conference (LPSC) XXXIX, League City, Texas, USA, abstract no. 1221.

Jiménes, A.R., Jain, A.K., Ceres, R., Pons, J.L., 1999. Automatic fruit recognition: A survey and new results using range/attenuation images. *Pattern Recognition* 32, 1719-1736.

Jones, K.H., 1998. A comparison of algorithms used to compute hill slope as a property of the DEM. *Computers & Geosciences* 24, 315-323.

Kalleson, E., Corfu, F., Dypvik, H., 2009. U-Pb systematics of zircon and titanite from the Gardnos impact structure, Norway: Evidence for impact at 546 Ma? *Geochimica et Cosmochimica Acta* 73, 3077-3092.

Kearey, P., Brooks, M., Hill, I., 2002. *An Introduction to Geophysical Exploration*, 3rd edn. Blackwell Publishing, Oxford, UK, 262 pp.

Keating, P., 1995. A simple technique to identify magnetic anomalies due to kimberlite pipes. *Exploration and Mining Geology* 4, 121-125.

Keating, P., Sailhac, P., 2004. Use of the analytic signal to identify magnetic anomalies due to kimberlite pipes. *Geophysics* 69, 180-190.

Keller, E.A., Blodgett, R.H., 2006. Impacts and extinctions, In: Lynch, P. (Ed.), Natural Hazards: Earth's Processes as Hazards, Disasters, and Catastrophes, Pearson Prentice Hall, Upper Saddle River, 314-337.

Kenkmann, T., 2002. Folding within seconds. *Geology* 30, 231-234.

Kenkmann, T., Dalwigk, I.v., 2000. Radial transpression ridges: A new structural feature of complex impact craters. *Meteoritics & Planetary Science* 35, 1189-1201.

Kenkmann, T., Jahn, A., Scherler, D., Ivanov, B.A., 2005. Structure and formation of a cenrtal uplift: A case study at the Upheaval Dome impact crater, Utah, In: Kenkmann, T., Hörz, F., Deutch, A. (Eds.), Large Meteorite Impacts III, Special paper 384, The Geological Society of America, 85-115.

Kim, J.R., Muller, J.-P., 2003. Impact crater detection on optical images and DEMs, In: International Society for Photogrammetry and Remote Sensing (ISPRS) Working Group IV/9: Extraterrestrial Mapping, Advances in Planetary Mapping 2003, Houston, Texas, USA.,

Kim, J.R., Muller, J.-P., Morley, J.G., 2004. Quantitative assessment of automated crater detection on Mars, In: 20th ISPRS Congress, Istanbul, Turkey, 816-821.

Kim, J.R., Muller, J.-P., van Gasselt, S., Morley, J.G., Neukum, G., High Resolution Stereo Camera (HRSC) Collaborative Team, 2005. Automated crater detection, a new tool for Mars cartography and chronology. *Photogrammetric Engineering & Remote Sensing* 71, 1205-1217.

Kleman, J., Borgström, I., 1994. Glacial landforms indicative of a partly frozen bed. *Journal of Glaciology* 40, 255-264.

Koeberl, C., 2004. Remote sensing studies of impact craters: How to be sure? *C. R. Geoscience* 336, 959-961.

Koeberl, C., 2007. The geochemistry and cosmochemistry of impacts, In: Davis, A. (Ed.), Treatise of Geochemistry, Volume 1 (online edition), Elsevier, Amsterdam, 1.28.1-1.28.52.

Kouli, M., Seymour St., K., 2006. Contribution of remote sensing techniques to the identification and characterization of Miocene calderas, Lesvos Island, Aegan Sea, Hellas *Geomorphology* 77, 1-16.

Krøgli, S.O., Dypvik, H., 2010. Automatic detection of circular outlines in regional gravity and aeromagentic data in the search for impact structure candidates. *Computers & Geosciences* 36, 477-488.

Krøgli, S.O., Dypvik, H., Chicarro, A., Rossi, A.P., Etzelmüller, B., 2009a. An impact crater detection tool (ICDY) applied to Martian and terrestrial digital elevation models, In: International Conference on Comparative Planetology: Venus-Earth-Mars, ESA/ESTEC Noordwijk, The Netherlands, abstract.

Krøgli, S.O., Dypvik, H., Chicarro, A.F., Rossi, A.P., Pesonen, L.J., Etzelmüller, B., in prep. The Impact Crater Discovery (ICDY) tool applied to geospatial data from Finnmark, Northern Norway.

Krøgli, S.O., Dypvik, H., Etzelmüller, B., 2007a. Automatic and semi-automatic detection of possible meteorite impact structures in the Fennoscandian shield using pattern recognition of spatial data, In: ScanGIS'2007: The 11th Scandinavian Research Conference on Geographical Information Science, Ås, Norway, 227-235.

Krøgli, S.O., Dypvik, H., Etzelmüller, B., 2007b. Automatic detection of circular depressions in digital elevation data in the search for potential Norwegian impact structures. *Norwegian Journal of Geology* 87, 157-166.

Krøgli, S.O., Dypvik, H., Etzelmüller, B., 2009b. Correlation of radial profiles extracted from automatic detected circular features, in the search for impact structure candidates, In: Geomorphometry 2009, Zurich, Switzerland, 50-54.

L'Heureux, E., Ugalde, H., Milkereit, B., Boyce, J., Morris, W., Eyles, N., Artemieva, N., 2005. Using vertical dikes as a new approach to constraining the size of buried craters: An example from Lake Wanapitei, Canada, In: Kenkmann, T., Hörz, F., Deutch, A. (Eds.), Large meteorite impacts III, Special paper 384, The Geological Society of America, 43-50.

Le Feuvre, M., Wieczorek, M.A., 2006. The assymetric cratering history of the Moon and terrestrial planets, In: First international conference on impact cratering in the Solar system, ESTEC, Noordwijk, The Netherlands, abstract no. 295683.

Lidmar-Bergstrøm, K., Ollier, C.D., Sulebak, J.R., 2000. Landforms and uplift history of southern Norway. *Global and Planetary Change* 24, 211-231.

Lowman, P.D., Jr., 1997. Extraterrestrial impact craters. *Oklahoma Geological Survey Circular* 100, 55-81.

McCall, G.J.H., 2009. Half a century of progress in research on terrestrial impact structures: A review. *Earth-Science Reviews* 92, 99-116.

McHone, J.F., Greeley, R., Williams, K.K., Blumberg, D.G., Kuzmin, R.O., 2002. Space shuttle observations of terrestrial impact structures using SIR-C and X-SAR radars. *Meteoritics & Planetary Science* 37, 407-420.

Melosh, H.J., 1989. *Impact Cratering: A Geologic Process*, 1st edn. Oxford University Press, New York, 240 pp.

Michael, G., Neukum, G., 2007. Refinement of cratering model age for the case of partial resurfacing, In: Lunar and Planetary Science Conference (LPSC) XXXVIII, Houston, Texas, USA, abstract no. 1825.

Michael, G.G., 2003. Coordinate registration by automated crater recognition. *Planetary and Space Science* 51, 563-568.

Midtun, R.D., 1988. Karasjokgrønnsteinsbeltet. Regional geofysikk og geologisk tolking (Karasjok greenstone belt. Regional geophysical and geological interpretation). *Norges Geologiske Undersøkelse Skrifter* 88, 1-19 [in Norwegian].

Mihàlyi, K., Gucsik, A., Szabò, J., 2008. Drainage patterns of terrestrial complex meteorite craters: A hydrogeological overview, In: Lunar and Planetary Science Conference XXXIX, Houston, Texas, USA, abstract no. 1200.

Murray, J.B., Guest, J.E., 1970. Circularities of craters and related structures on Earth and Moon. *Modern Geology* 1, 149-159.

Neukum, G. 1983. Meteoritenbombardement and datierung planetarer oberflächen, University of Munich. Habilitation dissertation for faculty membership, 186 pp.

Neukum, G., Ivanov, B.A., Hartmann, W.K., 2001. Cratering records in the inner Solar System in relation to the lunar reference system. *Space Science Reviews* 96, 55-86.

Neukum, G., Werner, S.C., Ivanov, B.A., 2006. The characteristics of the impact crater production size-frequency distribution on solar system planetary bodies, their relationship to asteroidal and cometary impacts, and cratering chronologies for the terrestrial planets, In: First international conference on impact cratering in the solar system, Noordwijk, the Netherlands, abstract no. 313244.

Nixon, M.S., Aguado, A.S., 2002. *Feature Extraction & Image Processing*. Newnes Elsevier, Oxford, 350 pp.

O'Sullivan, D., Unwin, D.J., 2003. *Geographic information analysis*. John Wiley & Sons, New Jersey, 436 pp.

Oberbeck, V.R., Aoyagi, M., Murray, J.B., 1972. Circularity of Martian craters. *Modern Geology* 3, 195-199.

Olaya, V., 2009. Basic land-surface parameters, In: Hengl, T., Reuter, H.I. (Eds.), Geomorphometry, Consepts, Software, Applications, 33, Elsevier, Amsterdam, 141-169.

Olesen, O., Henkel, H., Lile, O.B., Mauring, E., Rønning, J.S., 1992. Geophysical investigations of the Stuoragurra postglacial fault, Finnmark, northern Norway. *Journal of Applied Geophysics* 29, 95-118.

Olesen, O., Sandstad, J.S., 1993. Interpretation of the Proterozoic Kautokeino Greenstone Belt, Finnmark, Norway from combined geophysical and geological data. *Norges Geologiske Undersøkelse Bulletin* 425, 43-64.

Pesonen, L.J., 1996. The impact cratering record of Fennoscandia. *Earth, Moon, and Planets* 72, 377-393.

Pesonen, L.J., Koeberl, C., Hautaniemi, H., 2003. Airborne geophysical survey of the lake Bosumtwi meteorite impact structure (southern Ghana) - geophysical maps with descriptions, In: Jahrbuch der geologischen bundesanstalt, 142, 581-604.

Peulvast, J.-P., 1985. Post-orogenic morphotectonic evolution of the Scandinavian Caledonides during the Mesozoic and Cenozoic, In: Gee, D.G., Sturt, B.A. (Eds.), The Caledonian Orogen - Scandinavia and Related Areas, Wiley, Chichester, 979-995.

Pike, R.J., 1977a. El'Gygytgyn, probably world's largest meteorite crater (Comment). *Geology* 5, 262-263.

Pike, R.J., 1977b. Size-dependence in the shape of fresh impact craters on the moon, In: Roddy, D.J., Pepin, R.O., Merrill, R.B. (Eds.), Impact and Explosion Cratering, Pergamon Press, New York, 489-509.

Pike, R.J., 1995. Geomorphometry - progress, practice and prospect. *Z. Geomorph. Suppl.* 101, 221-238.

Pike, R.J. 2002. A bibliography of terrain modeling (geomorphometry), the quantitative representation of topography - Supplement 4.0, U.S. Geological Survey, 465 pp.

Pilkington, M., Grieve, R.A.F., 1992. The geophysical signature of terrestrial impact craters. *Reviews of Geophysics* 30, 161-181.

Plescia, J.B., Saunders, R.S., 1979. The chronology of the martian volcanoes, In: Lunar and Planetary Science Conference (LPSC) 10th, Houston, Texas, USA, Pergamon Press, 2841-2859.

Plesko, C.S., Werner, S.C., Brumby, S.P., Asphaug, E.A., Neukum, G., High Resolution Stereo Camera (HRSC) Investigator Team, 2006. A statistical analysis of automated crater counts in MOC and HRSC data, In: Lunar and Planetary Science Conference (LPSC) XXXVI, Houston, Texas, USA, abstract no. 2012.

Prinz, T., 1996. Multispectral remote sensing og the Gosses Bluff impact crater, central Australia (N.T.) by using Landsat-TM and ERS-1 data. *ISPRS Journal of Photogrammetry & Remote Sensing* 51, 137-149.

Reimold, W.U., Cooper, G.R.J., Romano, R., Cowan, D.R., Koeberl, C., 2006. Investigation of Shuttle Radar Topography Mission data of the possible impact structure at Serra da Cangalha, Brazil. *Meteoritics & Planetary Science* 41, 237-246.

Riis, F., 2002. The Ritland crater structure, In: The 25th Nordic Geological Winter Meeting, Reykjavik, Iceland,

Riis, F., Dypvik, H., Krøgli, S.O., 2008. The Ritland crater - an early Cambrian impact structure in West Norway, In: 33rd International Geological Congress, Oslo,

Riis, F., Dypvik, H., Krøgli, S.O., Nilsen, O., in press. The Ritland impact structure, SW Norway. *Meteoritics & Planetary Science*.

Risbøl, O., Gjertsen, A.K., Skare, K. 2007. Flybåren laserskanning og registrering av kulturminner i skog. Fase 2 (Airborne laser scanning of cultural remains in forest. Phase 2). *NIKU Rapport 18,* [In Norwegian with English abstract], 34 pp.

Risbøl, O., Gjertsen, A.K., Skare, K. 2008. Flybåren laserskanning og registrering av kulturminner i skog. Fase 3 (Airborne laser scanning of cultural remains in forest. Phase 3). *NIKU Rapport 22,* [In Norwegian with English abstract], 43 pp.

Roberts, L.G. 1965. Machine Perception of Three-Dimensional Solids. *Optical and Electro-Optical Information Processing*, MIT Press, 159-197 pp.

Ronca, L.B., Salisbury, J.W., 1966. Lunar history as suggested by the circularity index of lunar craters. *Icarus* 5, 130-138.

Salamuniccar, G., Loncaric, S., 2008. Open framework for objective evaluation of crater detection algorithms with first test-field subsystem based on MOLA data. *Advances in Space Research* 42, 6-19.

Sawabe, Y., Matsunaga, T., Rokugawa, S., 2006. Automated detection and classification of lunar craters using multiple approaches. *Advances in Space Research* 37, 21-27.

Schmidt, J., Dikau, R., 1999. Extracting geomorphometric attributes and objects from digital elevation models - semantics, methods and future needs, In: Dikau, R., Saurer, H. (Eds.), GIS for Earth Surface Systems, Gebrüder Borntraeger, Berlin, 153-173.

Scott, R.G., Pilkington, M., Tanczyk, E.I., 1997. Magnetic investigations of the West Hawk, Deep Bay and Clearwater impact structures, Canada. *Meteoritics & Planetary Science* 32, 293-308.

Sindre, A., Olesen, O., Henkel, H., Erikson, L., Olsen, L., 1983. Geological and geophysical interpretation of a large gravity anomaly in the greenstone-gneiss-granite area of Finnmarksvidda, Norway. *Geoexploration* 21, 286.

Smereka, M., Duleba, I., 2008. Circular object detection using a modified Hough transform. *International Journal of applied mathematics and computer science* 18, 85-91.

Smith, W.H.F., Sandwell, D.T., 1997. Global sea floor topography from satellite altimetry and ship depth soundings. *Science* 277, 1956-1962.

Sobel, I.E. 1970. Camera Models and Machine Perception, Stanford University. Ph.D. Thesis.

Sollid, J.L., Sørbel, L., 1994. Distribution of glacial landforms in southern Norway in relation to the thermal regime of the last continental ice-sheet. *Geografiska Annaler* 76, 25-35.

Sonka, M., Hlavac, V., Boyle, R., 1999. *Image processing, Analysis and Machine Vision*, second edition. Brooks/Cole Publishing Company, Pacific Grove, USA, 828 pp.

Strøm, K., 1948. The geomorphology of Norway. *Geographical Journal* CXII, 19-27.

Szèkely, B., Karàtson, D., 2004. DEM-based morphometry as a tool for reconstructing primary volcanic landforms: Examples from the Börzsöny Mountains, Hungary. *Geomorphology* 63, 25-37.

Thackrey, S.N.D., Walkden, G.M., Dunn, G. 2006. Geological aspects of terrestrial impact cratering rates; simulating the processes and effect of crater removal. *40th ESLAB First International Conference on Impact Cratering in the Solar System*. ESTEC Noordwijk, Netherlands.

Trefil, J.S., Raup, D.M., 1990. Crater taphonomy and bombardment rates in the Phanerozoic. *The Journal of Geology* 98, 385-398.

Trier, Ø.D., 1995. Goal-directed evaluation of binarization methods. *IEEE Transactions on pattern analysis and machine intelligence* 17, 1191-1201.

Turtle, E.P., Pierazzo, E., Collins, G.S., Osinski, G.R., Melosh, H.J., Morgan, J.V., Reimold, W.U., 2005. Impact structures: What does crater diameter mean?, In: Kenkmann, T., Hörz, F., Deutsch, A. (Eds.), Large meteorite impacts III: Geological Society of America Special Paper, 384, 1-24.

Ugalde, H.A., Artemieva, N., Milkereit, B., 2005. Magnetization on impact structures - constraints from numerical modeling and petrophysics, In: Kenkmann, T., Hörz, F., Deutch, A. (Eds.), Large Meteorite Impacts III, Special paper 384, The Geological Society of America, 25-42.

Urbach, E.R., 2007. Classification of objects consisting of multiple segments with application to crater detection, In: 8th International Symposium on Mathematical Morphology, Rio de Janeiro, Brazil, 81-82.

van der Werff, H.M.A., Bakker, W.H., van der Meer, F.D., Siderius, W., 2006. Combining spectral signals and spatial patterns using multiple Hough transforms: An application for detection of natural gas seepages. *Computers & Geosciences* 32, 1334-1343.

Webb, K.E., Hammer, Ø., Lepland, A., Gray, J.S., 2009. Pockmarks in the inner Oslofjord, Norway. *Geo-Marine Letters* 29.

Werner, S.C. 2006. Major aspects of the chronostratigraphy and geologic evolutionary history of Mars. Berlin, Freie Universität Berlin. Doctoral dissertation, 160 pp.

Williams, G.E., Schmidt, P.W., Boyd, D.M., 1996. Magnetic signature and morphology of the Acraman impact structure, South Australia. *AGSO Journal of Australian Geology & Geophysics* 16, 431-442.

Woodcock, C.E., Strahler, A.H., 1987. The factor of scale in remote sensing. *Remote Sensing of Environment* 21, 311-332.

Zumsprekel, H., Bischoff, L., 2005. Remote sensing and GIS analyses of the Strangways impact structure, Northern Territory. *Australian Journal of Earth Sciences* 52, 621-630.

Öhman, T., Aittola, M., Kostama, V.-P., Raitala, J., Korteniemi, J., 2008. Polygonal impact craters in Argyre region, Mars: Implications for geology and cratering mechanics. *Meteoritics & Planetary Science* 43, 1605-1628.

Appendix: List of impact structures

Impact structures mentioned in the thesis and their parameters according to Earth Impact Database (2009).

Crater name	Location	Diameter (km)	Age (Ma)	Target Rock
Acraman	South Australia, Australia	90	~ 590	C
Barringer	Arizona, U.S.A.	1.186	0.049 ± 0.003	S
Bosumtwi	Ghana	10.5	1.07	C-Ms
Brent	Ontario, Canada	3.8	396 ± 20	C
Gardnos	Norway	5	500 ± 10	C
Gosses Bluff	Northern Territory, Australia	22	142.5 ± 0.8	S
Lappajärvi	Finland	23	73.3 ± 5.3	M
Lonar	India	1.83	0.052 ± 0.006	C
Manicouagan	Quebec, Canada	100	214 ± 1	M
Mjølnir	Norway	40	142.0 ± 2.6	S
Ritland*	Norway	2.5	600-500?	C
Serra da Cangalha	Brazil	12	< 300	S
Strangways	Northern Territory, Australia	25	646 ± 42	M
Suavjärvi	Russia	16	~ 2400	C-Ms
Tenoumer	Mauritania	1.9	0.0214 ± 0.0097	M
Upheaval Dome	Utah, U.S.A.	10	< 170	S
Vredefort	South Africa	300	2023 ± 4	M
Wanapitei	Ontario, Canada	7.5	37.2 ± 1.2	C
Wolfe Creek	Western Australia, Australia	0.875	< 0.3	S
Zhamanshin	Kazakhstan	14	0.9 ± 0.1	M

Abbreviations: C - Crystalline Target; C-Ms - Metasedimetary Target; M - Mixed Target (i.e. sedimentary strata overlying crystalline basement); S - sedimentary target (i.e. no crystalline rocks affected by the impact event). *Ritland is not yet part of the Earth Impact Database.

I

Automatic detection of circular depressions in digital elevation data in the search for potential Norwegian impact structures

Svein Olav Krøgli, Henning Dypvik & Bernd Etzelmüller

Krøgli, S.O., Dypvik, H. & Etzelmüller, B.: Automatic detection of circular depressions in digital elevation data in the search for potential Norwegian impact structures. *Norwegian Journal of Geology,* Vol. 87, pp. 157-166.Trondheim 2007. ISSN 029-196X.

Presently, 174 impact craters are proven on Earth, and of these 10 are located in Finland, 6 in Sweden and only 2 in Norway (Gardnos and Mjølnir). A pattern matching algorithm (correlation) based on 100 m digital elevation data was used in a regional study to discover circular depressions in the search for possible new Norwegian impact structures. By applying this technique to detect depressions of 5 – 10 km diameter in Finnmark, northern Norway, about 23 large circular structures were found in a 14,000 km^2 area of Precambrian rocks. Circular features are clearly displayed in the detected structures. The large number of candidates in this area, however, makes field inspection inconvenient and time consuming, and supplementary screening methods should be considered to help reduce the number.

Krøgli, S.O., Dypvik, H., Etzelmüller, B., Department of Geosciences, University of Oslo, P.O. Box 1047 Blindern, No - 0316 Oslo, Norway. E-mail: s.o.krogli@geo.uio.no , henning.dypvik@geo.uio.no, bernd.etzelmuller@geo.uio.no

Introduction

Impact structures are formed by collisions of comets and asteroids with planets or moons, and these crater structures may be preserved for millions of years. The general understanding of impact cratering and its significance for the Earth's development has increased dramatically during last decades. This is a result of intensive exploration of our solar system and the geological structure of planets. Planetary surface analysis shows that most of the planets have geomorphologies strongly influenced by impact cratering (Lowman 1997). Today we know that impact processes and crater formation have been (and will be) important processes for the development of our solar system (Melosh 1989; Montanari & Koeberl 2000).

On Earth 174 impact structures have been found so far (Earth Impact Database 2006). These craters seem unevenly distributed, partly the result of observations being focused on populated areas, rather than on less accessible locations. In Fennoscandia eighteen proven structures (Earth Impact Database 2006) have been found; ten in Finland, six in Sweden and only two in Norway (Gardnos and Mjølnir) (Fig. 1). The number of suggested ones is much higher (Abels et al. 2002), and in Norway we have a new, very promising candidate in the Ritland structure (Rogaland) (Fig. 1). Due to the varied surface geology and its areal extent it is difficult to calculate the expected number of impact structures of 5 – 10 km diameter in Norway. In this experiment we have searched for 5 – 10 km diameter structures in a 14,000 km^2 area of Precambrian rocks in Finnmark (Fig. 2).

When attempting to detect impact craters a simple but appropriate question might be: What do impact craters look like, and are such structures present in Norway? Normally the crater itself and its circular shape are regarded as important arguments for impact identification, in addition to structural and mineral evidence (Montanari & Koeberl 2000). The first possible registration of a crater is therefore often related to the identification of a circular surface structure. As the proven structures have large diameters (0,015 - 300 km (Earth Impact Database 2006)) and are dispersed over large areas, aerial photos, optical- and radar satellite images (e.g. Araujo et al. 2001; Chicarro et al. 2003; Earl et al. 2005) and coarse digital elevation models (DEM) (e.g. Portugal et al. 2004) have been commonly used in screening surveys.

There are mainly two important families used in pattern recognition of impact structures (Di Stadio et al. 2002); a) voted methods like the circular Hough Transform (e.g. Matsumoto et al. 2005; Portugal et al. 2004) and b) matching methods (e.g. Magee et al. 2003). In the approach presented below we used a digital matching technique, known from image analysis (e.g. Efford 2000; Gonzalez & Woods 1993) and automatic photogrammetric elevation generation (e.g. Heipke 1997; Schenk 1999).

The objective of this study was to develop an automatic technique to identify potential impact structures on the basis of morphometric analyses of a continuous topographic surface. Based on elevation data the aim was to find impact structure candidates, with a geometric shape matching the shape of a typical terrestrial impact

Fig. 1. The distribution of confirmed and proposed impact structures in Fennoscandia (Norway: 42 Gardnos, 73 Mjølnir, 91 Ritland). The figure is modified from Abels (2006).

crater of 5 – 10 km diameter. Analyses of the formation mechanics of the candidates must be evaluated by subsequent field inspections and laboratory analysis.

Geological setting

Norway comprises the western part of the Scandinavian Peninsula. The bedrock geology of Norway is dominated by Precambrian basement rocks (e.g. granites, gneisses, amphibolites and meta-sediments) and Caledonian successions (mostly Precambrian rocks and metamorphic Cambro-Silurian sediments stacked in nappe units). Limited areas of Devonian to Permian sediments and volcanics are also present (Fig. 2). The larger part of the bedrock is, however, covered by various Quaternary formations of mainly marine, glacial and fluvial origin. Geomorphologically the present topography of Norway is governed by peneplanation and stripping of marine strata during the Mesozoic (Lidmar-Bergstrøm et al. 2000; Peulvast 1985), a Tertiary uplift (Gjessing 1967; Strøm 1948) and related fluvial-dominated landscape formation in a warmer and partly drier climate than today (Gjessing 1967; Lidmar-Bergstrøm et al. 2000; Strøm 1948), followed by numerous Quaternary glaciations (Kleman & Borgström 1994). The latter accentuated the Tertiary fluvial valley pattern, while areas in central and northerly mountainous areas underwent little or no erosion due to the thermal conditions of the ice sheets (Lidmar-Bergstrøm et al. 2000, Sollid & Sørbel 1994).

Impact structures can be expected in all kinds of terrain, but with varying preservation potential. The oldest rocks, e.g. Precambrian gneisses and meta-sediments, are normally the hardest and may therefore have a good chance of displaying impact structures, due both to high age and competence. In contrast, the younger Cambro-Silurian formations, less consolidated sedimentary rocks and loose sediments will, as target rocks, not preserve impact structures as well. The Caledonian orogeny may also have altered possible earlier structures. The last glaciations in Scandinavia both eroded and covered (by sedimentation) possible pre-Quaternary impact structures. Based on this information, Finnmark appears as a suitable test area for further impact studies (Fig. 2).

Impact crater morphology

When celestial bodies (asteroids and comets) collide with planets or moons, the shape of the resulting crater is dependent on target material and the size, velocity and angle of the impacting body. The shapes and sizes of impact structures change with crater diameter, and fresh-appearing impact structures on the Moon illustrate this size-morphology relationship (Melosh 1989). The smallest impact craters have a simple bowl-shaped appearance, and as crater diameter increases, rim terracing and central peaks are more common. Crater morphology displays the same progression throughout the solar system, including the Earth, but the less well preserved terrestrial impact structures make them more challenging to classify (Earth Impact Database 2006). On Earth, the three basic types of impact structure are 1) simple structures, with a raised rim surrounding a bowl-shaped depression, 2) complex structures, larger in diameter, with a central peak, surrounded by an annular trough and a slumped rim (e.g. Grieve 1990; Melosh 1989) and 3) the even larger and more rare peak ring craters, consisting of a central peak (possibly with a depression) and possibly several ring structures creating annular basins (e.g. Turtle et al. 2005). The transition between simple and complex craters occur at diameters of about 2 km or 4 km, in sedimentary or crystalline rocks respectively (Grieve 1990).

Global processes acting on the surface of the Earth will eventually leave more poorly preserved impact structures (Turtle et al. 2005), which can be hard to distinguish from their surroundings. Their appearance then reflects geologic activity and post-impact physical processes (e.g. erosion, subduction). Fresh looking craters (e.g. Barringer crater, Arizona, USA) are easily recognized, but older impact structures may be eroded and filled with sediments. High velocity impacts produce circular craters, even at angles of low incidence (Melosh 1989). The presence of a circular-shaped depression is characteristic for

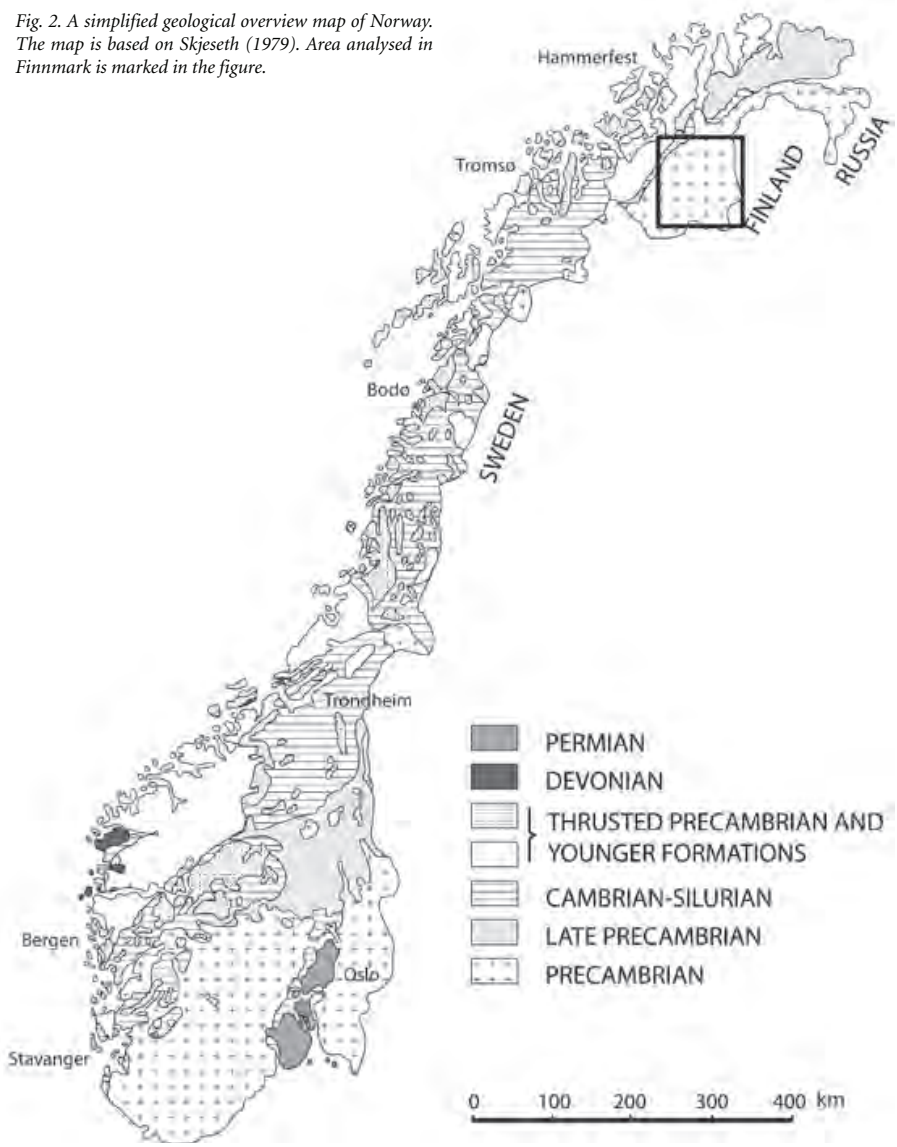

Fig. 2. A simplified geological overview map of Norway. The map is based on Skjeseth (1979). Area analysed in Finnmark is marked in the figure.

fresh impact structures and provides important information for use in the following analyses.

The geologically active Earth causes terrestrial impact structures to exhibit a high degree of variation as regards morphological characteristics and few fresh examples are left (Earl et al. 2005; Turtle et al. 2005). Still, some size characteristics are needed in order to construct a proper template. When searching for impact structures between 5 and 10 km in diameter, size-morphology relations for plausible impact structure depths, as presented in Grieve & Pesonen (1992), were used in the analysis. They divide the final morphology of complex terrestrial craters according to whether the target rocks are sedimentary or crystalline. This is due to the strength differences between the two. Complex craters are shallower when formed in sedimentary target material than in crystalline target material. In this analysis the equation (1) for sedimentary targets is used (Grieve & Pesonen 1992).

$$d_a = 0.12D^{0.30} \quad (1)$$

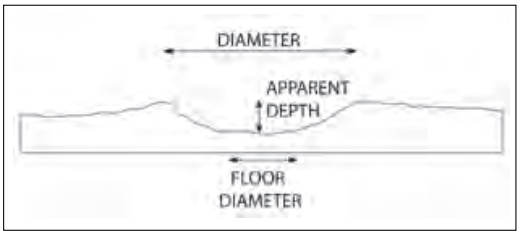

Fig. 3. Characteristic crater dimensions (diameter, apparent depth and floor diameter) displayed on a topographic profile. Modified from Pike (1977).

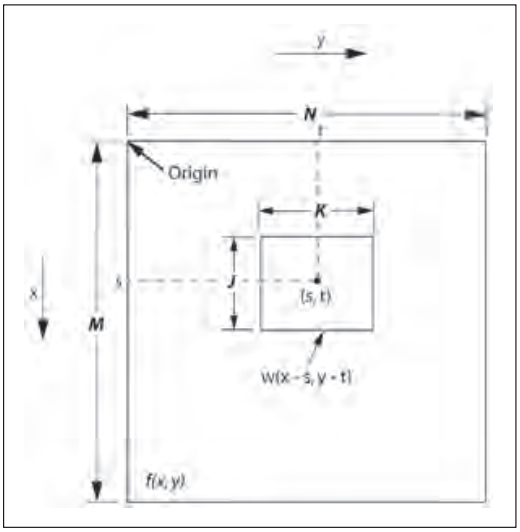

Fig. 4. Image and template arrangement for obtaining the correlation of respectively f(x,y) of size M x N and w(x,y) of size J x K at points (s,t), according to equation (3). The origin of f(x,y) is at its top left and the origin of w(x,y) at its centre. For any value of (s,t) inside f(x,y), the application will yield one correlation value. As s and t vary, w(x,y) moves around the image area (Gonzalez & Woods 1993).

where d_a is apparent depth (km), and D is diameter (km) (Fig. 3). The sedimentary target rock equation is chosen because this gives a shallower depth than the crystalline equation and may fit better the possibly new Norwegian impact structures after years of erosion.

A relation between crater diameter and floor diameter (2) based on lunar statistics (Pike 1977) is used to determine the size of a flat crater floor in the model.

$$D_f = 0.031 D_r^{1.765} \quad (2)$$

where D_f is the crater floor diameter, and D_r is the rim-crest diameter. It does not apply to craters less than 5 km in diameter (Pike 1977). The use of a rim-crest diameter in this equation and a probably apparent diameter in equation (1), implies that the crater floor diameter may be a bit undersized.

Data and methods

Digital elevation data

This study is based on digital elevation data in the computer represented as regular square grid models or arrays of elevation values. Such digital representation of the topographic surface is static and scale dependent since the size of the cells (pixels) building the terrain model is unchangeable (Burrough & McDonnel 1998). The matrix structure will allow programming of relatively complex algorithms, which can be easily used for digital elevation model (DEM) manipulation. Thus, this type of grid structure provides good possibilities for modelling any type of surface, and to investigate spatial interactions of features, being close or remote from the processed location (DeMers 2002). The resolution (scale) of the grid data is the relation between pixel size and size of the cell on the ground (Burrough & McDonnel 1998). When using grid-based DEMs to recognize landforms it is important to consider the resolution relative to the landform size (DeMers 2002). For the search of impact structures of 5 – 10 km diameter, we found a 100 m resolution satisfactory for these first analyses. A 3 x 3 kernel neighbourhood mean filter was applied to the elevation data to reduce noise.

Matching by local correlation

Template matching is a technique to measure the similarity between an unknown image and a known image acting as a feature model or template (Gonzalez & Woods 1993). Correlation analysis was used to describe the similarity between the known image (template) *w(x,y)* of size J x K within an image *f(x,y)* of size M x N, where it is assumed that J ≤ M and K ≤ N (Fig. 4). The result of each correlation analysis is an image, the size of image *f(x,y)*, where each pixel consists of a correlation value. The calculations are performed in the image region where *w* and *f* overlap, and high values of correlation indicate a match between *w(x,y)* and *f(x,y)* (Gonzalez & Woods 1993). Near the edges of image *f*, there will be no full overlap with *w*, and hence along the borders of the image *f(x,y)* there will be an area, half the size of *w*, where no correlation calculations are performed.

In our study we used spatial domain methods, where the procedures operate directly on the pixel values, while frequency domain methods operate on the results of a Fourier transform. The algorithm presented is based on a spatial domain matching procedure for calculating correlation coefficients (Gonzalez & Woods 1993), equation (3):

$$\gamma(s,t) = \frac{\sum_x \sum_y [f(x,y) - \bar{f}(x,y)][w(x-s,y-t) - \bar{w}]}{\left\{ \sum_x \sum_y [f(x,y) - \bar{f}(x,y)]^2 \sum_x \sum_y [w(x-s,y-t) - \bar{w}]^2 \right\}^{1/2}} \quad (3)$$

where s= 0, 1, 2, …, M - 1, t= 0, 1, 2, …, N - 1, $\overline{w}$ is the average value of the pixels in *w(x,y)* (computed only

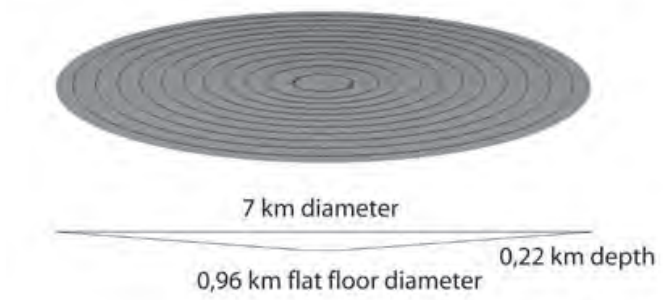

Fig. 5. An impact crater model, a circular depression template, of 7 km in diameter derived from equations (1) (Grieve & Pesonen 1992) and (2) (Pike 1977) shown as a shaded model with a depth contour interval of 20 m (above) and as a cross section (below). The template refers to w(x,y) in the correlation coefficient equation (3) and in Fig. 4.

once), $\bar{f}(x,y)$ is the average value of $f(x,y)$ in the region coincident with the current location of w, and the summations are taken over the image coordinates (pixels) common to both f and w. The correlation coefficient $\gamma(s,t)$ is scaled (normalised with respect to both image and template) in the range -1 to 1, independent of scale changes in the amplitude of $f(x,y)$ and $w(x,y)$ (Gonzalez & Woods 1993). Correlation analysis works well only if the size and orientation of the feature of interest are known and this information is used to design an appropriate template. If the size and orientation of the feature varies, a range of templates needs to be generated and each of them correlated with the image (Efford 2000). The automatic detection algorithm calculates the correlation between two datasets with a grid structure. It is a combination of C++ code and Arc Macro Language (AML). Input to the algorithm are an elevation data grid, $f(x,y)$, where the search for impact structures will take place, and a template grid, $w(x,y)$, smaller in size and representing the circular depressions to be found. Output of the algorithm is a map consisting of a similarity value (correlation coefficient) between the image and the template for every pixel position $\gamma(s,t)$ (Fig. 4).

Impact structure templates

In the correlation analysis performed, the unknown image represents the topography of the study area, in this case a part of Norway and consists of a DEM, while the template is a smaller DEM representing a theoretically defined impact crater. The general crater morphology forms the basis for creating this crater-shaped template (model). By using equations (1) and (2) to create templates and then including a degree of variation in the analysis, a match with terrestrial formations should be possible. Six templates of diameters 5 km, 6 km, 7 km, 8 km, 9 km and 10 km were made, based on these equations. They have a circular shape and the crater rim-walls were given a linear outline due to their most likely appearance after years of erosion. The crater floor is stipulated flat (Fig. 5). These models were used as templates in the regional analysis (template matching). They have the same resolution as the image, and the pixel values are of the same type and range as the pixels in the image.

Test area

The algorithm was tested on a synthetic 2,000 km^2 flat area, including one depression and one peak. The depression and the peak represent opposite, but similar geometries as the 5 km diameter template. By running a correlation analysis with a 5 km template and the test area, the correlation matching pattern of the template with "itself" is displayed. The correlation values show that in an ideal situation with a complete match, the pattern makes a circular formation with a correlation high of 1 and a negative correlation high of -1 (Fig. 6). A positive correlation as high as possible is preferred in the analysis, but also a value that picks out some candidates. The correlation coefficients tend, in a larger area, to be approximately normally distributed. A global threshold based on Niblack`s (1986) method is set to $t = \mu + w \cdot c$, where μ is the mean value, σ is the standard deviation of the correlation coefficient values, and w is an input weight. The threshold will divide the coefficient values into two classes, interesting (high values) and not interesting (low values). To keep the most promising candidates in each diameter size class, the same rule (a value of w) applies to all (5 – 10 km) correlation value images. It will still be a low correlation coefficient (ca. 0.50 – 0.65 for w = 2 – 2.5) compared to more ideal statistical solutions. This is a necessity because of the high variability of the circular depressions to be detected.

Pixel values above the threshold and within the immediate eight-cell neighbourhood of other pixels with higher values than the threshold, were spatially connected into a region. Area and perimeter were calculated for each region. The attribute roundness for a region can be described by $4\pi \cdot area / perimeter^2$, where the value for a circular disk is 1, otherwise less than 1. Identified candidates were regions having a roundness value above the algorithm input-*roundness* parameter.

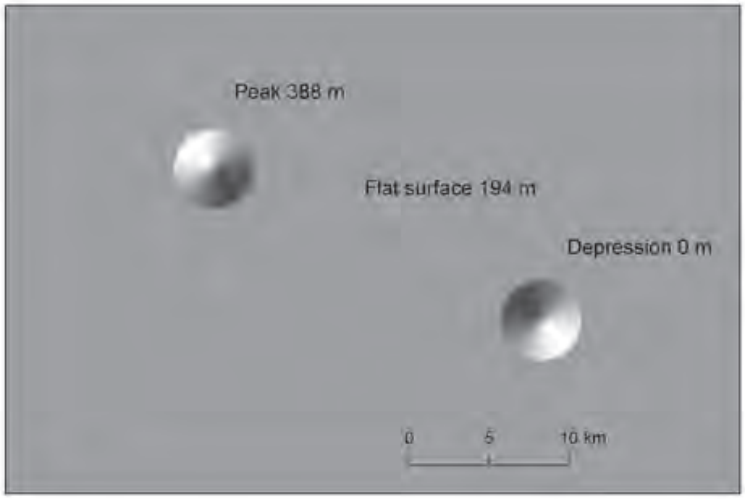

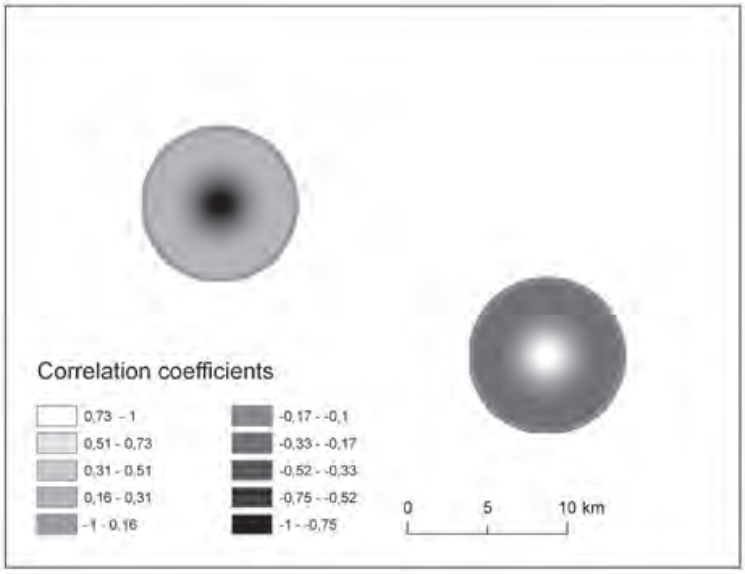

Fig. 6. The test area (abowe) is constructed as a flat surface broken by a peak and a depression with similar geometry as the 5 km diameter template. Correlation values (below) are only calculated in non flat areas, showing a circular pattern in an ideal correlation situation.

Results

Figure 7 displays the various steps using the 8 km template, parameters w = 2.3 and *roundness = 0.5*. These parameters and the range of templates (5 – 10 km) were applied on an area 14,000 km^2 in the county of Finnmark, northern Norway (Fig. 2), an area of mostly Precambrian basement rocks. The analysis yielded 23 circular depressions when not counting overlaps between the templates (Fig. 8). This procedure detects areas with different grades of circular shapes. When studying the detected structures in more detail, they also show hits of circular features in other close diameter intervals, although the templates was set to specific diameter values. In such cases the template may hit and correlate with a curved feature (wall) which is part of a smaller or larger structure.

102 structures were detected in a primary analysis of digital elevation data covering Norway with the 5 km diameter template, w = 2.5 (threshold then becomes 65.98) and *roundness* = 0.5. This number is too large for realistic field investigations, but during the screening studies we still want to keep a relative high number of structures for further analysis. The Gardnos impact structure, now seen as a circumform hanging valley, is located between the villages Gol and Nesbyen. In the regional analysis it gave the following maximum correlation coefficient values inside its boundaries: 0.52 (5 km), 0.47 (6 km), 0.41 (7 km), 0.35 (8 km), 0.37 (9 km) and 0.41 (10 km). Even if it turns up with a relative high cor-

relation coefficient in the 5 km case, this is partly due to coincidences of later landscape formation, which may to some extent reflect the impact event.

Discussion

The geometrical analyses display several circular features, partially matching the pre-described structure, and thereby sites of potential impact structures. Of these, at the best, only very few might have impact origin, when compared to the size distribution in Finland (4 impact structures in the interval 5 – 10 km) and Sweden (2 impact structures in the interval 5 – 10 km). The high number of potential Norwegian structures (102 of approximately 5 km diameter for Norway and 23 of 5 – 10 km diameter for a 14,000 km^2 area in Finnmark) and consequently a large number of false candidates are not suitable for a time saving search method. There are ways to restrict or vary the method:

1) The crater template appearance can be based on other equations or models, and thereby give different representations of impact structures (e.g. a template with non-linear walls).
2) The correlation coefficient threshold is the factor that determines how similar to the template the potential areas would appear, and a higher threshold (weight) would leave less circular depressions. A higher roundness value will leave fewer candidates.
3) The DEM and template spatial resolution will affect the results, and other resolutions may lead to different discoveries. But it is not necessarily true that a DEM with a finer resolution will give an increased spatial accuracy in terms of landform identification, since a finer-grained DEM may be more sensitive for other types of errors (DeMers 2002).

The Hough transform was developed to identify lines in images (Hough 1962). This technique, modified to identify circles or ellipses, and by applying different pre- and post-processing procedures, has shown promising results in detecting circular shapes in satellite images and DEMs of planetary bodies (e.g. Bruzzone et al. 2004; Earl et al. 2005; Kim et al. 2004; Matsumoto et al. 2005). In the presented template matching of this paper, the use of DEMs as input gives us an opportunity to take advantage of the horizontal profile (e.g. a depression) in addition to the vertical profile (circular shape). The variability of terrestrial impact structures in relation to topography requires a method that can handle this. The possibilities of the presented method to vary the threshold, the roundness value and vary the templates (e.g. topographic depression, linear or curved walls, flat or open crater floor), make template matching a convenient choice of technique.

A drawback is the computational time. The analysis performed with template diameters of 5 – 10 km in the

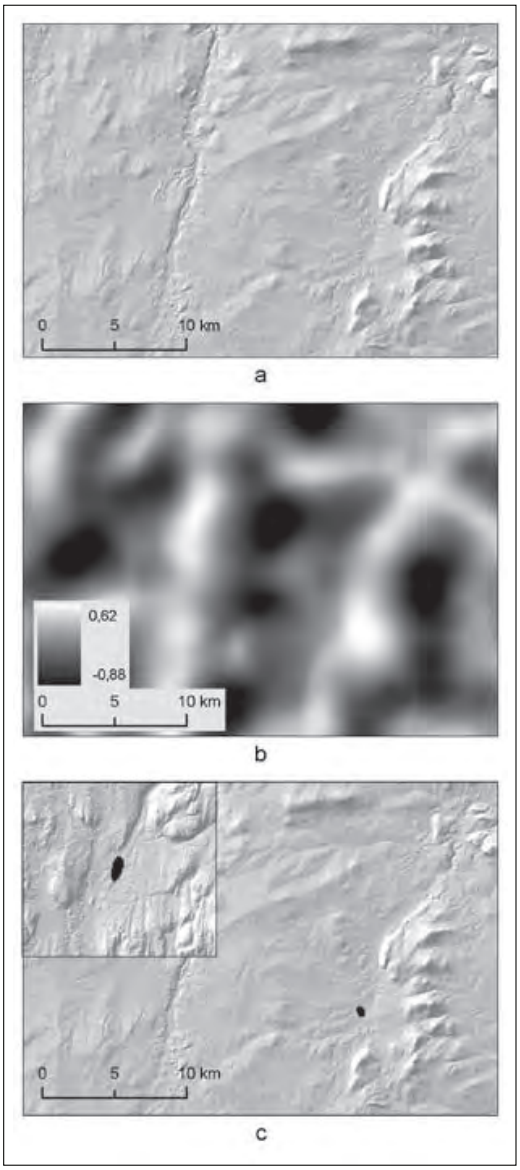

Fig. 7. Part of the area covered in Fig. 8, showing the steps of the algorithm: A shaded elevation model of the elevation data (a), a map of correlation values as computed by the algorithm for the 8 km diameter template (b). The correlation coefficients have values between -0.88 and 0.62, marked by dark to bright pixels. These values are divided into two classes by a threshold of 0.59 (w = 2.3), where black coloured pixels have higher values than the threshold and pixels of lower values than the threshold are not displayed (c). The black coloured pixels are then grouped. In this small area the result is one group (c). A roundness value is then calculated for the group which is kept, because it has a roundness value above the input parameter (roundness = 0.5). An inserted map in the upper left corner (c) displays a group, at the same scale but from a different location, with a roundness value below the input parameter and subsequently will be removed.

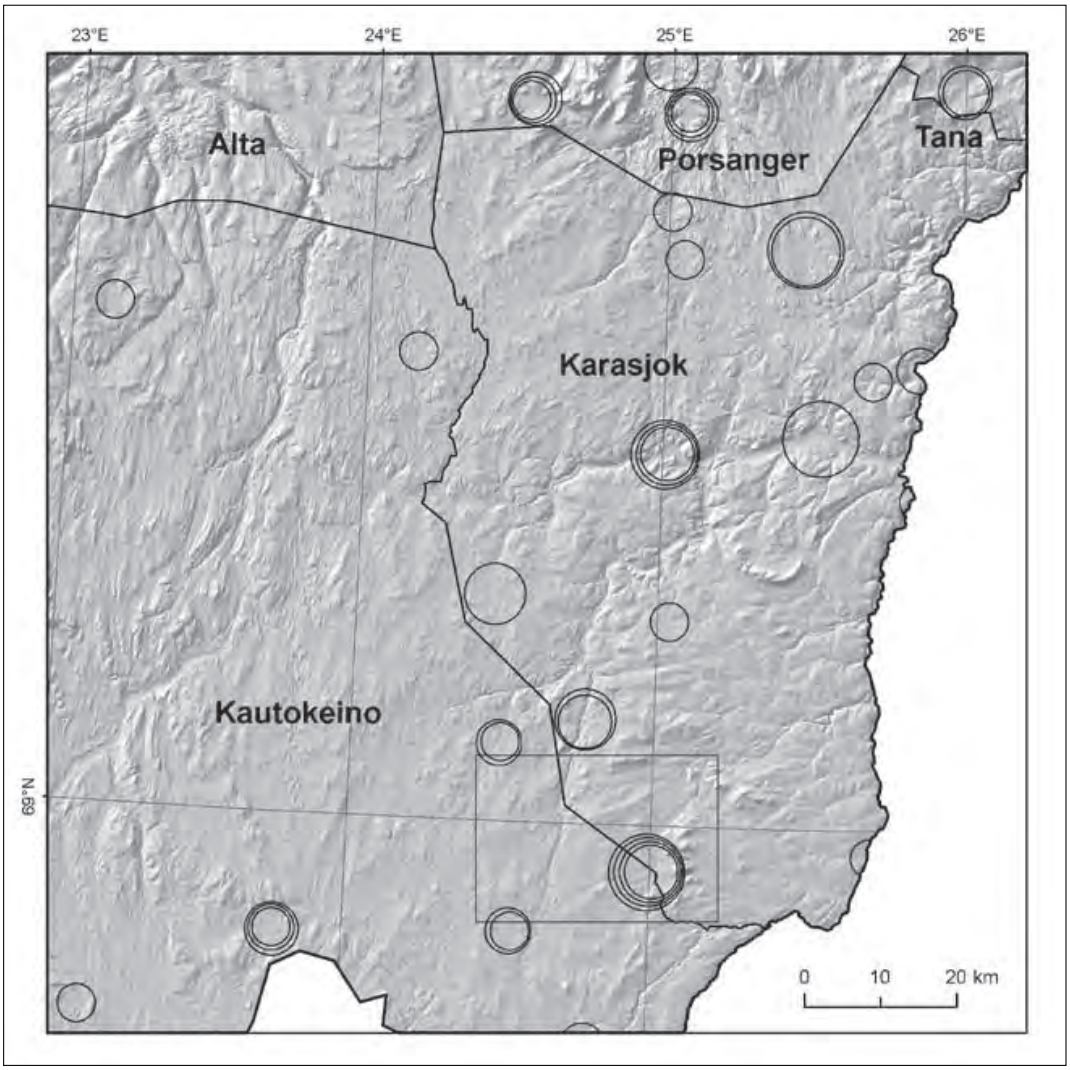

Fig. 8. An area of Finnmarksvidda including the municipality Karasjok and parts of Kautokeino, Alta, Porsanger and Tana, displaying detected circular depressions. For regional location see Fig. 2. The circular depressions are shown with circular symbols of diameters 5 – 10 km, the diameter referring to the template diameter detecting the individual structure. It shows 23 depressions, not counting overlaps between templates. The position of Fig. 7 is shown by the inserted square. Map projection: UTM EUREF89/WGS84 zone 35.

Finnmark area took several hours, and with larger templates it would take even longer. There is a possibility to compute the correlation in the frequency domain, using a fast Fourier transform algorithm to obtain the forward and inverse transforms. This is often a more effective solution (Gonzalez & Woods 1993). The spatial domain method used here is still a preferred option because of the convenient grid structure of the elevation data, and thereby an easier result interpretation.

The correlation function was normalized for amplitude changes via the correlation coefficient and for orientation via its circular symmetry, but it can be difficult to obtain normalization for changes in size. Such changes involve spatial scaling, a process that requires a high amount of computation (Gonzalez & Woods 1993). In the presented analysis such normalization was not performed, but six different-sized templates were used to inspect the range of potential structures in the 5 – 10 km interval. An inspection of the results showed that the method gave hits of circular features of diameter values close to the template diameters as well. In this way the intervals between the templates may be covered.

The diameter/depth and diameter/crater floor diameter relations of equations (1) and (2) were used to create the applied templates. It is a huge simplification to describe the shape of impact structures with just these two size morphology equations. In addition to the active surface processes working on the Earth and changing the crater appearance, the initial crater size depends on the target's surface gravity conditions (e.g. Lowman 1997). The crater floor equation is based on statistics from the Moon and a transfer of the relationship to the Earth may introduce some error. However, application of a too specified crater morphology can be misleading, since similarly sized terrestrial impact craters often exhibit contrasting characteristics (Earl et al. 2005). It is the template simplification and a correlation threshold set to less than the maximum result correlation coefficient value that makes it possible to pick out areas in the landscape, but finally resulting in a large number of circular depressions.

A high match percentage means that the structure has approximately the same shape as the circular template, but it could have been formed in several ways. Equation (1) is based on data from only five craters (Grieve & Pesonen 1992) and equation (2) is based on lunar statistics. This rather confined foundation, and the high degree of variation of known impact structures, contributes to the analytical uncertainty. The large number of candidates might call for a manual inspection of the digital data before field investigations, for example to exclude the less promising sites based on non crater-like features. Another solution could be to filter the results with other data or additional analysis. This could involve comparing the theoretical circular sites with geological or geophysical information, a possible part of the automatic detection. An improved exercise would need to compute different time models reflecting the various environmental settings through geological time, presently an immense task. Therefore the next step to evaluate the formation mechanisms of the detected depressions would be field inspections of the various structures.

Conclusions and further studies

From this study the following conclusions can be drawn:

a) An automatic correlation algorithm based on gridded DEMs on a regional scale seems suitable to identify depressions with circular features. This is a first approach and represents an oversimplification regarding automatic impact crater search.
b) These morphometrical DEM analyses provide a powerful and inexpensive tool for first landform assessments of circular-shaped features of approximately 5 – 10 km diameter, given the 5 – 10 km diameter templates. By combining these results with other regional digital information, we hope to reduce the large number of potential impact structures.

This study represents a first screening analysis for potential impact structures in Norway. In addition to analyses of digital elevation data, future programs will explore other types of available regional digital information. This could be satellite data (e.g. radar) and geophysical data (e.g. gravity, magnetic). Geophysical characteristics have been studied for many impact structures and a negative, often circular, gravity anomaly which changes density after impact, is common (Pilkington & Grieve 1992). Magnetic anomalies display large variations across impact craters, but a magnetic low is often a dominant effect (Pilkington & Grieve 1992). The nature of the geophysical signatures implies that using different digital terrain and image analysis techniques (e.g. geomorphometry, Hough transforms), and considering just the circumform shape and not a depression, might be rewarding. Different data may be analysed separately or in combination in order to reduce the number of potential impact structure candidates, and hopefully to find new promising ones.

Acknowledgments: This study was funded by the University of Oslo (Department of Geosciences, the Faculty of Mathematics and Natural Sciences, Central Administration) and the Research Council of Norway (NFR#170617/v30). The analyses were carried out at the Laboratory of Remote Sensing and GIS at the Department of Geosciences, Division for Physical Geograpy, University of Oslo. Based on an earlier template version (deeper) and a manual inspection of the resulting sites, 1200 structures were presented on a website (www.geo.uio.no/groper) (only in Norwegian). A national school project was launched in cooperation with The Research Council of Norway, where interested classes or students could visit and do the first simple observations of the structures (NFR#171890). This public involvement may have triggered increased public interest in science. In this connection we thank Marianne Løken, Thomas Keilman and Kate Alice Furøy (The Nysgjerrigper Science Knowledge Project, Research Council of Norway) for their inspiring support. The review comments by H. Henkel and S.C. Werner significantly improved the manuscript. Thanks to guest editor Odleiv Olesen for editorial handling of the manuscript. We want to thank all individuals and institutions.

References

Abels, A. 2006: <http://www.geophysics.helsinki.fi/tutkimus/impacts/maps.html> (Accessed: 1 Feb 2006)

Abels, A., Plado, J., Pesonen, L.J. & Lehtinen, M. 2002: The impact cratering record of Fennoscandia - a close look at the database. *In* Plado, J. & Pesonen, L.J. (eds.): *Impacts in Precambrian Shields*, 1-58. Springer, Berlin Heidelberg.

Araujo, A.A., Hadad, R. & Martins Jr, P. 2001: *Identification of pattern in satellite imagery - circular forms*. Nonlinear Image Processing and Pattern analysis, XII, Proceedings of SPIE, 25-34.

Bruzzone, L., Lizzi, L., Marchetti, P.G., Earl, J. & Milnes, M. 2004: *Recognition and detection of impact craters from EO products.* Proceedings of ESA-EUSC 2004 - Theory and Applications of Knowledge-Driven Image Information Mining with Focus on Earth Observation, Madrid

Burrough, P.A. & McDonnel, R.A. 1998: *Principles of Geographical Information Systems*. Oxford University Press, Oxford, 333 pp.

Chicarro, A., Zender, J., Lictenegger, J., Abels, A., Barbieri, M. & Paoloni, S. 2003: *ERS Synthetic Aperture Radar Imaging of Impact Craters.* ESA Publications Division, Noordwijk, 69 pp.

DeMers, M.N. 2002: *GIS modeling in raster.* John Wiley & Sons, New York, 203 pp.

Di Stadio, F., Costantini, M. & Di Martino, M. 2002. Craters - executive summary: Survey of algorithms for automatic recognition of impact craters. *Telespazio-EO Doc.No. 190.193-SPA-ES-001 - Issue 1.0.* Rome, Italy, ESA contract report, http://www.esa.int/gsp/completed/ExecSumAll01_A19.pdf, 28 pp.

Earl, J., Chicarro, A., Koeberl, C., Marchetti, P.G. & Milnes, M. 2005: *Automatic recognition of crater-like structures in terrestrial and planetary images.* Lunar and Planetary Science XXXVI, Lunar and Planetary Institute, Houston, USA, abstract no. 1319.

Earth Impact Database. 2006: <http://www.unb.ca/passc/ImpactDatabase/> (Accessed: 1 Mar 2006)

Efford, N. 2000: *Digital Image Processing, a practical introduction using Java.* Addison-Wesley, Harlow, 340 pp.

Gjessing, J. 1967: Norway's paleic surface. *Norsk Geografisk Tidsskrift 21*, 69-132.

Gonzalez, R.C. & Woods, R.E. 1993: *Digital Image Processing,* 1st Edition. Addison-Wesley, Reading, Massachusetts, 703 pp.

Grieve, R.A.F. 1990: Impact cratering on the Earth. *Scientific American* 262, 44-51.

Grieve, R.A.F. & Pesonen, L.J. 1992: The terrestrial impact cratering record. *Tectonophysics 216*, 1-30.

Heipke, C. 1997: Automation of interior, relative, and absolute orientation. *ISPRS Journal of Photogrammetry & Remote Sensing 52,* 1-19.

Hough, P.V.C. 1962: *Methods and Means for Recognizing Complex Patterns.* U.S. Patent No. 3069654 pp.

Kim, J.R., Muller, J.-P. & Morley, J.G. 2004: *Quantitative Assessment of automated crater detection on Mars.* XXth ISPRS Congress, Istanbul, Turkey, pp. 816-821.

Kleman, J. & Borgström, I. 1994: Glacial landforms indicative of a partly frozen bed. *Journal of Glaciology 40*, 255-264.

Lidmar-Bergstrøm, K., Ollier, C.D. & Sulebak, J.R. 2000: Landforms and uplift history of southern Norway. *Global and Planetary Change 24*, 211-231.

Lowman, P. 1997: Extraterrestrial impact craters. *Oklahoma Geological Survey Circular 100*, 55-81.

Magee, M., Chapman, C.R., Dellenback, S.W., Enke, B., Merline, W.J. & Rigney, M.P. 2003: *Automated identification of Martian craters using image processing.* Lunar and Planetary Science XXXIV, Lunar and Planetary Institute, Houston, USA, abstract no. 1756.

Matsumoto, N., Asada, N. & Demura, H. 2005: *Automatic crater recognition on digital terrain model.* Lunar and Planetary Science XXXVI, Lunar and Planetary Institute, Houston, USA, abstract no. 1995.

Melosh, H.J. 1989: *Impact cratering, A Geologic Process.* Oxford University Press, New York, 240 pp.

Montanari, A. & Koeberl, C. 2000: *Impact stratigraphy; the Italian record.* Springer-Verlag, Berlin-Heidelberg-New York, 364 pp.

Niblack, W. 1986: *An Introduction to Digital Image Processing.* Prentice Hall, Englewood Cliffs, 115-116 pp.

Peulvast, J.-P. 1985: Post-orogenic morphotectonic evolution of the Scandinavian Caledonides during the Mesozoic and Cenozoic. *In* Gee, D.G. & Sturt, B.A. (eds.): *The Caledonian Orogen - Scandinavia and Related Areas*, 979-995. Wiley, Chichester.

Pike, R.J. 1977: Size-dependence in the shape of fresh impact craters on the moon. *In* Roddy, D.J., Pepin, R.O. & Merrill, R.B. (eds.): *Impact and Explosion Cratering*, 489-509. Pergamon Press, New York.

Pilkington, M. & Grieve, R.A.F. 1992: The geophysical signature of terrestrial impact craters. *Reviews of Geophysics 30,* 161-181.

Portugal, R.S., de Souza Filho, C.R. & Bland, P.A. 2004: *Automatic crater detection using dem and circular coherency analysis - a case study on south american craters*. 67th Annual Meteoritical Society Meeting, Rio de Janeiro, Brazil, abstract no. 5096.

Schenk, T. 1999: *Digital photogrammetry.* TerraScience, Laurelville, Ohio, 428 pp.

Skjeseth, S. 1979: *Innføring i Norges geologi*. Landbruksforlaget Oslo, 37 pp.

Sollid, J.L. & Sørbel, L. 1994: Distribution of glacial landforms in southern Norway in relation to the thermal regime of the last continental ice-sheet. *Geografiska Annaler 76*, 25-35.

Strøm, K. 1948: The geomorphology of Norway. *Geographical Journal CXII*, 19-27.

Turtle, E.P., Pierazzo, E., Collins, G.S., Osinski, G.R., Melosh, H.J., Morgan, J.V. & Reimold, W.U. 2005: Impact structures: What does crater diameter mean? *In* Kenkmann, T., Hörz, F. & Deutch, A. (eds.): *Large meteorite impacts III: Geological Society of America Special Paper 384*, 1-24.

II

This article is removed.

III

This article is removed.

Extended abstract I

Automatic and semi-automatic detection of possible meteorite impact structures in the Fennoscandian shield using pattern recognition of spatial data

Svein Olav Krøgli, Bernd Etzelmüller and Henning Dypvik

Department of Geoscience, University of Oslo,
PO Box 1047 Blindern, N-0316 Oslo, Norway
s.o.krogli@geo.uio.no

Abstract. The search for impact structures in Norway is still in its infancy and compared to Sweden (6) and Finland (11) the number of discovered Norwegian structures (2) is low. This initiated a systematic search for possibly new impact structures in Norway by geographic information and image analysis on available regional geodata. Such data might be digital elevation models (DEM), satellite data (optical, radar), bedrock, lineaments and probably most promising, geophysical data (e.g. gravity, aeromagnetic). A matching algorithm using a DEM and impact crater templates has been performed, and a circular Hough transform algorithm is tested on the same data.

1 Introduction

The search for impact structures in Norway is still in its infancy and compared to Sweden (6) and Finland (11) the number of discovered Norwegian structures (2) is low [1]. This initiated a systematic search for new impact structures in Norway. Areas inhabiting impact structure characteristics, named here possible meteorite impact structures, are searched by geographic information and image analysis on regional geodata.

Impact structures are formed by collisions of comets and asteroids, with planets or moons, and these crater structures may be preserved for millions of years. Fresh impact craters are characterized by their circumform shape [8]. The active Earth (e.g. erosion, sedimentation, subduction) will eventually leave more poorly preserved impact structures [12], which can be hard to distinguish from their surroundings. The circular shape, even if less apparently, makes impact structures ideal objects for the applications of automatic detection methods. Candidates may be detected, but field observations are needed to determine if the structure has an impact origin (shock metamorphic features).

1.1 Joint project

The Norwegian search project is part of a cooperation program between the European Space Agency (ESA-ESTEC), the Universities of Oslo and Helsinki

along with the Geological Surveys of Norway and Finland. The project objectives are to develop a workable automatic search algorithm and to discover new impact structures in Fennoscandia.

2 Data

In order to detect candidates, available regional digital information will be explored for circular shapes. Such data might be digital elevation models (DEM), satellite data (optical, radar), bedrock, lineaments and probably most promising, geophysical data (e.g. gravity, aeromagnetic). Geophysical characteristics have been studied for many impact structures and a negative, often circular, gravity anomaly which changes density after impact, is common [9]. Magnetic anomalies display large variations across impact craters, but a magnetic low is often a dominant effect [9].

3 Methods

Two of several techniques in use to detect circular features in digital data are matching and voting algorithms. Variations of the Hough transform voting technique are the most common in the field of planetary impact crater counting, e.g. [2].

Using a matching algorithm, a first systematic search for possible Norwegian impact structures was based on an automatic scan of DEMs [7]. The DEM resolution applied were 100 m. Topographic crater templates (circular depressions), representing typical impact structures in the interval 5-10 km, were made based on depth/diameter relations from terrestrial impact structures [5] and lunar impact structures [8] [10]. The circular shaped templates of fixed diameters were cross-correlated with the DEM. The template matching output is an image the size of the DEM, consisting of a value of similarity between the template and the DEM in each pixel. The similarity is calculated by a correlation coefficient [4],

$$\gamma(s,t) = \frac{\sum_x \sum_y [f(x,y) - \bar{f}(x,y)][w(x-s,y-t) - \bar{w}]}{\left\{\sum_x \sum_y [f(x,y) - \bar{f}(x,y)]^2 \sum_x \sum_y [w(x-s,y-t) - \bar{w}]^2\right\}^{1/2}}, \quad (1)$$

where w(x,y) is the template, f(x,y) is, in this application, the DEM and the correlation is obtained at point (s,t). A post-processing step, including a threshold to separate between low and high match pixels, grouping of high match pixels and a group classifier will gain areas of interest, potential impact structures.

The nature of the geophysical signatures of impact structures implies considering just the circumform shape and not a circular depression (the template matching), might be rewarding. A method that can solve this is the Hough transform. The Hough transform was developed to identify lines in digital images [6]. This technique, modified to identify circles, and by applying different

pre- and post-processing procedures (edge detection, result filtering), has shown promising results in detecting impact structures on satellite images and DEMs of planetary bodies, e.g. [2].

A circular Hough transform attend the problem of the probability that a set of pixels (from now on called gradient pixels) lies in a circular pattern. It is often an edge detection of an image that results in these gradient pixels. An advantage of the Hough transform is that if the circular object itself is a bit occluded, the transform still manages to detect the structure. It is also independent of position, rotation and scale [11]. Given an image of gradient pixels and a radius r, potential circle centres are calculated for each gradient pixel. The potential circle centre are all pixels a distance r away from the gradient pixel. These potential circle centres are accumulated in a matrix and the procedure is repeated for all gradient pixels. If the radius is not known, the Hough transform must be calculated for several values of radius. The circle accumulation matrix gets a dimensionality of three, each cell in the accumulation matrix categorized by a potential circle centre (a,b), which must be inside the original image, and a radius r, inside a radius interval set prior to the analysis. This because a circle is parameterized by three parameters a,b,r,

$$(x_1 - a)^2 + (x_2 - b)^2 = r^2 \ , \tag{2}$$

where the circle has centre (a,b) and radius r [4], [11]. The frequency of the accumulated cells tell if several of the gradient pixels belong to the same circle. A high value indicate that a circle probably are present in the original image (Fig. 1).

4 Results

4.1 Template matching

A DEM covering a 7,000 km^2 area of Precambrian rocks in Finnmark resulted in 23 structures partly matching the templates, using a correlation coefficient of 36. They display different varieties of circular shapes (Fig. 2), and most likely have several different origins. The results detects more structures than what is the expected number of impact structures of this diameter interval in an area of this size.

4.2 Circular Hough transform

The analyses is performed on a gray level (8 bit) image, a shaded elevation model calculated from a part of the digital elevation model used in the template matching. The image is smoothed using a low pass filter and gradient pixels are found using the Sobel edge detection operator and a threshold of 80. A radius interval from 20 to 60 pixels (ca. 5-10 km) was set prior to the analyses and a threshold of 60 was applied to the accumulation matrix (Fig. 3 and 4).

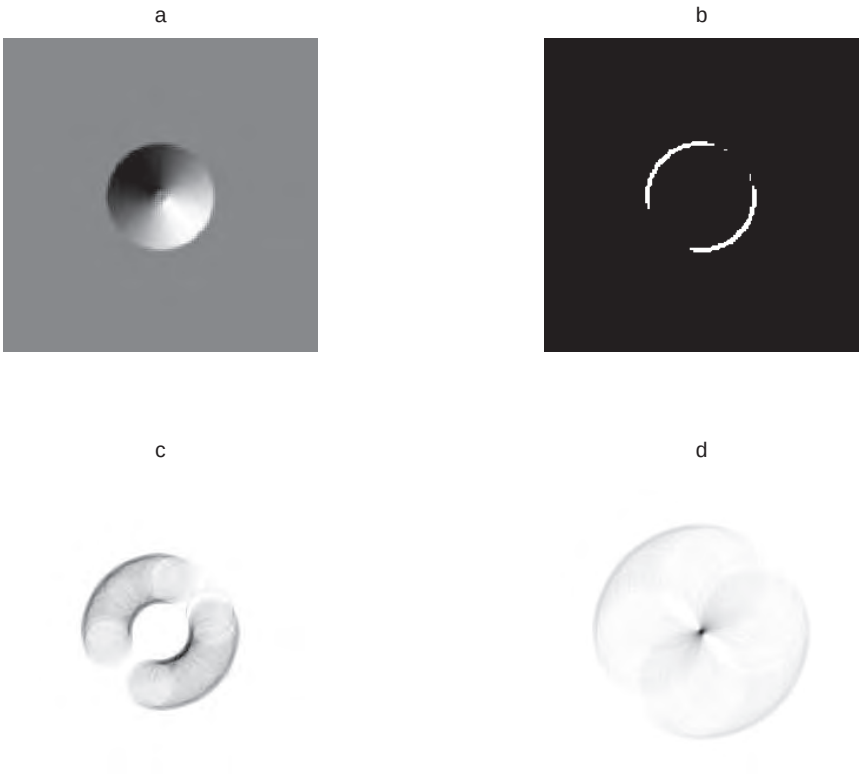

Fig. 1. A shaded elevation model of a synthetic circular depression made for the template matching analyses a), having a radius of approximately 45 pixels. b) displays a thresholded (threshold = 100) gradient image (white pixels are gradient pixels), and the results of a Hough transform with radius 20 and 45 pixels are shown in c) and d) respectively. The peak in Fig. d) have a larger value than the peaks in c), indicating that this peak is a probably circle centre.

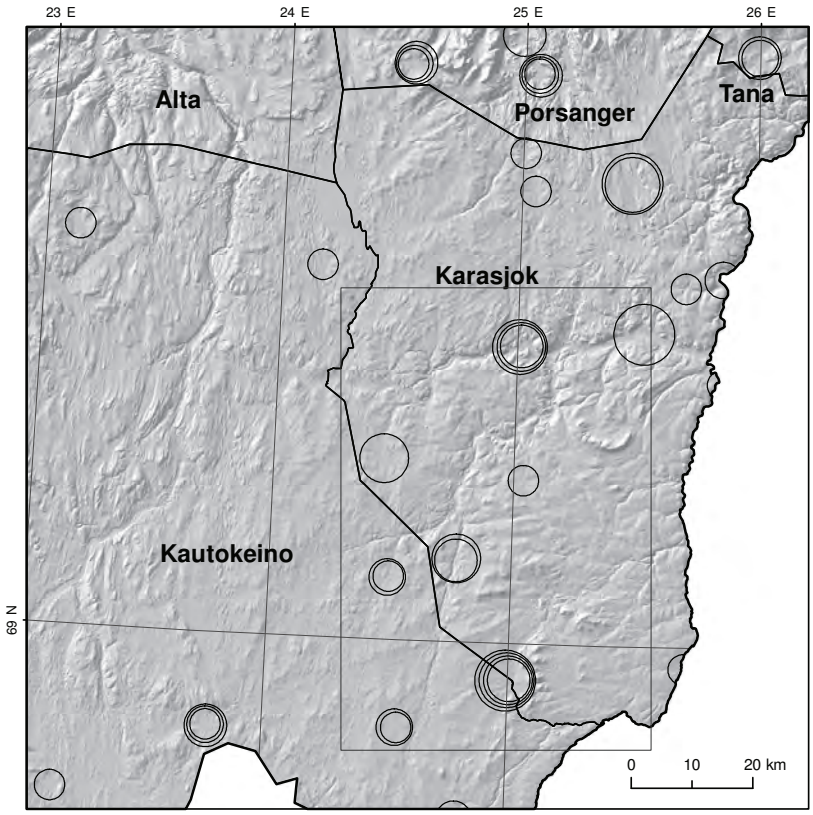

Fig. 2. An area of Finnmarksvidda displaying detected circular depressions [7]. The circular depressions are shown with circular symbols of diameters 5-10 km, the diameter referring to the template diameter detecting the individual structure. It shows 23 depressions, not counting overlaps between templates. The position of Fig. 3 and 4 is shown by the square. Map projection: UTM EUREF89/WGS84 zone 35.

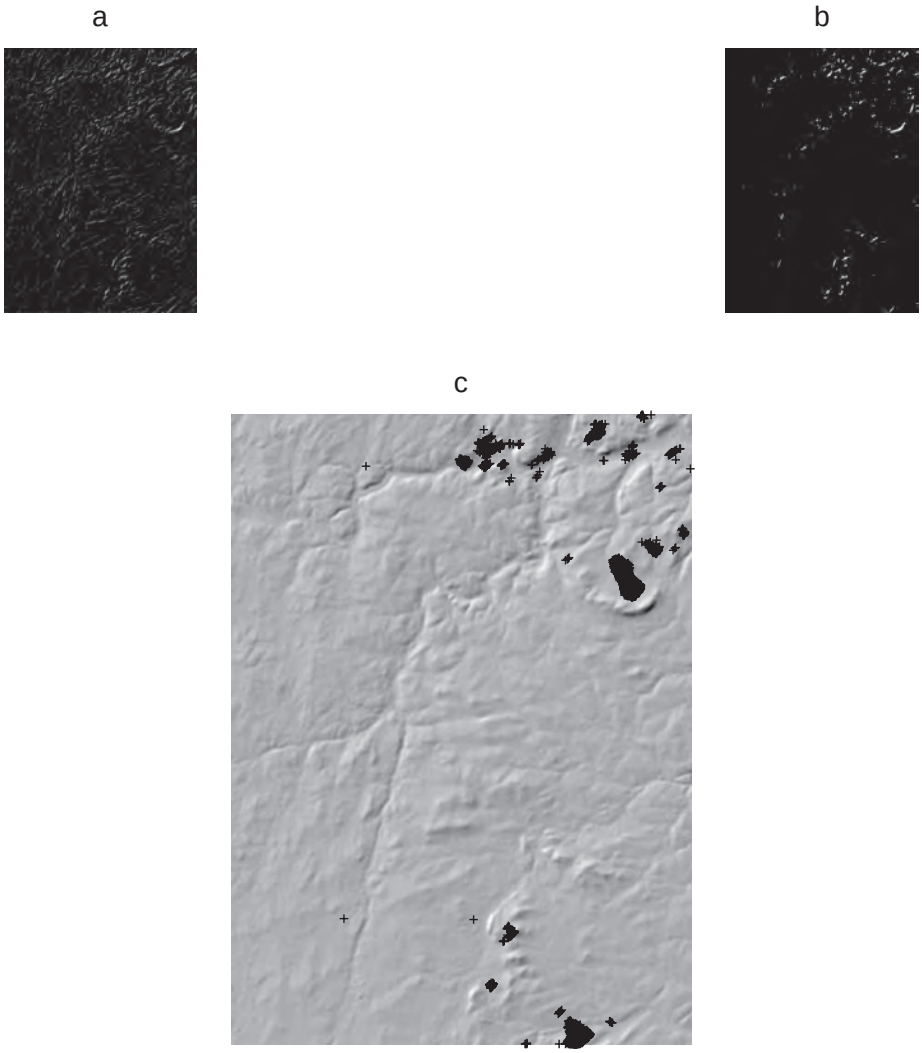

Fig. 3. A gradient image of part of the area of Finnmarksvidda displayed in (Fig. 2) calculated by the Sobel operator is shown in a), and results after a threshold of 80 on this image b). c) displays detected circular centres having a from 20 to 60 pixels, approximately 5-10 km in this resolution.

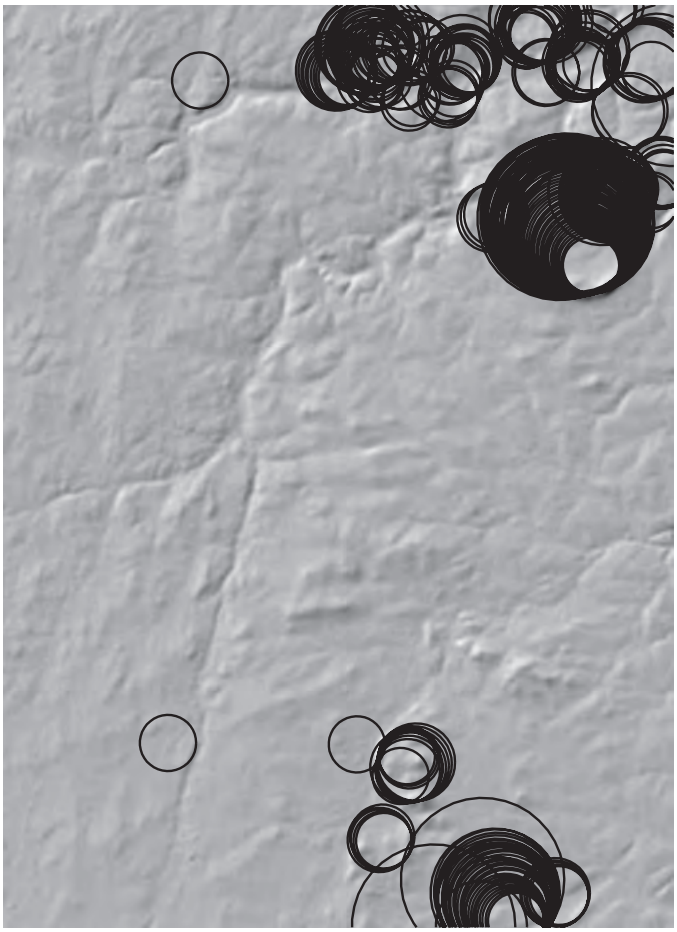

Fig. 4. Circles with radius r from circle centres (Fig. 3c). The clearly visible half circular structure in north east (Fig. 3c) is found by most radiuses, indicating that a stricter accumulation threshold could have been used, but on the expense of loosing some of the other structures.

5 Discussion

The template matching detects a high number of possible meteorite impact structures, exceeding what could have been expected. The use of a higher correlation coefficient would have reduced this number, but the variability of the topography and impact structures defend such a low value.

The Hough transform enforce some decisions to be made, e.g. how to find proper gradient pixels (in addition to edge detection methods, terrain parameters like slope and curvature might be explored) and how to decide a threshold for the gradient image and the accumulation matrix. The thresholds in this Hough analyses was based on visual inspection. Global thresholds were used, but there exists locally adaptive threshold methods that might improve the results. Enough gradient pixels to capture structures are needed, but not to many. The threshold of the accumulation matrix settle whether a cell is a potentially circle centre or not. If a circle is occluded it will lead to a lesser cell value of that (a,b,r) combination, still it may be a high enough value to detect the circle. Gradient pixels of an uneven or noisy circle accumulate not only to a specific cell, but rather a cluster of cells, where the cluster mass centre may represent the circle centre.

The Hough transform analyses was performed on a gray level image, but a digital elevation intensity image might also be used, leading to other decisions and results. Generalized Hough transforms are developed to deal with more complex shapes, e.g. circles not exactly circular, and could be a future direction of the impact structure detection analyses.

Crater detection on e.g. Mars deals with more clearly visible structures. The Hough transform analysis showed that structures not clearly visible in the original image might not be detected. Applying this technique to terrestrial environments may force minor adjustments, but also enable the possibility to perform the analysis on a broad set of geodata. These results suggests further analysis, including incorporation of other methods, fusion of different data and combination of results.

Acknowledgements. Geophysical data are provided by the Geological Survey of Norway (NGU). Project is supported by The Research Council of Norway.

References

1. Abels, A., Plado, J., Pesonen, L.J. and Lehtinen, M. The Impact cratering Record of Fennoscandia A New Look at the Database. In Plado, J., Pesonen, L.J., editors, *Impacts in Precambrian Shields*,:1-58. Springer, 2002.
2. Earl, J., Chicarro, A., Koeberl, C., Marchetti, P.G. and Milnes, M. Automatic recognition of crater-like structures in terrestrial and planetary images. *Lunar and Planetary Science XXXVI*, Lunar and Planetary Institute, Houston, USA, abstract no. 1319, 2005
3. Earth Impact Database. (http://www.unb.ca/passc/ImpactDatabase/) (Accessed: 1 Jun. 2007).

4. Gonzalez, R.C. and Woods, R.E. *Digital image processing*, 1th. ed., Addison-Wesley, Reading, Massachusetts, 1993.
5. Grieve, R.A.F. and Pesonen, L.J. The terrestrial impact cratering record. *Tectonophysics* 216: 1-30, 1992.
6. Hough, P.V.C. *Methods and Means for Recognizing Complex Patterns.* U.S. Patent No. 3069654, 1962.
7. Krøgli, S.O., Dypvik, H. and Etzelmüller, B. Automatic detection of circular depressions in digital elevation data in the search for potential Norwegian impact structures. *Norwegian Journal of Geology* 87: 173-182, 2007.
8. Melosh, H.J. *Impact cratering, A Geologic Process*, University Press, 1989.
9. Pilkington, M. and Grieve, R.A.F. The Geophysical Signature of Terrestrial Impact Craters. *Reviews of Geophysics* 30: 161-181, 1992.
10. Pike R.J. Size-dependence in the shape of fresh impact craters on the moon. In Roddy, D.J., Pepin, R.O., Merrill, R.B. editors, *Impact and Explotion Cratering*: 489-509. University Press, 1977.
11. Sonka, M., Hlavac, V. and Boyle, R. *Image Processing, Analysis, and Machine Vision.* 2nd. ed., PWS Publishing, Pacific Grove, USA, 1999.
12. Turtle, E.P., Pierazzo, E., Collins, G.S., Osinski, G.R., Melosh, H.J., Morgan, J.V. and Reimold, W.U. Impact structures: What does crater diameter mean? In Kenkmann, T., Hrz, F., Deutch, A., editors, *Large meteorite impacts III*, Geological Society of America Special Paper 384: 1-24, 2005.

Extended abstract II

Correlation of Radial Profiles Extracted from Automatic Detected Circular Features, in the Search for Impact Structure Candidates

S. O. Krøgli[1], H. Dypvik[1], B. Etzelmüller[1]

[1]Department of Geosciences, University of Oslo
P. O. Box 1047, NO-0316 Oslo, Norway
Telephone: 0047 22856656
Fax: 0047 22854215
E-mail: sveinkro@geo.uio.no, henning.dypvik@geo.uio.no, bernd.etzelmuller@geo.uio.no

1. Introduction

Impact cratering is a common geological process in the Solar System and most planetary bodies display geomorphologies strongly influenced by impacts (Lowman 1997). Fresh impact craters are normally characterized by a circular morphology (Melosh 1989). This surface expression is modified on Earth by active geological processes. The variation of terrestrial impact structure expressions suggests a simple characteristic to use in automatic detection, usually the circular shape. Automatic techniques may detect candidates in regional data, but field and laboratory analysis are required to possibly confirm an impact origin by finding shock metamorphic effects or traces of meteorites (Koeberl 2004).

A first approach to detect candidates was conducted comparing typical impact crater morphologies and topography (Krøgli et al. 2007). Size-dependency scaling characteristics, e.g. relations of crater diameter, crater floor diameter and crater depth, have been established for heavily cratered areas like the Moon (Pike 1977). On Earth the catalog presently consists of 176 proven impact structures (Earth Impact Database 2009). Despite the low number, size-dependencies have also been established for terrestrial impact structures (e.g. Grieve and Pesonen 1992). To search crater-like circular depressions Krøgli et al. (2007) calculated correlations between circular templates, based on terrestrial and lunar size relations, and digital elevation models.

The geophysical properties of impacted target areas may also change during impact and can be found as anomalies in e.g. gravity and magnetic potential field data. Fracturing and brecciation of target rocks and the presence of low-density sedimentary infill cause a circular gravity low, while a central uplift of heavier rocks from deeper crustal levels may cause a circular gravity high (e.g. Grieve and Pilkington 1996). There has not been found a one to one relationship between shapes of magnetic anomalies and impact structures, but circularity may often be present (French 1998). An algorithm that detects circular orientations of slope values has been constructed to search impact structure candidates, treating regional gravity and aeromagnetic data as surface models. The algorithm, that also works on DEMs, examines only the outline of possible circular features.

Both methods (template matching and circular oriented slope values) detected features with different degrees of circularity. The number of detected features depends on the choice of threshold, but is usually large and requires further manual or automatic analysis to refine the number before field investigations. Results can be compared to maps of e.g. geology and drainage patterns and to additional methods and

data (e.g. multispectral images). An approach to reduce the number of candidates is presented here as a filter technique, removing candidates from symmetry measurements.

2. Symmetry in Circular Features

The symmetry measurements are based on correlation coefficients between radial profiles in automatic detected circular features. For each circular feature the algorithm extracts eight profiles from the DEM or geophysical surface, radiating from centre to the length of the radius. These profiles are placed in a matrix consisting of a number of columns equal to the number of profiles (default eight) and a number of rows equal to the number of pixels in profiles (depending on radius). First only a part of the matrix, the first three pixels of each profile, is included in the correlation coefficient calculations. When counting pixels the first pixel of a profile is on the circular outline and the next pixel one step towards centre, and so on. A profile is marked if it does not correlate with any of the other profiles. The matrix then includes the pixels on the next step towards centre. Again a correlation coefficient calculation between profiles is performed, this time without marked profiles. This continues until all profiles are marked (no more correlation) or the end of profiles is reached (Fig. 1). Two profiles may then go the whole distance to the centre, even if situated at opposite sides. The percentage of pixels included in correlated profiles compared to total number of pixels in profiles is saved.

3. Results and Discussion

Fig. 2 displays the effect of symmetry filtering on automatic detected circular features. The reasoning behind equalizing two features having similar total profile distances is to keep features that have few but long correlation profiles, e.g. in just a corner or half of the circle. They may represent impact structures where only parts of the earlier circularity is present. Opposite, one could include a weight in order to reward if all the eight profiles are correlated a distance. The latter may exclude valleys, where two opposite ridges may have some of the characteristics of a partly circular feature. In the presented algorithm the profiles are extended from the rim an inwards, calculating correlation coefficients for each step, leaving out non-correlating profiles. This emphasizes the rim area and downgrades the middle area, which may be promising in an impact structure candidate detection. Initiating the calculations with a minor number of pixels could miss out profiles that would correlate at a later stage, if more pixels had been included. A future filter value might be calculated incorporating correlation results of profiles starting both from the outline and from the centre, or even including complete profiles. The choice of eight profiles, always with the same profile configuration, influence results. It is the profile shapes that are correlated, indicating that the profiles might be located at different elevations. Fig. 2 displays that the filter reduce the number of automatic detected impact structure candidate sites based on non-symmetrical characteristics.

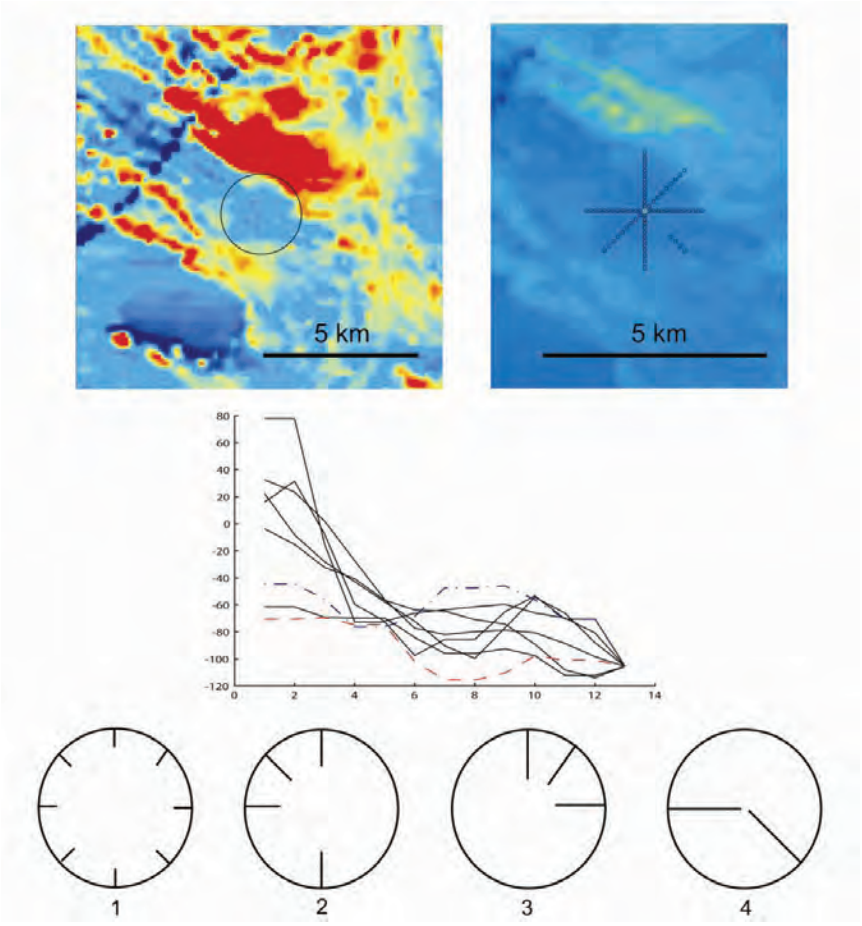

Figure 1. (Above left) Automatic detected circular feature in aeromagnetic potential field data (100 m spatial resolution, Finnmark, northern Norway). (Above right) Length of profile correlations for feature on left image. Correlation threshold 80%. Six profiles correlate the whole distance. The north-west profile does not correlate with any other. There is a gap in the circular border at that place. The south-east profile stops correlating after a while. (Middle) The eight profiles. The dashed (red) profile is the one not correlating with the others, while the dash-dotted (blue) profile stopped correlating at step 5. The y-axis is exaggerated. (Below) Four circles that display equal total profile correlation distances. If a few profiles correlate a longer distance, e.g. in a quarter of the circle (#3), it will get the same value as if all profiles correlate a smaller distance (#1). Fig. 1 is marked in Fig. 2d.

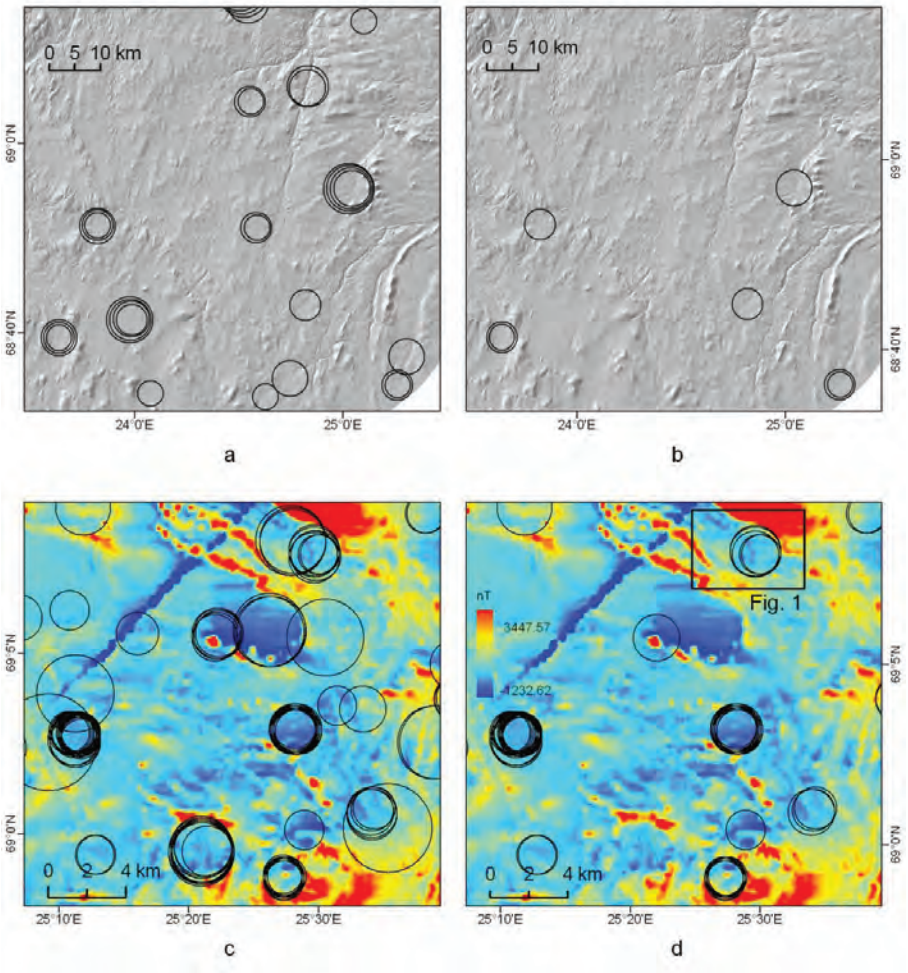

Figure 2. Figures (b) and (d) display features with a symmetry value higher than 75%, and are the filtered results of the automatic detected circular features in (a) and (c). The circular features are found by the methods of template matching on a DEM (a) and the circular outline algorithm on aeromagnetic data (c). (a) and (c) display two different areas of Finnmark, northern Norway. Both models have a spatial resolution of 100 m. The location of Fig. 1 is shown in (d).

Acknowledgements

Geophysical data were kindly provided by the Geological Survey of Norway (NGU). The project is supported by the Research Council of Norway (#170617). The comments of the Geomorphometry 2009 referees' and Programme Committee are highly appreciated.

References

Earth Impact Database. 2009: http://www.unb.ca/passc/ImpactDatabase (Accessed: 3 Mar 2009)

French BM, 1998, *Traces of Catastrophe: A Handbook of Shock-Metamorphic Effects in Terrestrial Meteorite Impact Structures*. Lunar and Planetary Institute, Houston, 120 pp.

Grieve RAF and Pesonen LJ, 1992, The terrestrial impact cratering record. *Tectonophysics* 216, 1-30.

Grieve RAF and Pilkington M, 1996, The signature of terrestrial impacts. *AGSO Journal of Australian Geology & Geophysics* 16, 399-420.

Koeberl C, 2004, Remote sensing studies of impact craters: How to be sure? *C. R. Geoscience* 336, 959-961.

Krøgli SO, Dypvik H and Etzelmüller B, 2007, Automatic detection of circular depressions in digital elevation data in the search for potential Norwegian impact structures. *Norwegian Journal of Geology* 87, 157-166.

Lowman PD, Jr., 1997, Extraterrestrial impact craters. *Oklahoma Geological Survey Circular* 100, 55-81.

Melosh HJ, 1989, *Impact Cratering: A Geologic Process*. Oxford University Press, New York, 240 pp.

Pike RJ, 1977, Size-dependence in the shape of fresh impact craters on the moon, In: Roddy DJ, Pepin RO and Merrill RB (eds.) *Impact and Explosion Cratering*, Pergamon Press, New York, pp. 489-509.